UNIVERSITÀ degli STUDI di CATANIA
Dipartimento di Agricoltura, Alimentazione e Ambiente
Di3A

UNIVERSITÀ DEGLI STUDI DI CATANIA

Agricultural, Food and Environmental Science

XXXIV° Cycle

TREATMENT WETLANDS AS RELIABLE SOLUTIONS FOR WATER POLLUTION CONTROL: LESSONS LEARNED IN MEDITERRANEAN CONDITIONS

Alessandro Sacco

Advisor:
Prof. Ing. Giuseppe Luigi Cirelli

Co-advisor:
Prof. Ing. Simona Consoli

Coordinator:
Prof. Alessandro Priolo

Ph. D. attended during 2019/2022

Everything should be made as simple as possible, but not simpler.

Albert Einstein (1879 – 1955)

Acknowledgements

I dedicate this work to Federica and the girl she carries in her womb. They are my heart, strength, and hope for the future.

I would like to express my gratitude to Professor Giuseppe Cirelli for being a solid reference point. His valuable guidance led me during my research journey. I thank all Catania's hydraulic team for their great support during these years. A great thanks to the PhD coordinator, Professor Alessandro Priolo, for his dedication and charismatic motivation. A special thanks to Nicolas Forquet and the REVERSAAL team of INRAE – Lyon. A super hug to the "Aula Aquatec fellowship": Angela, Giuseppe, Liviana, Manuela, Salvatore and Serena they are friends and best colleagues of ever! To them, I would dedicate the best "Prosecco" rigorously opened by "flex", hammer, axe, sword, or blade (in the most favorable case). I also want to thank the "Aula Aquatec Followers" for their ever-watchful presence and the perfect timing!

A precious thank you to my parents for giving me the best gift: *Life.*

Index

Table Index

Table 1.1 - Advantages and disadvantages of horizontal flow (HF),

Figure Index

Research highlights

- The H-CW system exhibited positive performance even if treating two types of WW, highly different in terms of nutrient-richness.
- There is still a strong discrepancy between the Italian legislation for water reuse and the guidelines issued by the EU,
- K_s measurements, tracer test and the drainage equation for evaluating clogging in HSSF systems were applied.
- After 2.5 years of operation, the tested methods showed that clogging was in the initial stage.
- Tested methods properly assess the evolution of the clogging phenomenon in HSSF-TWs.
- The consistency of results obtained by tested methods demonstrates their reliability.
- Metal removal was mostly related to sediment and substrate processes.
- Plants exhibited limited impact in retention paths and through root system stabilisation.
- Assessment of metals removal processes in TWs can help management and maintenance operations.

Keywords: Clogging; Decentralized Water Treatment; Hydraulic conductivity; Hydraulic behavior; Legislation; Metals; Reuse; Stormwater; Treatment Wetlands; Tracer test**;** Wastewater treatment

Abstract

There current water crisis exists in numerous dimensions. There are many problems related to the issue of water stress and they are principally linked to the ineffective management of water resource. The new challenges of the 21st century have created the need to adopt sustainable strategies to mitigate the causes and effects of the water crisis by avoiding its progression. In this scenario, a new concept of nature-based solutions (NBSs) is constantly evolving. These approaches inspired and guided by nature are effective "low cost" tools capable of supporting sustainable development goals and improving the quality of human life. The treatment and reuse of wastewater through treatment wetlands (TWs) is an excellent example of a NBS and is recognized as one of the best practices for integrated water management in terms of circular economy and environmental protection. Water generated by specialized processes that need proper treatment should no longer be considered wastewater (WW) but rather an unconventional resource that could be used as a key factor for a valid strategy capable of relieving the pressure on freshwater. Thus, the treatment and reuse of these waters must be supported and researched further. In light of these considerations, this work aims to (i) examine and evaluate TWs as strategic approaches in the management of water resources in semiarid areas; (ii) evaluate the treatment efficiency of TWs as reliable natural infrastructures for the treatment of unconventional water in typical Mediterranean climate conditions; (iii) evaluate the potential reuse of WW and the main barriers that hinder its application in Italy; (iv) and to increase the knowledge on the hydraulic performance of horizontal flow constructed wetlands and their treatment efficiency in the various fields of application. The main results obtained concern: (1) The experimental evidence on the reliability of TWs as decentralized systems used in different fields of application (2) the confirmation of the potential of the reuse of WW in Sicily, although hindered by often

restrictive regulations; and (3) the development of a convenient and reliable approach for understanding the hydraulic behavior of TWs with horizontal subsurface flow.

Riassunto

Oggi la crisi idrica è una realtà. Sebbene il rischio connesso alla carenza d'acqua venga spesso considerato soltanto dal punto di vista quali-quantitativo esso esiste in numerose altre dimensioni. Infatti non è semplice prevedere l'esatta magnitudo del rischio e dei suoi effetti sulla salute umana, sull'ambiente, sull'economia e sullo scenario politico-sociale. Sono molte infatti le problematiche connesse a questo tema. Le nuove sfide del XXI° secolo hanno imposto la necessità di adottare politiche sostenibili per la gestione dell'acqua (in ogni sua forma) *conditio sine qua non* è possibile mitigare cause ed effetti della crisi. In questo scenario, un nuovo concetto di soluzioni basate sulla natura si sta costantemente evolvendo. Questi approcci ispirati e condotti dai processi che si svolgono in natura sono efficaci strumenti "low cost", capaci di supportare lo sviluppo sostenibile e migliorare la qualità della vita umana. Il trattamento e il recupero delle acque reflue tramite sistemi di fitodepurazione, è un eccellente esempio di soluzione basata sulla natura ed è riconosciuta come una delle migliori pratiche per la gestione integrata dell'acqua sia nell'ottica dell'economia circolare, sia in quella di tutela ambientale. Le acque generate da processi specializzati che necessitano di un adeguato trattamento non dovrebbero più essere considerate acque reflue, ma piuttosto una risorsa non convenzionale che potrebbe essere in grado di alleviare la pressione sull'acqua pulita. In questa prospettiva la politica di recupero e riutilizzo di queste acque, deve essere appoggiata e perseguita. Alla luce di tali considerazioni, il presente lavoro ha l'obiettivo di: (i) Esaminare e valutare i sistemi di trattamento di fitodepurazione come approcci strategici nella gestione delle risorse idriche delle aree semi-aride; (ii) valutare l'efficienza di trattamento di impianti di fitodepurazione come infrastrutture naturali affidabili per il trattamento delle acque non convenzionali nelle tipiche condizioni di clima mediterraneo; (iii) valutare il potenziale riuso delle acque reflue e le principali barriere che ne ostacolano un'applicazione

a scala reale, con particolare attenzione al caso dell'Italia; (iv) ampliare le conoscenze sulle prestazioni idrauliche di impianti di fitodepurazione a flusso orizzontale e sulla loro efficienza di trattamento nei diversi campi di applicazione. I principali risultati ottenuti riguardano: (1) le evidenze sperimentali sull'affidabilità di impianti di fitodepurazione come sistemi decentralizzati utilizzati in diversi campi di applicazione; (2) la conferma delle potenzialità del riuso delle acque reflue in Sicilia, sebbene ostacolata da normative spesso restrittive ed inadeguate; (3) la messa a punto di un approccio speditivo per la comprensione del comportamento idraulico del sistema di fitodepurazione a flusso sub-superficiale orizzontale.

Abbreviation and acronyms

Above-ground biomass (AGB)
Actual residence time (aRT)
Ammonium (NH^{4+})
Below-ground biomass (BGB)
Best Management Practice (BMP)
Biochemical oxygen demand (BOD_5)
Carbon dioxide (CO_2)
Chemical oxygen demand (COD)
Deficit irrigation (DI)
Decentralized Water Treatment Facilities (DWTF)
Dry weight (DW)
Electrical resistivity (ER)
Electrical resistivity imaging (ERI)
Electrical resistivity tomography (ERT)
European Union (EU)
Evapotranspiration (ET)
Falling head (FH)
French reed bed (FRB)
Free water surface (FWS)
Heat pulse (HP)
Hybrid treatment wetland (H-TW)
Hydraulic conductivity (K_s).
Hydraulic load rate (HLR)
Horizontal sub-surface flow (HF)
Mass Balance (MB)
Methane (CH_4)
Nature-based solutions (NBS)
Nitrate (NO^3)
Nitrite (NO^{2-})
Nitrogen (N)

Nominal residence time (nRT)
Non-point source (NPS)
Operation and maintenance (O&M)
Organic load rate (OLR)
Polyclic Aromatic Hydrocarbons (PAHF)
Person Equivalent (PE)
Phosphorous (P)
Residence time distribution (RTD)
Servizio Informativo Agrometeoro-logico Siciliano (SIAS)
Sodium adsorption ratio (SAR)
Soil water content (SWC),
Transpiration (T)
Suspended solids (SS)
Sodium chloride (NaCl)
Total Metal Retention (TMR)
Total suspended solids (TSS)
Total suspended solids rate (TSSLR)
Treatment wetland (TW)
United States Environmental Protection Agency (US EPA)
United States of America (USA)
Vertical sub-surface flow (VF)
Vertical sub-surface flow (VF)
Wastewater (WW)

1. Introduction

1.1 Problem statement

Nowadays, the water crisis is a reality. The risks linked to water scarcity are often considered only from a quantity and quality point of view, but they exist in several other dimensions. Therefore, is not easy to determine the precise magnitude of the issue and its potential and collateral consequences in terms of human health, and environmental, political, social and economic impacts. In the last twenty years, global events have shown how floods, storms and droughts affected approximately three billion people produced a financial crunch of almost US$700 billion. (UNESCO 2020). Drought accounted for 5% of natural disasters, affecting more than one billion people, killing twenty-two thousand, and causing US$100 billion in damage (Deberati et al., 2017). Additionally, population growth, urbanization, and climate change, exasperate the competition for hoarding water resources. As is well known, several human activities use up renewable freshwater. In particular, irrigation takes out about 66% of the total global wate; arid regions use up to 90%, domestic households use 10%, industry uses 20%, and evaporated water from reservoirs takes 4% (World Water Council, 2017). Furthermore, countries worldwide are already suffering water scarcity impacts and continuously demanding freshwater (Stefanakis, 2020) causing social and political issues. On one hand, this situation intensifies international tensions between different governments that share water resources. On the other hand, Institutions without clear agreements and cooperation policies often suffer points of instability in water management (World Water Council, 2017). The result is that the global water demand has increased by 600% over the past one hundred years (Wada et al., 2016). However, the water demand cannot exceed the water availability. While water demand is increasing, water availability is shrinking, and pollution threatens water quality (Ioannidou and Pearson, 2018; Boretti and Rosa, 2019). In particular,

water pollution can make water unfit not only for human life but also for agricultural and industrial sectors as well as ecosystem. Therefore, the water crisis is acquiring global standing, and mitigation measures have become a priority. Additionally, the economic crunch of recent years has forced many developed and developing nations to invest in reliable low-cost and energy saving strategies for water management. In this panorama, the global stakeholders pushing governments to adopt suitable strategic plans could still mitigate both the causes and the effects of the water crisis and avoid its progression. The European Union (EU) fought the water scarcity phenomenon by increasing regulations and policies to protect drinking water quality (2006/7/EC, European Commission 2006) and aquatic ecosystems, as ratified by the EU Water Framework Directive (2000/60/EC, European Commission 2000). Today, protecting the freshwater supply and ensuring its access for human health protection is a crucial challenge. It is a primary focus of the 6th goal of the 2030 Agenda for Sustainable Development (UN, 2018). The recycling approach is the core standpoint for all good practices regarding water, in all its shapes. In this optic, the water generated as a byproduct of specialized processes that need suitable preuse treatment should no longer be considered wastewater (WW) but rather an unconventional resource that could be a valuable strategy for alleviating freshwater pressure. On this premise, quite a new concept of nature-based solutions (NBSs) is evolving. NBSs inspired and maintained by nature, are feasible (cost-efficient/effective) and environmentally sustainable strategies intended to support society's development goals and safeguard human life (Cohen-Shacham et al., 2016). These solutions are carried out by the action of natural components (e.g., trees, soil, plant, microorganisms, etc.) and/or by the presence of complete ecosystems characterized by different complexity levels. The NBS are hypothesized to provide reliable and sustainable methods to tackle several global challenges enhancing the circular economy and urban innovation, while making resilient cities and water resource protection

possible (Haddis et al., 2020). In recent years, the European Commission set NBSs for water management as a crucial achievement goal of its agenda, defining them as an innovative approach with economic and social benefits through ecosystem services that can enhance natural capital and its resilience and renewal capacity. Consequently, NBSs are applied to address contemporary water management challenges across all sectors, including WW treatment and reuse. With respect to water issues, NBSs can enhance water availability and quality by means of natural processes and low energy demand (World Water Development Report 2018 by UN-Water). Treatment wetlands (TWs) are outstanding examples of NBSs, designed and built to treat contaminants in water through natural components (Somarakis et al., 2019). TWs can be assembled using local materials and are characterized by adaptability and resilience, providing multiple ecosystem services and economic advantages (Hansson et al., 2012, Ni et al., 2016). Hence, the implementation of TWs for water quality improvement and nonpoint source (NPS) pollution control has attracted worldwide interest for several years (Stefanakis A., 2016). The consideration of natural treatments has also been greatly stimulated in Italy since 2006. Law 152/2006 according to directives 91/271/CEE and 91/676/CEE of the EU provides general guidelines for water pollution control emphasizing natural approaches such as ponds and TWs (Cirelli et al., 2007)

1.2 TW as NBS: background, issues, and general views

The TW system can be defined as engineered ecological systems designed and built to treat water contaminants by means of natural service and nature-provided compounds. Only a few anthropogenic components are used to control the water level, hydraulic flow rate and its direction (US EPA 2000). The fundamental components employed in the TW technology are tanks, plant species, and porous media with specific sizes and ratios. In these systems, microorganisms perform different important processes such as

hydrolysis, mineralization, nitrification and denitrification. Plants carried out a crucial role as substrates where microorganisms develop; they maintain temperature, decrease wind speed, take up nutrients, support sedimentation and avoid resuspension of nutrients and sludge (Vymazal J., 2013). The plants used for phytoremediation strategies should have consistent biomass, an accelerated growth rate, and the capacity to accumulate metals in their aboveground tissue (Zeb et al., 2013). Although, TWs have a simple design and constructive features, they highlight good treatment performances to remove different types of pollutants (Birch et al., 2004; Marzec et al., 2018; Thalla et al., 2019). Furthermore, the slight energy demand and low operating costs have made this technology the most sustainable and low-impact choice for waters pollution control (Ghrabi et al., 2011). However, these positive features are compensated by a need for extensive surface area and a slow and inertial treatment process velocity. Originally, TW technology was established in Europe and United States (US) as an alternative low-energy demand system in small communities, on-site, mountain sites, and decentralized zones where centralized wastewater management is difficult to implement and/or in various villages, small industries and farms where operators are not often confident in conducting and afford conventional treatment systems (Stefanakis and Akratos, 2016). In these settings, the treatment technology should be robust and able to operate with slight maintenance and supervision (Nivala et al., 2013). There are several types of TWs, and many different designs and arrangements can be considered (Fonder and Headley, 2013). Since macrophytic vegetation types are used, the filtering media and the inflow flow WW to be treated are the major components of TW. Generally, their classifications (Figure 1.1) are based on two parameters: hydraulic flow regime and type of macrophytic growth. According to the hydraulic flow regime, TWs with subsurface flow can be categorized into horizontal sub-surface flow (HF), vertical subsurface flow (VF), and hybrid treatment wetlands (H-TWs). Generally, the hybrid TWs

can involve combinations of HF and VF-TWs, but any types of arrangements that enhance system treatment performance could be considered hybrid (Vymazal et al., 2013). The TWs could be further classified according to the life-form of the predominant macrophyte used in the systems including free-floating, floating-leaved, emergent, and submerged macrophytes. Commonly, TWs with emergent macrophytes are the most employed type of free water surface (FWS) systems in the EU and US (Vymazal et al., 2013)

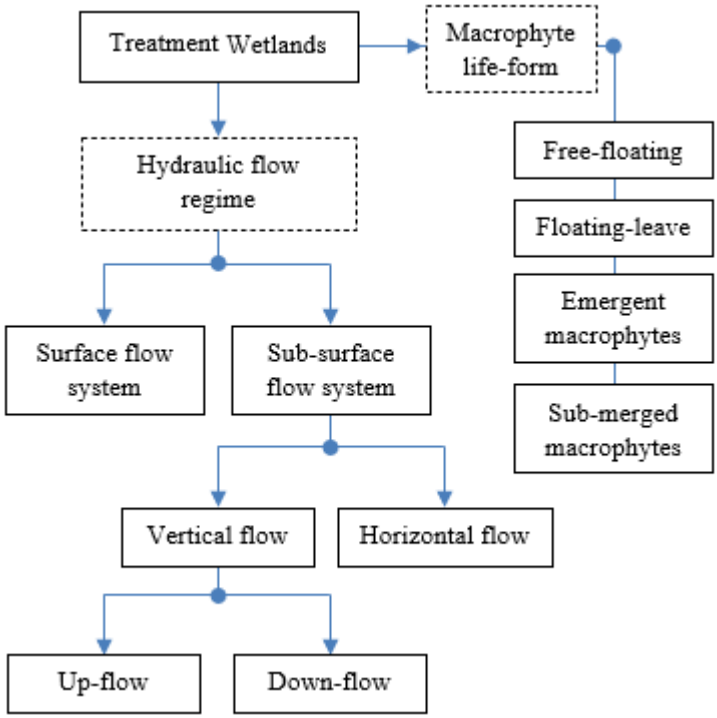

Figure 1.1– Schematic constructed wetlands classification according to hydraulic flow regime and macrophytes life-form

The FWS-TWs are channels, tanks or basins with an impermeable layer (clay or geo-textile) filled by a suitable medium

(rock, gravel, soil, etc.). The medium hosts emergent vegetation (*Typha* spp., *Scirpus* spp., and *Phragmites* spp.) that shades the water surface, prevent the growth/persistence of algae. Moreover, vegetation plays a role in pollutant removal through direct uptake, additionally providing a substrate for microorganisms that breakdown pollutants (Brix 1994; Wetzel 2001). The slow hydraulic and essentially laminar flow through the system allows synchronized physical, chemical, and biological processes, and they often act synergistically to remove pathogens (Stefanakis et al., 2014) primarily bacteria and viruses (Kadlec and Wallace 2008). Additionally, this technology allows water to flow gradually above the ground exposing it to the atmosphere and ultraviolet (UV) sunlight. Finally, FWS systems provide to numerous supplementary benefits such as the creation of a habitat for biodiversity instauration and conservation which are essential to many ecosystem services (Chen, 2011). TWs with subsurface flow (SSF) have been implemented for WW treatment in Europe since the early 1980s (Vymazal et al., 1996). After some years, worldwide database of results that showed impressive WW treatment by SSF was published (Brix, 1994). SSF-TWs are primarily designed for secondary or tertiary treatment of wastewater, and commonly use a pretreatment stage. The SSF system is a basin/tank filled by various types of porous media hosting plant species that survive under hydraulic saturated conditions. The WW flows over the surface or through the filter media activating physical, chemical, and biochemical reactions that contribute to WW quality improvement (US EPA, 2000). The substrate supports filtration process, provides a surface for microbial development. In comparison to FWS, the SSF systems have a lower area demand and higher rates of contaminant removal per unit of land. Generally, the SSF is more suitable than the FWS for human health safety, mosquito control and minimization of wildlife interactions (Kadlec, 2009). The HF-TWs are waterproof systems, filled with filtering media (in specific type, size and ratio). Plants are rooted in the hydraulic saturated layer, and water flows

slowly below the surface in connection with a network of aerobic and anaerobic zones. The media guarantees the possibility of the development of biofilms and plant roots (Rodriguez-Dominguez et al., 2020). HF reactions follow complex physical, chemical, and biological mechanisms (adsorption, filtration, sedimentation, oxidation/reduction reactions, precipitation, microbiological degradation, etc.) which are activated by the interaction of the media, plants, and microorganisms, the whole process is strongly mediated by the contact time between these components and WWs (Nivala et al., 2013). VF technology is widely applied NBS for WW treatment in Europe and in North Europe. Commonly, the removal of organic pollutants by the system does not depend strictly on temperature. The VF systems admit a high load rate and show good removal efficiency and a relatively low area demand in comparison to other TW types. The VF-TWs are characterized by highly oxidizing conditions and VF technology with intermittent loading is strongly efficient in removing different forms of organic carbon in terms of biochemical oxygen demand (BOD_5) and/or chemical oxygen demand (COD). They are also effective and suitable when aerobic processes such as nitrification are required (Langergraber and Haberl, 2001; Garcia et al., 2010). A well-considered positive aspect is the low area demand, which has increased VF technology implementation making it a widely growing treatment approach (Ayaz et al., 2012; Vymazal, 2013). VF technology has much higher maintenance and operational costs than HF units due to needing pumps that regularly dispense the hydraulic flow in the system. Recently developed H-TW systems have been used to increase the efficiency of the overall treatment process (Wu et al., 2015) to satisfy the exigent European water quality standards. Generally, hybrid systems present in the EU and the USA involve HF and VF units organized in different combinations depending on the needs. HF-TWs and VF-TWs act according to various mechanisms and often show different treatment performances. Indeed, they present a series of advantages and disadvantages (Table 1.1).

Table 1.1 - Advantages and disadvantages of horizontal flow (HF), vertical flow (VF), and free water surface (FWS) constructed wetland (Gorgoglione and Torretta, 2018)

System type	Advantages	Disadvantage
HF	(a) Long flowing distances possible; (b) Nutrient gradients can establish; (c) Formation of humic acids for nitrogen (N) and Phosphorous (P) removal; (d) Longer life cycle.	(a) Higher area demand (b) Careful calculation of hydraulics necessary for optimal oxygen-supply; (c) Equal wastewater supply is complicated.
VF	(a) Smaller area demand; (b) Good oxygen supply and nitrification; (c) Simple hydraulics; (d) High purification performance from the beginning.	(a) Short flow distances; (b) Poor denitrification; (c) Higher technical and maintenance demands; (d) Loss of performance esp. in P-removal (saturation).
FWS	(a)Addition to the "green space" in a community biochemical oxygen demand (BOD_5), total suspended solids (TSS), chemical oxygen demand (COD), metals, and organic material removal in a reasonable detention time; (b) N and P removal in a significantly longer detention time; (c) Minimization of mechanical equipment, energy, and skilled operator requirements.	(a) Higher area demand (b) Anoxic-environment and poor nitrification; (c) Mosquito development.

HF systems is known to have good treatment performance for removing organic matter and suspended solids (SS), but limited oxygen transfer affects its nitrification capacity. VF systems have considerable nitrification ability due to a well-defined oxygen network

in the system. There are several applications of hybrid systems (Rousso et al., 2019; Fernandez-Fernandez et al., 2020; Lavrnić et al., 2020; Ventura et al., 2021) each of which has defined a series of combinations that has shown different benefits. The classic combination of VF followed by HF has been used to treat municipal WW highlighting the improvement of nitrification processes, total suspended solids (TSS) reduction, and organic matter removal (Lee et al., 2009; Foladori et al., 2012; Vymazal, 2013;). Similarly, the sequence HF-VF in-series is highly reliable for organic matter and TSS treatment, showing good denitrification capacity (Justin and Zupančič, 2009). The HF-VF-FWS in-series arrangement was used to treat winery WW, this multiunit approach guaranteed the improvement of nitrification and denitrification processes, organic matter, TSS, and bacterial removal (Milani et al., 2020). As explained previously, the major drawback of TW implementation is the area footprint. Consequently, recent studies on TWs aim to discover innovative solutions and design/operational approaches to optimize the management and efficiency of TWs, maximize their longevity and tackle the extensive area demand (Zhao et al., 2020). Several studies and methods have been conducted to improve the knowledge on reducing footprints above and beyond achieving good quality effluent (Prost-Boucle and Molle 2012; Foladori et al., 2013). These studies have primarily focused on varying the hydraulics by recirculation of treated WW, using fill-and-drain cycles or artificial aeration, selecting new and/or reactive media and evaluating the effects of solids accumulation in the filtering media. Additionally, intensified TW variants are known and applied, largely based on different aeration modalities (e.g., tidal flow, artificial aeration and recirculation), with increased energy, chemical or operational inputs. Aerated TWs are examples of these variants, introduced and patented in the USA (Wallace, 2001). This system works by means mechanical aeration which pushes oxygen transfers enabling aerobic processes and improved reactions, especially when nitrification (and subsequent

total nitrogen removal) is a treatment purpose (Nivala et al., 2013). This means that in these systems, treatment processes are intensified, and high removal rates of organic matter and nitrogen can be reached. Thus, the system footprint can be significantly reduced (Stefanakis, 2020). Other variant systems include French reed bed (FRB), also called two-stage vertical flow. These systems have been well-known in France for several years, but are quite novel in many European countries (Rizzo et al., 2017). This technology involves two in-series treatment stages, with alternate feeding and resting periods to maintain permeability and oxygen content, and control of biomass growth (Morvannou et al., 2015). One innovative feature of FRB is that it can accept raw sewage in the first stage and does not require primary treatments (e.g., Imhoff or septic tank) reducing the effort required to implement and manage primary sludge treatment (Yadav et al., 2018). The sludge accumulates in the first stage for several years and is then removed (after its stabilization which typically occurs in 10-15 years), making it also suitable for reuse. Furthermore, FBRs allowed for a reduction in the area footprint, making these systems attractive, especially as an alternative for small towns (Paing et al., 2015). Despite a large number of TW variants, and the great variety of system types and configurations, a standardized design/operational approach has not yet been determined. Several studies suggest that TWs are often designed by means of a "black box" approach and that operational criteria are empirically based on previous experiences (Caselles-Osorio et al., 2007; Langergraber et al., 2009b; Pucher and Langergraber, 2018b). Nevertheless, every site is unique and the TWs will be site-specific and individually assembled to meet precise goals. Nowadays, thanks to the knowledge gained in implementing and managing TWs, more multilayered and accurate approaches have been developed and applied (Rousseau et al., 2004; Dotro et al., 2017; Li et al., 2018). They involve advanced calculations that take into account several variables such as hydraulic load rate (HLR), hydraulic retention time (HRT), organic load rate (OLR), nonideal flow patterns,

background pollutant concentrations, etc. The results of these studies have been used to recommend feasible ranges for the different factors (Table 1.2, summarizes the most studied and recognized as crucial TW design parameters), and highlighted that the design and operating parameters are vitally linked to optimizing TWs treatment performance, longevity, and sustainability. In addition, there are several handbooks on TW design (Kadlec and Knight, 1996; US EPA 2000; Bresciani and Masi, 2013; Scholz, 2011, 2015) that agree on different aspects such as setting up a simple design that allows for easy system maintenance, using natural energies and local materials, and incentivizing landscape integration, etc. Consequently, the conceptual planning phase is essential for making a successful TW. It should consist of identifying and properly using the key design parameters, understanding the TW processes and removal mechanisms that could have direct effects on the performance, operations and maintenance (O&M), and lifespan of TW. More than two decades of studies have proven that TWs have a strong ability to treat different types of pollutants (SS, organic matter, nutrients, bacteria, heavy metals, emergent pollutants, etc.). The treatment performance depends on complex mechanisms (physical, chemical and biological) that are catalyzed by several components (soil, plants, microorganisms, etc.) present or synergistically activated in the TW environment. In TWs, the substrate is the main supporting material for plant and microbial growth that can form a biofilm layer through it. Organic matter and SS are trapped by the substrate by means of sedimentation, filtration, and adsorption processes. Instead, the microbial population in TWs removes the organic matter by mineralization and gasification. In the TW aerobic zone the bacteria utilize the organic matter for their metabolism. In the anaerobic zone, organic matter will be decomposed into carbon dioxide (CO_2) and methane (CH_4) by anaerobic bacteria with fermentation.

Table 1.2 – Treatment wetlands (TWs) critical parameters and design criteria

TWs parameters	**Design and operational approaches**
Feeding modalities	TWs can operate continually or in batch-load mode depending on their configuration. Generally, the application of feeding/resting cycles may reduce clogging development (Sacco et al., 2021)
Hydraulic load rate (HLR)	Generally, HLR should be inversely proportional to hydraulic retention time (HRT), but it can vary according to site and TW configuration.
Hydraulic retention time (HRT)	HRT (theoretical) in TWs can varied between 6.3 and 11.6 days (Vymazal et al., 2017).
Organic load rate (OLR)	The OLR should be highly conservative to ensure TWs resilience and reliability. OLR between 8-12 g BOD_5 m^{-2} d^{-1} and 1-10 g TSS m^{-2} d^{-1} was suggested to treat secondary domestic WWs (Kadlec and Knight, 1996).
pH	Generally, TWs require neutral pH values. They could influence plants development (Rahman et al., 2020) and treatment performance (Carvalho et al., 2013).
Plants	Plants in TWs are able to directly uptake many organic pollutants in WWs (Li et al., 2014). A quite long list of macrophytes most frequently used in TWs was published (Vymazal et al., 2013).
Pre-treatment stages	Typically, pre-treatment stages (oxidation/sedimentation pond) are crucial to improve pollutants removal efficiency and alleviate clogging (Stefanakis et al., 2019),
Substrate	Commonly, medium selection and application depends on the availability of local materials and their costs. A list of medium types frequently used in TWs was published (Gorgoglione and Torretta, 2018).
Temperature	The microbial (nitrifying bacteria) degradation is possible at warm temperature (15–25 ◦C) (Matamoros et al., 2017). Generally, Lower temperature negatively affects TWs performance (Varma et al., 2021) Seasonality, has been recognized as important factor that impacts TW treatment efficiency (Vymazal et al., 1998).
Water depht	The Water depth is one of the important parameters for designing TWs. It is a quite variable and depending by TW configuration (Li et al., 2014).

Additionally, nutrients (N and P) are frequently targeted by TW treatment (Boog et al. 2018). On the one hand, they can cause serious environmental problems such as eutrophication of waterbodies (Frumin and Gildeeva, 2015). On the other hand, N in inorganic (ammonium, NH^{4+}, nitrite NO^{2-}, and nitrate, NO^{3-}) and organic forms is essential for living organisms. However, organic N in TW systems is easy to convert by microorganisms into NO_3-N leading to eutrophication of the receiving waterbody, so it becomes an important indicator of water pollution that needs to be adjusted. Several processes (adsorption, volatilization, plant uptake/adsorption, etc.) in the TWs may remove N from WWs and the ammonification and nitrification-denitrification processes are vital removal pathways around the root zone. Regarding P (organic and inorganic) that is present in different WWs, numerous studies (Vymazal, 2004; Wang et al., 2012; Bolton et al., 2019) have revealed that the most important way to remove P in TWs is through adsorption and precipitation facilitated by the substrate. In addition, P uptake/assimilation carried out by plants is usually high, especially at the beginning of the growing season (Vymazal, 1996) and if the biomass is harvested (Vymazal, 2004). TWs are applicable not only for chemical pollution control, but also for pathogen removal from WWs. The most frequent and well-validated removal mechanisms include adsorption, filtration, sedimentation and natural die-off (Wu et al., 2016). In recent years, TWs have also been applied to treat contaminants not commonly targeted in municipal WW treatment systems, such as heavy metals. They are primarily immobilized and retained by TW substrates through a range of processes that include sedimentation, adsorption, sulfate reduction with subsequent precipitation of metal sulfones (Hua and Hynes, 2016). Heavy metals are also taken up by plant roots and can be translocated upward to the aboveground parts (Vymazal and Březinová, 2016). The Table 1.3 summarizes typical pollutants present in the WWs and their removal mechanisms in the TWs.

Table 1.3 – Major pollutants and their removal mechanisms

Pollutant	Main removal mechanisms
Heavy metals	(a) Precipitation, (b) adsorption, (c) plants-uptake, (d) cation exchange, (e) complexation, (f) microbial redox.
Organic contaminants	(a) Microbial/substrate adsorption (b) aerobic/anaerobic bacteria decomposition.
Organic matter	(a) Filtration, (b) microbial aerobic/anaerobic degradation
Nitrogen (N)	(a) Ammonification-nitrification-denitrification, (b) volatilization, (c) plant uptake
Pathogens	(a) Filtration, (b) sedimentation, (c) natural die-off, (d) ultraviolet irradiation (FWS systems).
Phosphorous (P)	(a) Adsorption, (b) precipitation, (c) plants-uptake (export with harvesting).
Suspended solids	(a) Filtration, (b) sedimentation, (c) adsorption.

As previously explained, the TW substrate plays a crucial role in removing pollutants from WWs. On the one hand, the treatment mechanisms (filtration, sedimentation, ion exchange, physical adsorption, etc.) are crucial for the TW treatment process. On the other hand, they involve the accumulation of different types of solids, often recalcitrant (Kadlec R. H., 2009) that are converted to SS by means of microorganism activities (growth and reproduction) organized in biofilms (Kadlec and Wallace 2009), which reduce the free volume available for flow through the porous medium. As part of the treatment process, the TW porous medium will gradually become clogged due to different factors, mainly linked to WW characteristics, system design and operative modalities. The experiences with clogging a porous medium in TWs differ widely since the problem depends on many factors, often in disagreement with each other. The literature offers various information about the factors that could contribute to the clogging of porous media, indicating for instance the WW

characteristics as predominant (Winter and Goetz, 2003). Tanner et al. (1998) cited plant material (root and rhizome) development as the cause of the reduction in useful volume leading to a reduction in TW infiltration/percolation capacity. The presence of a large number of inert solids in porous media was attributed to the clogging phenomenon development process (Caselles-Osorio et al., 2007). Furthermore, it has been observed that the solids that occupy the porous medium and contribute to the development of clogging are of an organic nature (Pedescoll et al, 2009). Additionally, microbial growth and biofilm association have also been linked to phenomena leading to the progression of clogging (Wang et al., 2010). A recent critical review (Wang et al., 2021) has illustrated several factors implicated in the clogging development process (substrate porosity, hydraulic loading, oxygen supply conditions, organic loading, water depth, and plants). Of these organic loading and substrate porosity have the most significant influence. Similarly, clogging impacts in TW treatment performance, and its operation and lifespan are not yet clear. Several authors depict its negative effect on hydraulic behavior and treatment capacities (Caselles-Osorio and Garcia, 2006; Nivala and Rousseau, 2009; Gorgoglione and Torretta, 2018). Other studies have suggested that clogging improved the performance of TW at least initially (Karathanasis et al., 2003; Suliman et al., 2006; Xu et al., 2013). Recently, several authors have agreed that clogging could disturb TW treatment performance, long-term operations and time sustainability (Carrasco-Acosta et al., 2019; Yan et al., 2019; Zhou et al., 2020). The review of Matos et al. (2018), acknowledges that the progression of the clogging phenomenon in HF systems will lead to the formation of dead zones and preferential paths that will influence the hydraulic characteristics of the system causing direct impacts on the treatment performance. Other authors, did not observe any impact of clogging when it occurred (Marzo et al., 2018). Moreover, Vymazal, (2018) who compiled a large dataset from four HF-TWs found that the deposition process did not have a significant effect on

TW performance. Beyond these different interpretations, the scientific community is in agreement that the clogging phenomena can be quite complicated and challenging and complete understanding requires analysis of the whole system. Thus, a deep search of relationships between TW components and the interactions of these with the operation mode is needed as well as an identification of the influence of factors and impacts of each one. (Matos et al., 2018). Based on these premises, Clogging requires a precise understanding of TW hydraulics for their proper design and efficient operation. In agreement with recent studies (Liu et al., 2018; Licciardello et al., 2020), this phenomenon should be periodically monitored, especially in systems that have already been affected by clogging during their lifetime. In this optic, monitoring activities could be helpful for the application of restorative measures (i.e., replacing the dirty substrate, excavating, washing and reusing the substrate, direct application of chemicals to the filtering unit, or adding earthworms to the unit matrix). These saving approaches are more effective if the mechanisms and degree of clogging are well defined and understood. For these reasons, it has become increasingly crucial to identify a handily approach for clogging assessment with high accuracy, non-destructiveness, and simple realization. The literature provides several procedures for *in situ* detection of clogging. The traditional methods include clogging matter characterization proper to define the nature and degree of clogging despite a direct correlation of accumulated solids and the decrease of hydraulic conductivity and porosity is not easy to assess (Pucher and Langergraber 2018a). The hydraulic conductivity measurements and tracer testing evaluate hydraulic behaviour and are acknowledged as common approaches for clogging assessment (Nivala et al., 2012). As recognized, K_s of porous media decreases significantly once TW systems are in operation (Al-Isawi et al., 2015; Stefanakis et al., 2016; Licciardello et al., 2020). K_s values can be achieved using different approaches and at various points within TWs by surveying hydraulic gradients between specified points by using

Darcy's Law (Sanford et al., 1995; Suliman et al., 2006) as well as the falling head (FH) and constant-head (CH) methods (Pedescoll et al., 2009; Garcia-Artigas et al., 2020). However, the method limit is the reliability of the determined *Ks* values that depend on the accuracy of the hydraulic gradients (Sanford et al., 1995). Further disadvantages of these methods are that they require numerous measurement points inside the unit and a considerable disturbance due to the insertion of the tube into the matrix (Nivala et al., 2012). The scientific community largely uses the hydrodynamics of TWs obtained through tracer tests to study clogging phenomena on the flow in porous media. Tracer tests can be conducted at the system's outlet or at various points inside the bed to obtain a range of information. On the one hand, the tracer passage through the outlet allows identifying information about the impact of clogging on system hydraulics (Maloszewsky et al., 2005). On the other hand, measurements within the system provide notices about preferential flow paths, stagnant zones, and, ultimately, the possible causes of clogging (Knowles et al., 2011). In recent years, some studies have been explored the feasibility of the resistivity method to detect the clogging degree in SSF – TW. The clogged substrate has a strong water-holding capacity, which leads to low apparent resistivity in the draining phase. On these bases, the electrical resistivity method could be a good candidate to approach clogging phenomenon evaluation in TWs (Marzo et al., 2018; Liu et al., 2018). However, further investigation is needed to upgrade and explore the applicability of the resistivity method for quantifying clogging in the field and its characterization (Ergaieg et al., 2021). Other unusual techniques, such as ground-penetrating radar, nuclear magnetic resonance, and microbial fuel cell (Cooper P., 2005; Morris et al., 2011; Corbella et al., 2016), have been presented as clogging measurements to apply in the field. However, as they are complex, expensive and susceptible to several environmental factors, their accuracy and feasibility should be further discussed (Liu et al., 2018). A synthetic K_s value for HF-TWs can be obtained by simulating the

observed outflow volume using a mathematical model developed by Sanford et al. (1993) to predict the cumulative drainage volume from aquifers overlying sloping, impermeable layers. Darcy's law validates K_s values obtained from experiments by four rock-reed filters filled with different substrates and either planted with *Phragmites australis* or unplanted (Sanford et al., 1995). A drawback is that method needs system stopping, which can last up to several days for large HF-TW. Clogging is still a mystery box that gives few details and many possibilities. At present, there are many research methods to investigate TW clogging. Still, any technique has limitations, and a single measurement method provides little information about its spatial and temporal evolution. After two decades of experience with TW, we learn that the combination of multiple approaches seems the real promising trend on these premises (Nivala et al., 2012; Aiello et al., 2018; Licciardello et al., 2020; Wang et al., 2021).

2. Objectives and thesis outline

2.1 Thesis objectives

The General objectives of this work are:

(i) To increase knowledge on evaluating the hydraulic performance of horizontal TWs, with different designs, applications, and operational modalities;

(ii) To provide a general evaluation on water treatment scenario and promote strategic approaches and solutions in water resources management with specific insights on Mediterranean region;

(iii) To evaluate the reliability of TWs as feasible, effective and efficient treatment facilities for WW recover in Mediterranean climate.

Specific objectives are set in order to:

(i) To evaluate the hydraulic performance of the HF stage of a full-scale H-TW and the effects of clogging on the overall system;

(ii) Study the effectiveness of combining different approaches for monitoring the hydraulic behavior of the same HF unit, as a reliable tool for general method;

(iii) Assess the reliability and feasibility of a combined approach for assessing the occurrence of clogging and its potential spatial and temporal evolution;

(iv) Monitor the hydraulic behaviour of the HF units of a pilot scale H-TW from the start-up phase for the entire system lifespan;

(v) Define a properly and handily methodology for hydraulic conductivity at saturation (K_s) evaluation of different gravel filtering media at different spatial scales and operational modalities.

2.2 Thesis outline

A short overview of the thesis outline is provided to facilitate the reading and find commons points along all chapters.

Chapter 3 - Illustrates some issues related to stormwater and conventional wastewater (WW) reuse feasibility for green areas irrigation after being treated by a pilot hybrid treatment wetland (H-TW) in the Mediterranean climate. The system is operated to treat nutrient-poor effluent, like the stormwater runoff drained from the parking area and nutrient-rich domestic WW. Therefore, the treatment performance of H-TW for SWR treatment and recovery in the Mediterranean climate is evaluated.

Chapter 4 – This study defines and evaluates a handily approach to estimate K_s in saturated condition of gravel-based filtering media in the HF units. The system worked with the same hydraulic and loading condition of the pilot TW illustrate in *Chapter 3* compared with laboratory results obtained in previous monitoring campaigns. (1) The falling head (FH) method and a drainage equation to determine the porous medium's K_s and investigate the system's hydraulic performance. (2) A residence time distribution (RTD) analysis to evaluate the hydraulic flow dynamics and define the crucial parameters characterizing the TW. The effects of double feeding (operated to face typical local long dry periods and heavy/short rainfall

events) on the hydraulic system reliability are also evaluated.

Chapter 5 - This research aims to assess the capacity of the same method proposed in *Chapter 4* to determine the degree and variation in space and time of clogging in a full-scale HF-TWs for tertiary treatment of domestic WW produced by a retail store (SBR effluent), after five years of operation. The focus is put on identifying the most efficient combination of methods to assess clogging in HF-TWs.

Chapter 6 - This study investigates the pilot hybrid TW's reliability previously described in *Chapters 3* and *4*. To address the uncertainty associated with implementing representative monitoring during highly variable storm events, unique to Mediterranean conditions, a recipe for semi-synthetic stormwater was used to evaluate the removal efficiency of the system. This was characterized by metals and relative concentrations typically found in urban stormwater runoff. An intensive monitoring activity were carried out with the aim to analyze the quality of three matrices comprising the pilot H-W: water, biomass and volcanic gravel substrate.

Chapter 7 - In the present chapter, electrical resistivity imaging (ERI) was applied for monitoring the soil water motion patterns resulting from the adoption of water deficit scenarios in a micro-irrigated orange orchard (Eastern Sicily, Italy). The relationship of ERI with independent ancillary data of soil water content (SWC), plant transpiration (T) and in situ measurements of hydraulic conductivity at saturation using the falling head method was evaluated.

3. On the performance of a novel hybrid constructed wetland for stormwater treatment and irrigation reuse in Mediterranean climate[1]

Abstract

Decentralized water treatment facilities (DWFTs) have been described as one of the best practices (BMPs) for promoting effective water management programs in the framework of the circular economy, with the aim to easy the exploitation of freshwater supply. In many Mediterranean regions, wastewater (WW) reuse practice is still struggling for being accepted and it's clearly affected by legislation gaps and discrepancy among national and European perspectives. This work mainly investigates some issues related to stormwater and conventional WW reuse feasibility for green areas irrigation, after being treated by a pilot hybrid treatment wetland (H-TW) in Mediterranean climate. Experimental results are promising and suggest as viable the reclaimed water use in green area irrigation. Nevertheless, at the light of the EU guidelines proposal, the effluent water quality hereby reported fulfilled the minimum requirements for the intended use above mentioned but did not fully comply the stringent Italian standards.

Keywords: Decentralized water, treatment, stormwater, reuse, metals

A modified version of this chapter was published in [1] Ventura, D., Consoli, S., Milani, M., Sacco, A., Rapisarda, R., Cirelli, G.L., (2019c). On the performance of a novel hybrid constructed wetland for stormwater treatment and irrigation reuse in Mediterranean climate. [1]Innovative biosystems engineering for sustainable agriculture, forestry and food production, by Springer International Publishing AG, AIIA International Mid-Term Conference 2019

3.1 Introduction

Future urban scenarios could benefit from decentralized water treatment facilities (DWFTs) for effective water management of conventional and unconventional sources. In fact, De Feo et al. (2014) pointed out the unfeasibility to extend existing centralized water and wastewater (WW) systems to cope with the increasing level of urbanization, with consequent extra water demand and waste loads. Many WW facilities still remain vulnerable to the adverse effects of climate variability, with different frequencies in drought and flood all over the world. Moreover, in developed economies, like European Member States (MS), many infrastructures are ageing, while developing countries are facing challenging and costly investments for upgrading poor sewerage and drainage systems (SDS). In Italy, WW collection and treatment is largely lacking and insufficient, as reported by the European Community (EC), that considers 620 agglomerations in 16 regions in breach of the EU rules (EC, 2019). In particular, several EC infringement procedures and one condemnation of the Court of Justice, highlight absent or not complying infrastructures in 62 (>10.000 PE) and 5 (>2.000 PE) agglomerations in Sicily (CSEI, 2018). Begum et al., 2008) already described several stormwater reuse techniques used around the world, and sensitive urban design systems (SUDS) for urban green areas and sport fields irrigation have been particularly proposed. However, as reported by Goonetilleke et al. (2017), stormwater is still globally undervalued, because of related uncertainty and unreliability due to seasonal supply and therefore to quantitative and qualitative issues that could complicate the implementation of storage and treatment planning and designing strategies. In order to reduce the consequent counterproductive effects of combined quantitative and qualitative constraints, such as increased management and treatment costs, the intended use is a key concept allowing to use different water, with highly variable quality. To this aim, the adoption and the application of suitable existing technologies

should be fitted for given water reuse purposes. Regarding to that, the possibility to increase and define technical knowledge and management guidance can turn it into the chance to knowingly relay on extensive, more adaptive and self-supporting DWTFs. In the case of first flush rain water and stormwater runoff, Italian normative (Legislative Decree 152/06, Art. 113), specified that the Regions, subject to the authorization of the Ministry of the Environment, can regulate and manage, by means of specific rules and "case by case", these resources. On this regard, Lombardy and Emilia Romagna have promulgated the appropriate regional regulations, while the Sicily region, among others, does not have anyone yet. Stormwater runoff have been compared to industrial WW and their reuse, as well as for domestic and urban WW, is regulated by the Ministerial Decree (M.D.) 185/2003. However, the strictness of this law, which is reflected in costly monitoring activity, the absence of clear standard limits for specific intended use, and also the increasing tariffs to the expense of consumers for covering the reuse costs, generally discourages the spread of this practice (Ventura et al., 2019a). To optimize costly and time - consuming microbial monitoring analyses for WW reuse, the Italian Superior Institute of Health (Bonadonna et al., 2002) already proposed *Clostridium perfringens* as an effective indicator for old faecal contamination. However, the latter has never been included in the Italian standard limits for water reuse (M.D. 185/2003). Also, the recent EU proposal for water reuse (European Commission, 2018) recommended Escherichia coli and Clostridium perfringens, respectively, as the most appropriate indicators for pathogenic bacteria and protozoa assessment. Masi et al. (2018), highlighted how generally people are not willing to pay for wastewater reuse service and there is a need to demonstrate the reliability of costs-saving treatment technologies on the long term. The EU proposal for water reuse (2018) could be considered, in this context, as a first important step for easing and conforming its promotion and actualization at national level (Ventura et al., 2019a). Despite TWs are

well known treatment technologies and largely applied since several decades at international level (e.g.in Germany, since the end of 70's), however, there is a need to fill the knowledge gap on their technical performances, management procedures and design criteria (CSEI, 2018). As a step forward of previous case study on the reliability of a pilot hybrid constructed wetland (HF-TW) in treating typical stormwater runoff contaminants (metals and polycyclic aromatic hydrocarbons, PAHF) and alternative conventional rich-nutrient WW in the favorable climate of Mediterranean (Ventura et al., 2019b), this work mainly aims at investigating some issues related to treated WW reuse feasibility for green areas irrigation, with special regard to Italian and EU legislations.

3.2 Case study

The HF-TW is constituted by two identical parallel lines (1-2), with a common inlet (stabilization pond, monitoring points: in unit #1, out unit #2), a sub-surface horizontal flow unit (HF1-HF2, monitoring point: out unit #3), planted with *Canna indica*, and a free-water surface unit (FWS1-FWS2, monitoring point: out unit #4) with floating *Typha latifolia*, for each line. For further details on H-TW design, operating, site location, monitoring steps, metals and PAHF analytical methods, as also statistical approach, refer to Ventura et al., (2019b). For conventional water quality and overall removal efficiency (RE, %) relate to Marzo et al. (2018). Also, microbial indicators and pathogens were monitored: *Escherichia coli* and *Clostridium perfringens* spore were analyzed with the method of membrane filtration and culturing on suitable agar media. Overall, water quality parameters are shown as averaged values from treatment line 1 and 2 since non-parametric data analysis did not reveal any significant differences (*p-values* >0.05).

Table 3.1 - Average values and standard deviation (SD, ±) of physical parameters recorded at H-TW Inlet and Outlet during the three monitoring periods; dissolved oxygen (DO), electrical conductivity (EC, at 20 °C), pH and T (°C)

Period	**I**		**II**		**III**	
Point	**Inlet**	**Outlet**	**Inlet**	**Outlet**	**Inlet**	**Outlet**
DO (mg·L^{-1})	6.7 (1.8)	5.6 (2.5) 1[a]	4.9 (1.5)	8.4 (2.3) 0.08[a]	3.1 (0.7)	3.3 (0.1) 0.59[a]
EC (µS·cm^{-1})	1910 (388)	2851 (1443) 0.87[a]	114 (14)	471 (291) 0.35[a]	160 (73)	218 (30) 0.07[a]
pH	7.5 (0.3)	7.2 (0.2) 0.57[a]	6.7 (0.9)	7.5 (0.8) 0.92[a]	6.7 (0.7)	7.4 (0.01) 0.91[a]
T (°C)	28.9 (3.1)	26.5 (3) 0.87[a]	15.2 (1.9)	15.21 (1.4) 0.75[a]	23.9 (6.1)	21.7 (0.2) 0.75[a]

[a] Kruskal-Wallis test p-values calculated between identical treatment units (FWS1-FWS2: outlet point).

In Table 3.1 mean values of main physical parameters for each period are reported, at the general inlet and outlet of the hybrid system as also relative P-values for the latter (caption [a]). Electrical conductivity (EC) and dissolved oxygen (DO) values varied among I, II and III periods, along the treatment units (data not show), and generally between the inlet and the outlet of the plant, due to the different quality of WW treated, the seasonality and the hydraulic regime of each unit. The system design can clearly determine very variable biological and chemical dynamics occurring in within, particularly when a hybrid TW is set up. In fact, thanks to the arrangement of different TWs types all potential pollutants removal mechanisms can be exploited (Stefanakis and Akratos, 2016). Among the parameters reported in Table 3.1, the EC should be considered together with the SAR index for a proper evaluation of the ultimate effect on water infiltration rate

for pursuing suitable irrigation management practices (FAO, 1994). In Figure 3.1a the relationship between these two parameters in terms of soil structural stability is plotted, as already described by ANZECC (2000). The Figure 3.1b reports the mean EC and SAR values observed at the inlet and the outlet of the hybrid TW during the SBR effluent (I period) and runoff (II-III period) treatment. After the treatment, in both cases, a quite increase of both parameters can be noted. The EC increment could be explained by evapotranspiration (ET) processes taking place in the treatment units, while the photosynthetic activity occurring in the FWS units could have risen the pH values (as referred in Table 3.1), causing cations precipitation like Mg^{2+} and Ca^{2+} and therefore a slight SAR increase. By comparing the two graph HF, it seems that in this case, the TW treatment train could have played a positive role by making more favorable the EC and SAR relationship in the perspective of WW reuse for irrigation. However, too high proportion of sodium ($Na^{+)}$ ions relative to Mg^{2+} and Ca^{2+} could degrade the soil stability and reduce plants growth. Finally, the SAR index was always within the Italian standard limits for water reuse.

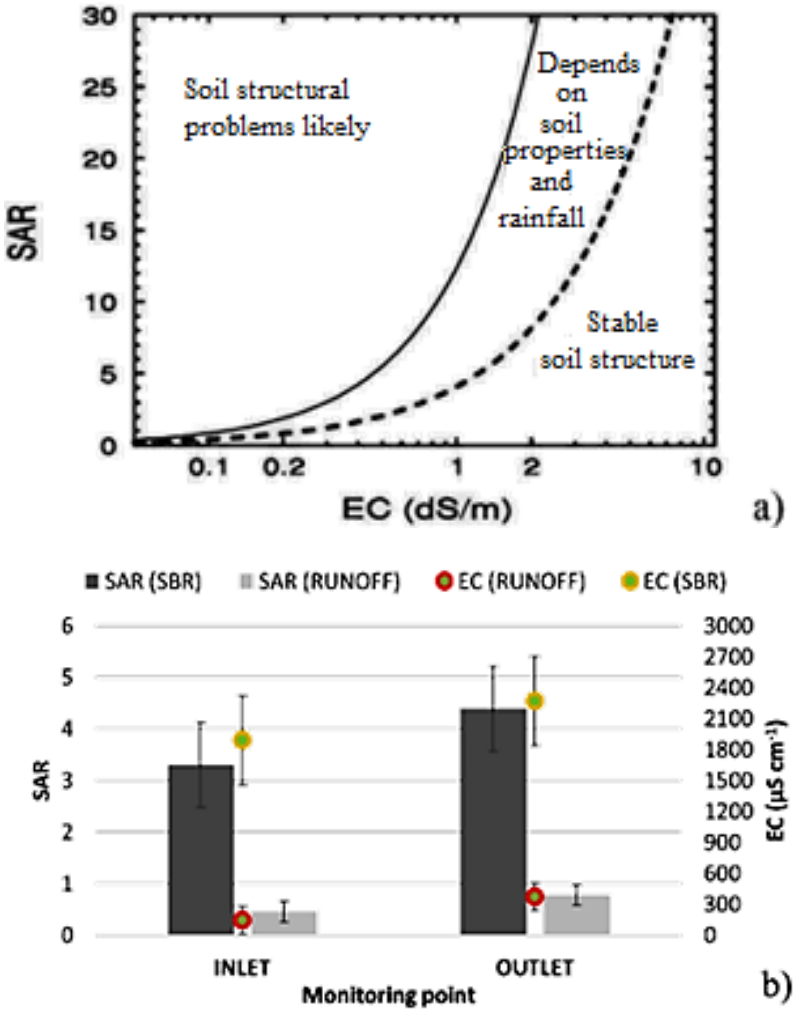

Figure 3.1 - Mean EC and SAR values detected at the inlet and outlet points of the hybrid TW during runoff and SBR effluent treatment (a); the relationship between SAR and EC for soil structural stability (b), as it appears in ANZECC (2000). Note that 1 dS m^{-1} = 1000 µS cm^{-}

In Figure 3.1, concentrations of main water quality parameters during SBR effluent treatment (I period) are reported as boxplots, at the inlet, the HF outlet and the final outlet of the HF-TW system. By comparing the partial RE (%) observed ad the HF outlet and the overall one (respectively: 64-45 TSS, 50-25 BOD_5, 35-16 COD, 25-38 TN, 35-41 TP), it was evident that the sub-surface horizontal flow units had better performance for organic matter and TSS removal, while the free water surface units for nutrients depletion. These trends were probably due to the instability of the novel system (data were collected since the start-up phase of the system and during the first year and a half of operations): macrophytes growth was, in fact, quite limited (FWS units were replanted after 6 month HF because the floating support was damaged and replaced) and algal proliferation occurred during warmer seasons was not confined and retained by the typical *Typha latifolia* huge root system, that was expected to act as a final filter. Outlet concentrations of TSS, BOD_5, COD, TN and TP were respectively: 62.5 (±37), 20.3 (±8), 47 (±13), 3.2 (±1.5), 46.3 (±21). These values were generally not complying with the Italian standard limits for reuse (tab. 2), except for COD and TP, but confirmed the self-defeating strictness of this legislation. According to the Table 3.2 of the European proposal for water reuse (EU, 2018) on reclaimed water quality criteria for agricultural irrigation in case of non-food crops (quality classes B and C), BOD_5 and SST limits refer to those reported in the European Directive on urban wastewater treatment (91/271/EEC): respectively 25 mg L^{-1} and 35 (<10.000 PE) or 70 mg L^{-1} (2.000-10.000 PE), while COD and nutrients limits are not reported. However, among the environmental hazards linked to reclaimed water use in agriculture, the same EU proposal cites the nutrients imbalance (the others are salinization, sodicity and toxicity) and reminds the importance of MS in knowledge gathered in order to limit concrete environmental risks.

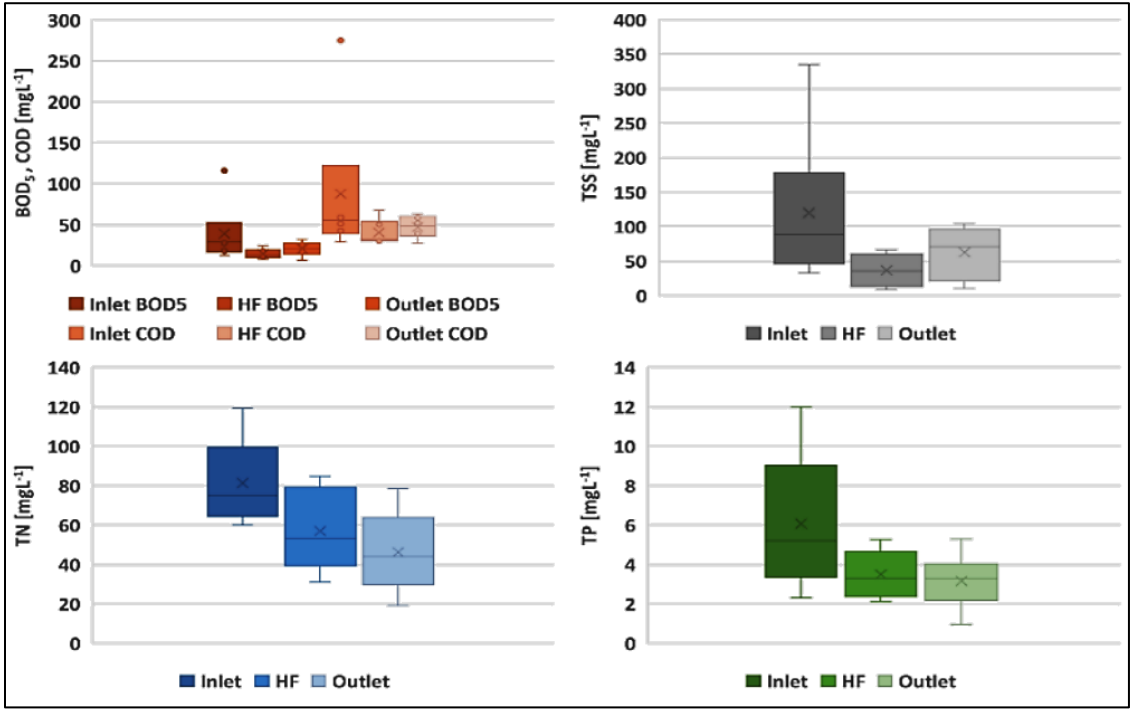

Figure 3.2 Boxplots of the concentrations of conventional quality parameters (BOD_5, COD, TSS, TN and TP) detected in water samples collected at the inlet, the HF outlet, and the final outlet of the H-TW, during I monitoring period (SBR effluent treatment)

Table 3.2 - Physical-chemical (mg L^{-1}), trace metals (mg L^{-1}), and microbiological (CFU 100 m L^{-1}) Italian standard limits for wastewater discharge and reuse Italian standard limits

Italian standard limits	TSS	BOD_5	COD	TN	TP	Tot. Cr	Fe	Ni	Pb	Cu	Zn	*Escherichia coli*
Wastewater discharge	80	40	160	35[c]	10	2	2	2	0.2	0.1	0.5	
Wastewater reuse	10	20	100	15	2	0.1	2	0.2	0.1	1	0.5	5.0×10^{3} [(d)]

[a] Legislative Decree 152 (2006), [m] ministerial Decree 185 (2003), [c] Limit for discharge into surface water bodies (as the rough sum of NH_4, $N\text{-}NO_2$ and $N\text{-}NO_3$), ([d]) Recommended value for P.E. >2,000, [e] Maximum value in 80% of samples, 100 is the max punctual value permitted; in case of natural systems, like lagooning and constructed wetlands, limits increase up to 50 UFC 100 m L^{-1} (80% of samples) and 200 UFC 100 m L^{-1} (max punctual value).

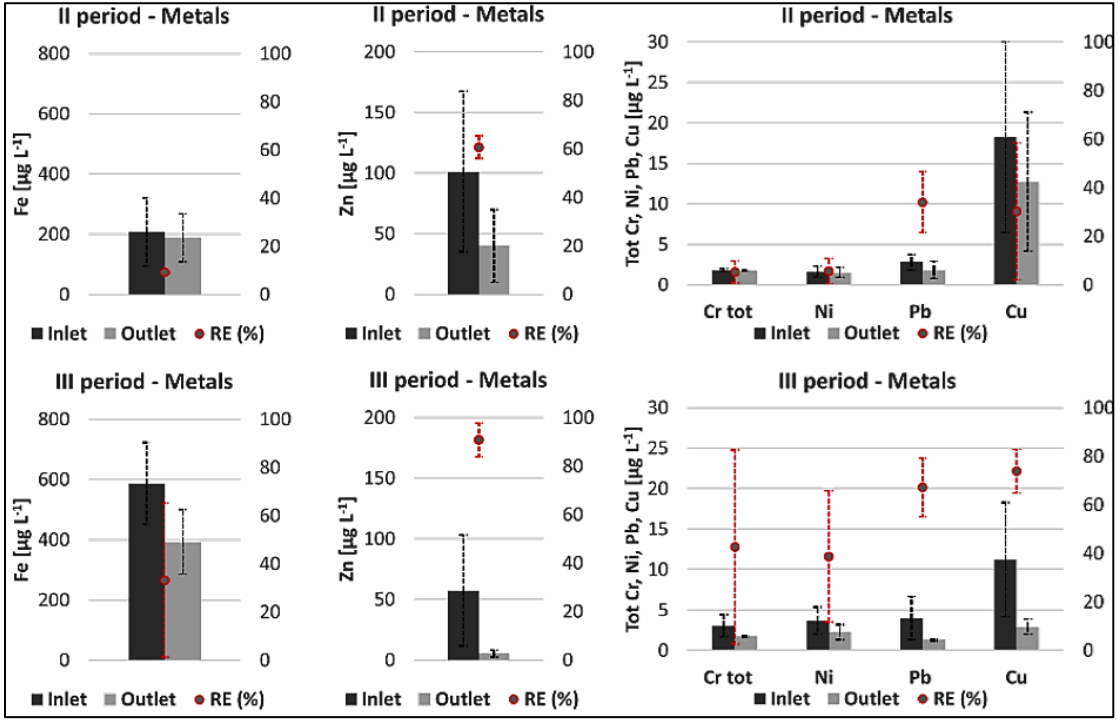

Figure 3.3 - Mean metals concentrations (µg L^{-1}), SD, removal efficiency (RE, %) (red points) and SD at the hybrid TW inlet (monitoring point #1) and outlet (monitoring point #4) during runoff treatment (II– III monitoring periods)

The presence of metals in stormwater runoff is strongly influenced by rainfall events and intensity, the hydraulic loads entering the treatment system and the physical state they are found (dissolved or particle-bound). Physical form, together with temperature, conductivity and pH variations can foster metals release in water and are crucial in major metals removal processes, like their association with granular media, precipitation as salts and biological uptake. Figure 3.3, reports mean metals concentrations (μg L^{-1}) and relative removal efficiency during II and III monitoring periods. They were always very low and clearly below the values imposed by Italian standard limits for reuse (Table 3.2), but a slight increase between II and III periods (except for Zn and Cu), allowed to observe higher RE during the last one (ranging from 33% (±32) for Fe to 91% (±7) for Zn). Mean *E. coli* concentrations (log UFC 100 ml^{-1}) were at the inlet and the outlet during I, II and III periods, respectively: 4.1 (±0.12) and of 1.5 (±0.4), with an overall RE of 2.6 (±0.4); 2 (±0.3) and 0.4 (±0.2), with an overall RE of 1.6 (±0.2); 1.5 (±1.3) and 0.09 (±0.2) with an overall RE of 1.4 (±0.6). Mean *C. perfringens* concentrations (log UFC/100ml) were at the inlet and the outlet during I, II and III periods, respectively: 3.3 (±0.2) and 1.3 (±0.2) with an overall RE of 2 (±0.3); 2.6 (±0.3) and 0.8 (±0.1) with an overall RE of 1.8 (±0.4); during the III period, *C. perfringens* was not determined. HF-TWs pathogens removal efficiency has been generally evaluated up to 4 u-log, and in some case, depending on the initial microbial load, further disinfection technology must be used. Thanks to the combination of different TWs types (which can promote prolonged HRTs like usually HF units do, and high DO concentrations ensured by VF stages), however, all potential pathogen removal 7 mechanisms can be encouraged (Stefanakis and Akratos, 2016). In this study, different effects of various treatment units, in function of the indicator or pathogen considered were observed, since main RE of *E. coli* occurred at the FWS outlet, while *C. perfringens* was removed already at the HF outlet. The latter is an obligate anaerobic, but in spite of its resistance

to environmental changes and disinfection processes, perhaps could have been inhibited by possible microbial predation activities and/or unfavorable environmental conditions occurrence (like atmospheric oxygen transferring in the rhizosphere of *Canna indica*). Finally, the sum of the PAHF species analyzed at the system inlet, had an average concentration of 0.038 µg L^{-1} (±0.017), which was clearly below respectively to 0.01 and 0.001 mg L^{-1}, the Italian standard limits relative to the total organic aromatic compounds and benzene for water reuse. However, despite the low concentrations detected, the overall removal efficiency was 81% (±31), and 78% (±11) was already observed at the outlet of the Pond. This could be in agreement with the major removal mechanism of PAHF in TWs described by Wojciechowska (2013) in terms of sedimentation (2013).

3.3 Conclusion

The H-TW system exhibited positive performance even if treating two types of WW, highly different in terms of nutrient-richness. On this regard, main considerations are reported in Ventura et al. (2019b). However, there is still a strong discrepancy between the Italian legislation for water reuse and the guidelines proposed by the EU, which clearly would require an implementation process for being integrated at national level. Even when considering conventional parameters and microbial indicators for water quality monitoring for reuse, quantitative and qualitative differences appear obvious. Therefore, the overcoming of this gap probably remains a key point to make effective the WW reuse practice in Italy, also because the intended use would be finally considered. Valuable resource like stormwater runoff would be then valorized. In fact, at the light of EU guidelines proposed, the effluent water quality reported in this case study would fulfil the minimum requirements for reuse in green area. irrigation, in contrast with the stringent Italian standard limits, which would not be fully complied.

4. Hydraulic performance of horizontal constructed wetlands for stormwater treatment: A pilot-scale study in the Mediterranean[2]

Abstract

Horizontal subsurface flow (HF) constructed wetlands (TWs) are widely adopted as a highly effective technique for stormwater treatment. However, the cumulative clogging phenomenon in HF is a complex and challenging operative issue affecting removal efficiencies and the lifespan of TWs. This paper aims to evaluate the reliability of a combined approach for assessing the occurrence of clogging and its potential spatial and temporal evolution in two pilot-scale HF-TW. The experimental TW system was fed with stormwater runoff from a parking area during the rainy season and sequential batch reactor (SBR) wastewater (WW) during the dry season. The falling head (FH) method and a drainage equation were used to determine the hydraulic conductivity at saturation (K_s) of the porous medium and investigate the hydraulic performance of the system. A residence time distribution (RTD) analysis was also performed to evaluate the hydraulic flow dynamics and define the crucial parameters characterizing the TW. The applied hydraulic measurement techniques highlighted that clogging was in the initial stages of development after 2.5 years of operation, likely associated with the presence of a pond and the partial retention of total suspended solids (TSS) by the HF system. Overall, the good consistency in the

A modified version of this chapter was published as Alessandro Sacco, Giuseppe Luigi Cirelli, Delia Ventura, Salvatore Barbagallo, Feliciana Licciardello (2021). Hydraulic performance of horizontal constructed wetlands for stormwater treatment: A pilot-scale study in the Mediterranean. Ecological engineering, Vol. 169, 106290
https://doi.org/10.1016/j.ecoleng.2021.106290

results of the applied methods supports their future application for predicting the occurrence of clogging phenomena in HF-TWs.

Keywords: Clogging Constructed wetlands Wastewater treatment Hydraulic conductivity Tracer test

4.1 Introduction

NPS pollution of water is becoming an increasing environmental issue (Fu et al., 2014; Wu et al., 2017). Frequently, stormwater runoff is reported as a carrier of various kinds of pollutants including toxic chemicals, hydrocarbons, trace metals, oils, and fats (Schmitt et al., 2015; Pálfy et al., 2017; Van Leeuwen et al., 2019). In response to these risks, the implementation of constructed wetlands (TWs) for NPS pollution control and water quality improvement has continuously grown worldwide. Compared with conventional wastewater (WW) treatment technologies for the control of stormwater pollution, horizontal subsurface flow (HF) TWs are a low-impact and sustainable choice (Tang et al., 2017) due to their structural simplicity, low maintenance requirements, and low operational costs (Ranieri et al., 2013). Several studies have highlighted the efficiency of TWs at removing different pollutants from various types of WW (Pedescoll et al., 2009) including stormwater runoff (Birch et al., 2004; Ventura et al., 2019). However, decades of development and management of TWs show that clogging is a widespread operational problem (Knowles et al., 2011). Clogging is a gradual and cumulative process (Nivala et al., 2012) that can negatively affect hydraulic performance and reduce the lifespan of HF TW systems (Caselles-Osorio et al., 2007; Aiello et al., 2016). The literature on clogging suggests various causes including the accumulation of solids inside HF units, design errors, and factors relating to incoming water quality (Pedescoll et al., 2013). In particular, the hydraulic performance of a filter medium is influenced by a range of factors including the type, system design, and operating conditions (Kandra et al., 2015). Yet, the

clogging phenomenon is not fully understood (Matos et al., 2018) and universal protocols for measurement and evaluation of clogging development are not available (Nivala et al., 2012). Nevertheless, many authors agree that the hydraulic conductivity at saturation (K_s) of porous media decreases significantly once these systems are put into operation (Al-Isawi, et al., 2015; Stefanakis et al., 2016; Licciardello et al., 2020); *Ks* values can, therefore, be a useful indicator of clogging in TWs. K_s values can be obtained using different approaches and at different points within TWs by measuring hydraulic gradients between specified points by using Darcy's Law (Sanford et al., 1995; Suliman et al., 2006) as well as the falling-head (FH) and constant-head (CH) methods (Pedescoll et al., 2009; Garcia-Artigas et al., 2020). In previous papers, different schemes, and equations for the FH method (based on Lefranc's test) were compared at multiple spatial scales (Licciardello et al., 2019) to identify the more reliable combination among those existing in literature (NAVFAC, 1980). However, FH method alone gives just partial and punctual information about clogging. A synthetic K_s value for HF systems can be obtained by simulating measured outflows based on the approach of Sanford et al. (1993), which predicts the cumulative drainage volume from aquifers overlying sloping, impermeable layers. Hydrodynamic conceptualizations achieved using residence time distribution (RTD) analysis can also be used to study clogging phenomenon in porous media. Tracer tests can be carried out both at the outlet of HF units or at various points within the system to determine a range of information. In particular, the passage of tracers through the outlet provides information about the impact of clogging on system hydraulics (Maloszewsky et al., 2005). On the other hand, measurements within the system can be useful to identify preferential flow path HF, stagnant zones, and, ultimately, the possible causes of clogging (Knowles et al., 2011). Currently, few studies have focused on investigating clogging development in TWs treating stormwater runoff (Tang et al., 2017). These systems are characterized by

stochastic loading and pollutants that differ from those present in domestic WWs (Kandra et al., 2015). In addition, in the Mediterranean region, TWs used to treat stormwater runoff require feeding with different influent during the dry season to avoid the TW drying and ensure its robustness (Ventura et al., 2019). Consequently, the clogging phenomenon may evolve differently in these systems. Hence, determining the accuracy and reliability of different measurement techniques, and their feasibility in terms of time and operator skill requirements, is crucial for effective clogging phenomenon evaluation. Furthermore, to verify consistency and suitability among the methods tested in clogged systems (Licciardello et al., 2020), it could be proper to apply the same approach to HF TWs with different clogging stages, influent types, design, and operating conditions. This paper investigates clogging phenomena in HF systems treating stormwater runoff during the rainy season and WW (preliminary treated by a sequential batch reactor, SBR) during the dry season in the Mediterranean region (generally, May-September). The main objectives of the study were to (1) analyze clogging development processes using different approaches, and (2) assess the reliability and consistency of these methods for monitoring the presence of clogging and its spatial and temporal evolution. The experimental campaign was carried out using two pilot-scale HF systems installed at a retail store area in Catania, eastern Sicily, Italy.

4.2 Material and methods

The TW pilot plant (Figure 4.1) consisted of a stabilization tank (pond) with a storage capacity of 6 m^3 that fed the system by means of two distinct parallel lines (L1 and L2), each including a filtering unit (HF1 and HF2) and a free water system (FWS1 and FWS2). The HF1 and HF2 tanks had the following dimensions: width = 1.5 m, length = 4.5 m, and height = 1.1 m. These units were filled by a 0.6 m-deep volcanic gravel porous material (porosity = 0.4 and grain size = 0.01–

0.03 m) and planted with *Canna indica* with a density of approximately four plants per $m^{2.}$ The FWS1 and FWS2 tanks had the following dimensions: width = 1.0 m, length = 3.5 m, and height = 1.0 m. These tanks were equipped with floating-supports for *Typha latifolia* plants, held a water depth of 0.8 m. A weather station (Campbell scientific GRWS100) was installed close to the TW pilot plant to record meteorological data (air temperature, wind speed and direction, rainfall, and relative humidity). The TW pilot plant has been operating since 2016 with a daily hydraulic flow rate of 1.0 m^3 per line provided by stormwater runoff during the rainy season (from October to April) and SBR effluent during the dry season (from May to September). Since the system's start-up phase, total suspended solids (TSS), chemical oxygen demand (COD), biochemical oxygen demand (BOD_5), total nitrogen (TN), and total phosphor (TP) have been monitored once per month during operational time at the TW inlet (pond). Average concentration values ($mg \cdot L^{-1}$) observed in the pond and the relative standard deviation (±SD) of TSS, COD, BOD_5, TN and TP were 7 (±0.05), 12 (±5.0), 21 (±7.0), 3 (±1.3), and 2.6 (±0.3), respectively, during stormwater (n = 18) feeding, and 120 (±28.0), 87 (±25.5), 39 (±15.0), 81 (±18.0), and 6 (±2.1), during SBR (n = 12) feeding. The frequency of feeding was between six (during stormwater feeding) and four (during SBR feeding) cycles per day. Pond's water was pumped into the HF systems, which accumulated in chambers equipped with submersible pumps to direct the flow to the FWS systems. Finally, the pilot plant effluents are discharged into a waterbody. Further details about the pilot TW system as well as its removal efficiency are reported by Ventura et al. (2019, 2021). The RTD analysis by means of tracer tests, FH method measurements and drainage simulations were carried out in October 2019 (stormwater feeding), when the canopy coverage in the systems was 100% and no rain events occurred during the days when the tests were conducted.

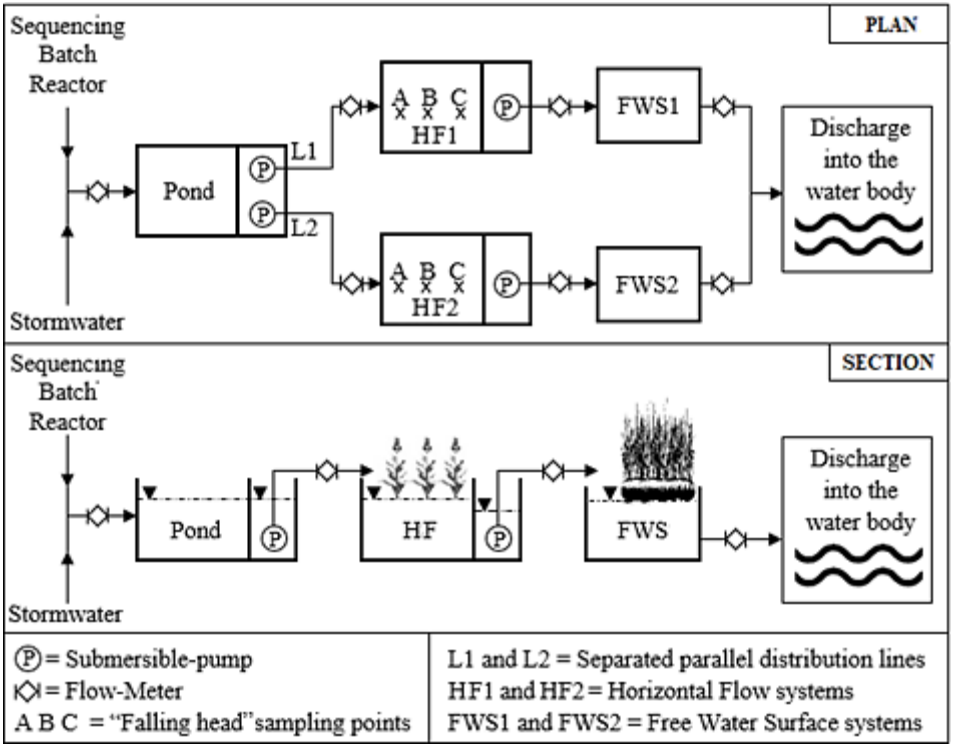

Figure 4.1 - TW pilot scale design and layout

4.2.1 Residence time distribution analysis

In a steady-state system without excluded zones, the actual residence time (*aRT*) equals the nominal residence time (*nRT*), which can be calculated by using Eq. 4.1:

$$nRT = \frac{V}{Q} \quad \text{(Eq.4.1)}$$

where V (m^3) is the volume of the TW system occupied by pore space, and Q ($m^3\ h^{-1}$) is the volumetric flow rate of water through the system. However, in TWs characterised by dispersion and mixed flows (Holland et al., 2004; Wahl et al., 2010), the *nRT* and *aRT* are not usually equal (Kadlec and Wallace, 2008). In this study, the RTD curve was derived experimentally by injecting an inert chemical tracer into the inlet at time zero and then measuring the tracer concentration C(t) at the outlet as a function of time. Sodium chloride (NaCl) was selected as the tracer due to its low cost and satisfactory reliability (Passos et al., 2018). The amount of NaCl was chosen based on influent's electric conductivity (EC) ranging between 650 and 850 µS cm^{-1}. At time zero, a conductivity meter (delta OHM – HD 2106.2) was used to measure the background EC value of the mixing water. The solution was then arranged in a bucket, stirring the tracer into the mixing water to achieve an average benchmark value of EC approximately ten-times higher than the background value (Keller and Bays, 2000). The solution (EC = 6,800 µS cm^{-1}) was then impulsively injected into the inlets of the HF systems using a pump. A conductivity probe (delta OHM – HD 2106.2) was positioned in the outlet pipe to record EC values at 5-min intervals. The outlet flows were measured using a flow-measurement device (B-Meters MUT 2200 EL). Finally, to extrapolate the RTD curve, the EC values (after subtracting the background EC value) were converted to NaCl concentrations (mg L^{-1}) using a linear standardisation curve (R^2 = 0.99). The method of

moments (Martinez and Wise, 2003; Holland et al., 2004; Aiello et al., 2016; Marzo et al., 2018) was applied to determine the RTD curve, for which two moments were used. The first moment (the centroid of the RTD curve) corresponded to *aRT*, giving the average time that the influent spent in the HF systems, calculated using Eq. (4.2):

$$aRT = \frac{\int_0^\infty t \cdot C(t)dt}{\int_0^\infty C(t)dt} \quad (4.2)$$

where *t* is the sampling time (s); *dt* is the change in the time between two successive samples, and *C*(*t*) is the tracer concentration at time *t* (mg L^{-1}). The second moment, also called "variance", expresses the dispersion of the average tracer concentration (Wang et al., 2006; Guo et al., 2017), calculated using Eq. (3):

$$\sigma^2 = \int_0^\infty (t - aRT)^2 \cdot \frac{C(t)}{\int_0^\infty C(t)dt} \quad (Eq.4.3)$$

The higher-order moments of the RTD curve were not considered in this study due to their increasing uncertainty (Wang et al., 2006). As suggested by Kadlec and Wallace (2009), the tracer mass recovered at the HF outlet was subsequently determined using Eq. (4):

$$M_{out} = \int_0^\infty Q(t) \cdot C(t)\, dt \quad (Eq.4.4)$$

where M_{out} is the tracer mass recovered at the HF system outlet (g); Q(t) is the outflow rate at time t (m^3 h^{-1}); and C(t) is the tracer concentration at the HF system outlet at time t (mg L^{-1}). The relative tracer mass recovery (%) was defined by Eq. (5):

$$Mass\ recovery\ (\%) = \frac{M_{out}}{M_{in}} \cdot 100 \quad (Eq.4.5)$$

where M_{out} is the racer mass recovered at the HF system outlet (g), and M_{in} is the total tracer mass recovered at the HF system inlet (g). The hydraulic efficiency (λ) can have varying effects on TWs performance (Persson et al., 1999; Kadlec and Wallace, 2009), was calculated using Eq. (6):

$$\lambda = \frac{\tau_p}{nRT} \quad \text{(Eq.4.6)}$$

where τ_p is the peak time reflecting the time after which the maximum tracer concentration was observed. Persson et al. (1999) classified λ into good ($\lambda > 0.75$), satisfactory ($0.5 < \lambda \leq 0.75$) and poor ($\lambda \leq 0.5$) bands. Finally, the short-circuiting parameter (θ), was calculated as an indicator of hydraulic performance (Tang et al., 2017) using Eq. (7)

$$\theta = \frac{t_{16}}{t_{50}} \quad \text{(Eq.4.7)}$$

Where t_{16} and t_{50} are the hydraulic residence times (HRT) when 16% and 50% of the tracer were recovered, respectively. For θ, the smaller the value is, the more severe the short-circuiting of TW flow is.

4.2.2 Hydraulic conductivity under saturated conditions

The K_s (m d^{-1}) of filtering unit substrates is frequently determined using the FH method based on the Lefranc's test (Nivala et al., 2012). The reliability and accuracy of this technique have been documented in several studies (Pedescoll et al., 2009; Ventura et al., 2019b; Licciardello et al., 2020). Among the different methods and equations that have been proposed, the "standpipe method" (Pedescoll et al., 2009; Licciardello et al., 2020) was selected for the K_s measurements performed in this study. For the FH test, two permeameters were assembled, one impervious (IMP) and one pervious (P). The layouts of these devices are shown in Table 2 and Table 3, respectively. The permeameters consisted of steel tubes with

a length of 0.65 m and an internal diameter of 0.10 m, which were connected to a 6.6 L plastic container by a ball-valve that added water in a single-pulse as required. A hole was subsequently drilled down in the HF TW filter medium until the water table was reached, into which the permeameters were placed and driven with force to a depth of 0.32 m. A pressure probe (STS–Sensor Technik Sirnach, AG) was also introduced inside the permeameters to measure the pressure variation as a result of water-level variations. These probes were connected to a data logger (Campbell Scientific CR220-R) that recorded four measurements per second until the infiltration of the water column was complete. A total of 12 (4 per sampling point) repeat measurements were made at variable distances from the inlet. In particular, three sampling points were set along a central alignment in both HF systems, with a distance of 1.0 m between one sampling point and the next. Finally, the pressure data were converted to water heights, and the average K_s values were calculated by averaging the 12 repeat measurements. Further details on the device design, dimensions, and construction of the experimental set-up are reported by Licciardello et al. (2019).

Table 4.1. Device layout and derivation of K_s using the IMP-permeameter and the FH method adapted from the NAVFAC Design Manual 7.01 (1986).

IMP-permeameter device layout	Equation
IMP-permeameter with material inside (**Standpipe**) 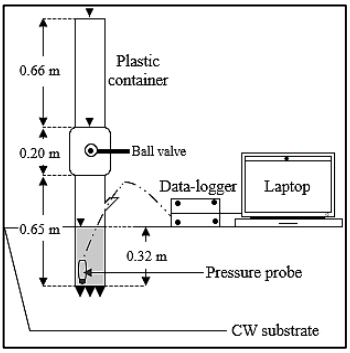	$K_s = \frac{2\pi R + 11L}{11(t_2 - t_1)} ln\left(\frac{h_1}{h_2}\right)$ $(Eq. 4.8)$ R (0.05 m) and L (0.32 m) are the radius and submerged length (m) of the tube, respectively, as defined in the NAVFAC Soil Mechanics Design Manual 7.01 (1986). h_1 and h_2 are the water levels (m) in the permeameter cell corresponding to time t_1 and t_2 (s), respectively.

Using the IMP permeameter with Eq. 4.8 (Table 4.1) is the most suitable method for measuring K_s in original (unclogged) gravels where the isotropic conditions are still valid and vertical and horizontal K_s are the same (Licciardello et al., 2019). When the clogging process is established, the vertical K_s starts to vary from the horizontal K_s. The P permeameter used with a calibrated equation (Eq. 4.9, Table 4.2) allowed K_s variations to be evaluated while accounting for the influence of clogging in the horizontal direction and saving time in comparison to other methods described in the literature (Licciardello et al., 2019).

Table 4.2. Device layout and derivation of K_s using the P-permeameter and the FH method adapted from the NAVFAC Design Manual 7.01 (1986).

	Equation
P-permeameter (with material inside) (total area = 3.11×10^{-4} m^2, distributed along 0.25 m) 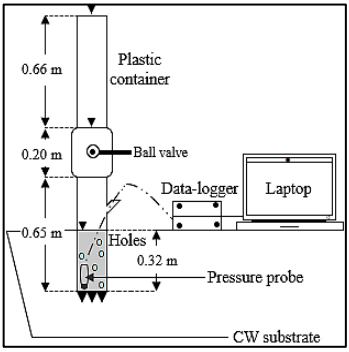	$K_s = \frac{2\pi R_{mod} + 11L_{mod}}{11(t_2 - t_1)} \ln\left(\frac{h_1}{h_2}\right)$ $(Eq. 4.9)$ R_{mod} (0.049 m) and L_{mod*} (0.18 m) are the radius (m) and submerged length (m) as calibrated by Licciardello et al. (2019). h_1 and h_2 are the water levels (m) in the permeameter cell corresponding to time t_1 and t_2 (s), respectively. *L_{mod} (0.18 m) is the calibrated value that allowed the use of an equation similar to Eq. 1 in the case of the P-permeameter. The submerged length in the field was 0.32 m.

To extrapolate the best fit between the observed and simulated water levels, the least squares regression was used (Licciardello et al., 2019) by summing and minimising the squared differences between the simulated and the observed curves, according to Eq. 4.10:

$$\sum_{t=0}^{n} (h_{obs}\ (t) - h_{sim}\ (t))^2 \rightarrow 0 \qquad \text{(Eq.4.10)}$$

where h_{obs} is the water table height (m) inside the permeameter at time t, and HF_{im} is the simulated data from Eq. 4.8 and Eq. 4.9.

4.2.3 Drainage tests

A synthetic K_s value for both filtering units was obtained by simulating a drainage condition from the HF systems. This approach

was successfully used by Sanford et al. (1993) to predict the cumulative drainage volume from aquifers overlying sloping and impermeable layers. The K_s value derived using Eq. 11 was validated by comparing values obtained using Darcy's Law in four rock-reed filters filled with different substrates (a sand-and-gravel mixture) with grain sizes ranging from 0.02 to 0.04 m and with/without common reed (*Phragmites australis*) planting (Sanford et al., 1995):

$$V = V^* \left(\frac{1 - \exp\left(-t \frac{3h(0,0) K_s \cos\beta}{sL^2} \left(1 - \frac{V^*}{V_i} \right) \right)}{1 - \frac{V^*}{V_i} \exp\left(-t \frac{3h(0,0) K_s \cos\beta}{sL^2} \left(1 - \frac{V^*}{V_i} \right) \right)} \right) \qquad \text{(Eq.4.11)}$$

where $V_i = (s \cdot w \cdot L \cdot h\,(0,0))$ (m^3) (initial volume of water for x = 0 and t = 0); $V^* = s \cdot w \cdot L \cdot (h\,(0,0) - h(0,t)) + \frac{1}{2} s \cdot w \cdot L^2 \tan\beta$ (m^3) (potential outflow due to drawdown and slope); V is the cumulative drainage volume (m^3); s is the drainable porosity ($m^3 \cdot m^{-3}$); x is the linear distance from the drain (m); t is the time at which the drainage volume is calculated (s); β is the slope of the impermeable layer ($m \cdot m^{-1}$); L is the length of the HF (m); w is the width of the HF (m); K_s is the saturated hydraulic conductivity ($m \cdot min^{-1}$); and h(0,0) is the hydraulic head when x = 0 and t = 0 (m); h(0,t) is the hydraulic head when x = 0 and t > 0 (m). A volume-meter (WS100, DS20 – SIN EMISOR) was also installed at the output of the HF systems, and drainage volumes were measured at 1-min intervals until the system was emptied. Five simulations (one per week) were conducted. Finally, a range of conductivity values was applied to Eq. (4.11) and K_s value producing the closest fit between the simulated and observed outflow curves, and that provided a simulated volume (VF_{im}) similar to the observed volume (V_{obs}) in the first part of the curve, was selected for the substrate for the drainage test.

4.2.4 Statistical analysis

A one-way analysis of variance (ANOVA) was performed to test the statistical significance of differences between the K_s average values obtained by applying the FH method (with the IMP-permeameter), the drainage test, and the unclogged gravel obtained by Licciardello et al. (2019) in each of the HF test units. The data obtained by means of the FH method (using the IMP-permeameter) were assumed to be normally distributed, and the tests were performed using *Minitab* software. To assess eventual differences between the K_s values obtained in HF1 and HF2 for each of the applied methods, the Kruskal-Wallis test (R Core Team 2014) was performed (significance was assumed where $p < 0.05$).

4.3 Results

4.3.1 Residence time distribution analysis.

Observed and simulated RTD curves at the outlets of HF1 and HF2 are shown in Figures 4.2 and 4.3, respectively.

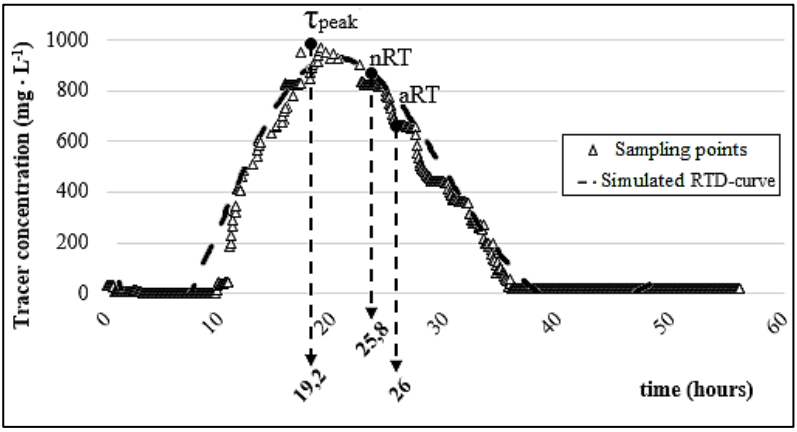

Figure 4.2 - Observed and simulated RTD curves for the HF1 outlet.

HF1 had an average flow rate of 0.051 $m^3 h^{-1}$ corresponding to a *nRT* of 25.8 h. The percentage of the tracer mass recovered at the outlet was 81% in accordance with the indicators of Kadlec and Wallace (2008), which confirmed the applicability of the tracer test. The *aRT* calculated using the method of moments was 26 h (σ^2 = 5 h); the τ_p was 19.2 h; and the hydraulic efficiency of the system (λ_{HF1}) was 0.74, which is satisfactory according to the indicators of Persson et al. (1999); finally, the short circuit parameter (θ_{HF1}) was 0.69. The RTD analysis performed at the HF2 outlet is shown in Figure 4.3, characterized by parameter values very similar to those obtained for HF1. In particular, during the tracer test, the average flow rate was 0.051 $m^3 h^{-1}$, which corresponded to a *nRT* of 25.8 h.

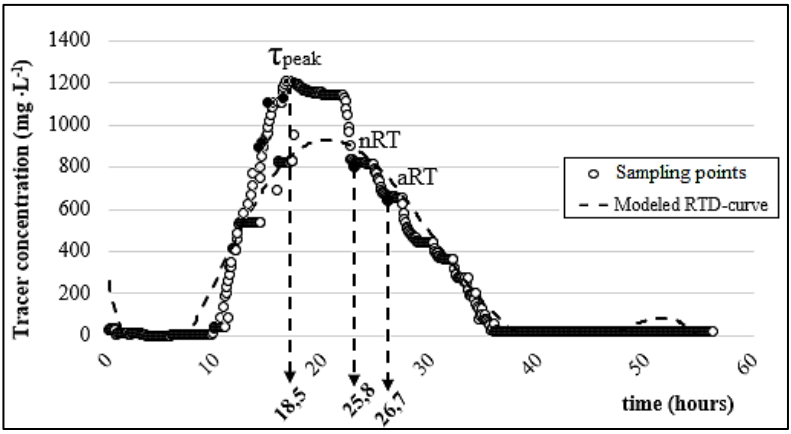

Figure 4.3 - Observed and simulated RTD curves for the HF2 outlet.

The percentage of tracer mass recovered at the outlet was 86%, which further demonstrates the efficiency of the experimental set-up (Kadlec and Wallace, 2008). The *aRT* was 26.7 h (σ^2 = 4.7 h); the τ_p was 18.5 h; and the hydraulic efficiency of the unit (λ_{HF2} = 0.71) was satisfactory (Persson et al., 1999); and the short circuit indicator (θ_{HF2}) was 0.66.

4.3.2 Hydraulic conductivity under saturated condition

K_s values based on the application of the FH method observed with both permeameters at points A, B, and C were alike (Table 4.3) as well as being very similar to those reported by Licciardello et al. (2019) for the unclogged gravel (average = 12,135 ± 1,591 m d^{-1}). Moreover, K_s values were analogous to those observed during the sampling campaign carried out in 2018 (Licciardello et al., 2019).

Table 4.3 - K_s average ± standard deviation (SD, n = 4 per sampling point) values at each sampling point (A, B, and C) measured using the FH method with both IMP and P permeameters in HF1 and HF2 units.

Sampling points	IMP-permeameter		P-permeameter	
	HF1	HF2	HF1	HF2
	K_s (m·d^{-1}) ±SD	K_s (m·d^{-1}) ±SD	K_s (m·d^{-1}) ±SD	K_s (m·d^{-1}) ±SD
A	12,783 ± 1,948	12,324 ± 1,876	12,603 ± 1,679	12,566 ± 1,034
B	13,184 ± 1,610	13,215 ± 1,446	12,215 ± 1,567	12,326 ± 1,081
C	11,806 ± 694	12,003 ± 751	12,122 ± 2,299	12,122 ± 1,152

4.3.3 Drainage tests

The drainage tests reported in Table 4.4 were carried out five times in both of HF units. The K_s values giving the best fit between identified and the simulated cumulative outflows are also reported in Table 4.4. The average K_s values were 11,714 ± 428 m d^{-1} and 11,677 ± 1,067 m d^{-1} for HF1 and HF2, respectively.

Table 4.4 - Simulated K_s values giving the best fit between observed and modelled cumulative outflows in HF1 and HF2 obtained during drainage tests; measurement timespan (MTS); and differences between observed (V_{obs}) and simulated (V_{sim}) cumulative outflows.

Test	HF1 K_s (m d^{-1})	HF2 K_s (m d^{-1})	HF1 MTS (min)	HF2 MTS (min)	HF1 $V_{obs} - V_{sim}$ (m^3)	HF2 $V_{obs} - V_{sim}$ (m^3)
1	12,261	13,050	74	78	0.04	0.07
2	11,779	12,022	66	67	0.01	0.03
3	11,877	11,523	68	67	0.01	0.03
4	11,098	10,086	61	61	0.02	0.02
5	11,553	11,704	67	63	0.04	0.02

4.3.4 Statistical analysis

The *p-values* obtained by the ANOVA analysis were 0.42 and 0.48 for HF1 and HF2, respectively, indicating that in both cases, there was no significant difference between the average K_s values obtained using FH method (using the IMP-permeameter), the drainage equation, and of the unclogged gravel reported by Licciardello et al. (2019). Moreover, the Kruskal-Wallis test showed that the differences in Ks values (n = 5 for each method) between the HF systems were not statistically significant for either method (p = 0.6 and 0.7 for the FH method and drainage test, respectively

4.4 Discussion

The RTD analysis of both HF systems revealed good hydraulic performance and satisfactory hydraulic efficiency values (λ_{HF1} = 0.71; λ_{HF2} = 0.73) in agreement with the Persson et al. (1999) indicators. Furthermore, for both HF systems, *nRT* and *aRT* values were very similar, suggesting that the hydraulic flow was close to ideal conditions (Kadlec and Wallace, 2009). This likely reflects no or very

slight development of clogging. On the other hand, the short circuit indicator values (θ_{HF1} = 0.69; θ_{HF2} = 0.66) were very similar to that reported by Tang et al. (2017) for filtering units characterized by an inert substrate (in zeolite) with dimensions of $d_{0.1}$ = 0.02 m, and $d_{0.5}$ = 0.03 m) planted with *Canna indica*, which is comparable to systems where clogging has begun to develop. Furthermore, K_s values of both units were very similar to the average value of the unclogged gravel (12,135 ± 1,591 m d^{-1}; p = 0.42 and 0.48 for HF1 and HF2, respectively), indicating that clogging remained in the initial phase. Several reasons might explain the clogging evolution observed in both HF units after 2.5 years of operation, which were characterised by an alternative treatment of SBR influent (for five-month HF of the year) and stormwater runoff (for seven-month HF of the year). During the latter, characterized by very low TSS and organic matter concentrations, HF units have a sort of resting time without solids accumulation that may delay the clogging impact increasing the system lifespan in the Mediterranean environment. Secondly, we observed that most of the TSS present in the influent were trapped in the pond at the initial stages of the TW system, indicating its vital role. Similarly, Ventura et al. (2021) reported an average TSS concentration of 120 mg L^{-1} at the inlet of the pond during SBR effluent feeding (May–September 2017), falling to 69 mg L^{-1} at the outlet of the pond and 37 mg L^{-1} at the outlet of the HF systems. Furthermore, similar TSS removal trends occurred when the stormwater runoff was treated (related to very low concentrations, data are not shown). These observations demonstrate the importance of the sedimentation capacity of ponds. A similar conclusion was also acknowledged by Caselles-Osorio et al. (2007), which established an effective and reliable combination of HF and maturation ponds, especially for TSS and organic matter removal, emphasizing the importance of a primary stage of treatment to avoid fast clogging of granular media due to solids accumulation... A third factor that could explain the limited clogging is that HF systems did not retain about 50% of TSS. This

could be due to the small grain sizes of sediments relative to the coarse grains constituting the filtering media (porosity of 0.4) as reported also by other authors. Kandra et al. (2015) conducting lab experiments with a zeolite substrate (0.02 m average-sized) suggested that these coarse filters may not be effective in trapping fine solids due to the difference between the free pore size and sediments in the influent. It should be noted during the SBR feeding period, the TSS concentrations measured at the outlets of both HF systems were within Italian limits for discharge in waterbodies. Moreover, during the stormwater runoff feeding period, TSS concentrations were also below the more restrictive Italian standard limits for reuse (Licciardello et al., 2018; Ventura et al., 2019b).

4.5 Conclusion

The FH method, RTD analysis, and simple drainage equation were used to evaluate the hydraulic behaviour of pilot-scale HF TWs supplied by stormwater runoff during the rainy season (October–April) and SBR effluent during the dry season (May–September) in the Mediterranean region. K_s measurements were carried out based on two innovative permeameters and a calibrated equation. All the investigations demonstrated that clogging remained in the initial stages of development. In particular, the RTD analysis highlighted the good hydraulic performance of both HF systems. Furthermore, the K_s values obtained after 2.5 years of operation using the FH method and the drainage equation were statistically similar to those obtained during the initial stages of operation under similar conditions (Licciardello et al., 2019). The limited development of clogging in HF systems is likely explained by (1) the stormwater feeding that provided to HF units a resting period without solids accumulation; (2) the presence of a settling pond at the beginning of the TW plant and (3) the difference between the free pore size and sediments in the influent.

The consistency of results obtained with K_s values obtained using these different methods (i.e., at the outlets based on the drainage equation, at various points within the systems based on the FH method, and along the main treatment path based on tracer tests) demonstrates their collective reliability. Based on these observations, the combined application of these approaches can be used in the future to assess the evolution of the clogging phenomenon in HF-TWs.

5. Evaluation of Different Methods to Assess the Hydraulic Behavior in Horizontal Treatment Wetlands[3]

Abstract

While there have been numerous studies on the rate and development of clogging in horizontal subsurface treatment wetlands (HF-TWs) and, consequently, the effects on its hydraulic characteristics, research has not shown a clear understanding of the processes. The existing methods for measuring the impact of clogging provide limited information on the extension and degree of the phenomenon. This study aimed to evaluate the capacity of various measurement techniques to assess the degree and variation in space and time of clogging in HF-TWs. Hydraulic conductivity at saturation (K_s) measurements were conducted using a newly implemented scheme, the drainage equation method, and traditional tracer tests, which were carried out in a full-scale HF-TW system, located in Sicily, Italy, during 2019. After five years of operation, the results highlighted a severe decrease in K_s (<1000 m day^{-1}) in the inlet zone (despite the fact that the filter gravel was replaced in 2017), a very high reduction of K_s along the central path inside the HF unit, a nonuniform flow through the HF-TW, the presence of stagnant zones, and a reduction of the porosity of the HF unit gravel. Nonetheless, the mean values of the physical–chemical and bacteriological parameters at the hybrid treatment wetland (hybrid TW) outlet indicated that the partial clogging had no significant effect on the quality of the discharged water. Moreover, the results obtained using the different measurement

A modified version of this chapter was published as [3]Feliciana Licciardello, Alessandro Sacco, Salvatore Barbagallo, Delia Ventura, and Giuseppe Cirelli (2020) "Evaluation of Different Methods to Assess the Hydraulic Behavior in Horizontal Treatment Wetlands" *Water* 12, no. 8: 2286. https://doi.org/10.3390/w12082286

techniques (in terms of both the K_s values and the flow distribution inside the HF unit) were consistent with each other and with results obtained previously for the same system. Finally, the most efficient combination of methods to assess clogging in HF-TWs was identified.

Keywords: clogging; hydraulic behavior; constructed wetlands; wastewater treatment

5.1 Introduction

The clogging of horizontal subsurface treatment wetlands (HF-TWs) is inevitable and not a new phenomenon. Its development and impacts on the design and operation of these systems must be taken into account to avoid reductions of their lifetime (Knowles et al., 2011; Dotro et al., 2017; Langergraber et al., 2019) Clogging is also a complex phenomenon, because sets of mechanisms act differently during the lifetime of HF-TWs (Kadlec and Wallace, 2009). Cleaning the HF unit media in the inlet zone of TWs (where microbial biomass formation primarily occurs) may be unavoidable and should be regularly scheduled. On the other hand, designers have to take into account that the clean-unit K_s will change significantly once the system is put into operation and that HF-TWs must nonetheless be able to operate efficiently. The K_s value, which is largest at start-up, will decrease with time as plant roots, microbial biofilms, and chemical precipitatesgradually occupy spaces. While there have been numerous studies on the rate and development of clogging and, consequently, on the changes to the hydraulic characteristics of HF-TWs, research has not acquired a clear understanding of the processes (Tang et al., 2020). In addition to techniques that measure the properties of clog matter (elucidating the nature and the degree of clogging (Caselles-Osorio et al., 2007; Pedescoll et al., 2009) tomography (allowing for the production of a 3D image of the distribution of the clogging and its concentration in the filter) (Garcia-

Artigas et al., 2020) all the other approaches are based on the evaluation of HF-TW hydraulic behavior. In particular, one of the main effects of clogging is a reduction of the hydraulic conductivity (K_s) at saturation of the porous media (Stefanakis And Akratos, 2014; Barreto et al., 2015; Al-Isawi et al., 2015). The K_s values at saturation can be obtained by surveying the hydraulic gradients between points in the filter media and then applying Darcy's law (Sanford et al., 1995; Rodgers and Mulqueen, 2006; Suliman et al., 2006). A limitation of this method is that the reliability of the determined K_s values depends on the accuracy of the hydraulic gradients (Sanford et al., 1995). K_s measurements can be made by falling- and constant-head tests, which were specifically developed to detect the potentially high hydraulic conductivity of wetland gravels (Knowles and Davies, 2012; Pedescoll et al., 2011) In particular, the in situ falling-head method, used by Pedescoll et al. (2009) and Garcia-Artigas et al. (2020) to determine the K_s in several HF-TW units, is based on the Naval Facilities Engineering Command Design manual (NAVFAC, 1980). The equation that is used for the determination of K_s depends on the geometry of the cavity (that is, the ratio between the radius R and length L) and, consequently, of the chosen scheme (NAVFAC, 1980; Licciardello et al., 2019). A disadvantage of these methods is that they require numerous point measurements inside the HF unit (to measure the vertical K_s) and also along a vertical profile (to determine the horizontal K_s), if an impervious permeameter is used. The latter limitation was recently overcome by the implementation of a pervious permeameter with a calibrated equation to consider the effect of clog matter on the horizontal direction of flow and also to save time (Licciardello et al., 2019) It should be noted that these methods involve a certain degree of disturbance due to the insertion of the tube into the substrate (Nivala et al., 2012). A synthetic K_s value for HF-TW units can be obtained by simulating the measured outflow through an equation developed in (Sanford et al., 1993) to predict the cumulative drainage volume from aquifers overlying sloping,

impermeable layers. The K_s values obtained using the drainage equation were validated by a comparison with values obtained by Darcy's law in four rock-reed filters filled with different substrates (from 2 to 4 cm in a sand and gravel mixture) and either planted with *Phragmites australis* or unplanted (Sanford et al., 1995). A disadvantage of this method is that the system must be stopped during the experiment, and the stoppage can last up to several days for large HF-TWs. The hydrodynamic visualizations obtained through tracer tests can also allow for the study of the effect of clogging phenomena on the flow in a porous medium, e.g., using sodium chloride (NaCl), rhodamine dye, or potassium bromide (Bowmer et al., 1987; Knowles et al., 2010; Marzo et al., 2018). Tracer tests can be conducted both at the outlet of the system or at various points inside the HF unit to obtain different information. The clogging impacts on the hydraulics of the whole unit can be investigated by monitoring the tracer passage through the outlet (Maloszewsky et al., 2006), while the measurements inside the unit are required in order to identify preferential flow path HF and, eventually, possible causes of clogging (Knowles et al., 2010). While there are different available approaches, numerous research reports indicate that no individual method could quantitatively assess clogging phenomena in HF-TWs (Nivala et al., 2012; Aiello et al., 2016; Marzo et al., 2018). To better monitor the clogging evolution in HF-TWs, different combinations of approaches are suggested. In Aiello et al. (2016) K_s measurements, the quantification of clog matter, and tracer tests (NaCl) are combined for full-scale investigations into HF-TWs. In Marzo et al. (2018) K_s measurements, tracer tests (NaCl), and geophysical techniques are integrated to highlight a progressive increase in clogging in a full-scale HF-TW in Sicily. The latter is a hybrid treatment wetland (hybrid TW) system that functions as a secondary wastewater treatment system of the IKEA® store, located in the industrial district of Catania, Sicily, Italy. Because K_s measurements and tracer tests highlighted a partial clogging in January 2017, a restoration measurement was carried out

in the inlet zone of the HF-TW unit in April 2017. Since there is no single method that can quantitatively measure the clogging in HF-TWs (Nivala et al., 2012) and due to the fact that each has different advantages and disadvantages, it can be useful to identify an approach, or eventually a combination of approaches, that allow for a complete understanding of clogging development in a treatment wetland in the most time-efficient and easily repeatable way. This paper aims (1) to assess the degree and variation in space and time (also by comparison with previous experimental campaigns) of clogging in the HF-TW system functioning as a secondary wastewater treatment system of the IKEA® store, and (2) to identify the most efficient way to evaluate the phenomenon in HF-TW systems. In order to reach these objectives, an experimental campaign integrating traditional and innovative methods to assess the hydraulic behavior in HF-TWs was carried out in the HF unit of the hybrid TW system of the IKEA® store, which had already been partially clogged in the past. In particular, traditional tracer tests were compared with K_s measurements in a newly implemented scheme (i.e., by using a pervious permeameter with a calibrated equation) and the drainage equation method. To ensure that the HF-TW conditions were the same, the three methods were carried out consecutively in February 2019; it was not possible to perform them simultaneously due to the characteristics of the individual methods

5.2 Materials and Methods

5.2.1 Full-Scale HF-TWs Characterization

The selected HF-TW was chosen as a case study to assess clogging using various measurement techniques. The HF-TW system is part of the hybrid TW system that functions as a secondary wastewater treatment system for the IKEA® store, located in the industrial district of Catania, Italy (37◦26054.2” N 15◦02005.2” E, 11 m a.s.l., Figure 5.1). The area is semiarid and characterized by average annual precipitation of about 760 mm. The values for temperature and

humidity were in the range of 1.6–40 ◦C and 8–100%, respectively, in 2018. The average monthly precipitation was 55 mm during January and February 2019. No rains occurred in the days during which the measurements were made or on the three previous days. The treatment plant includes a screening unit and a SBR. The SBR was designed for treating wastewater produced by toilets and the food area of the store, with a maximum flow rate of 30 m^3 day^{-1} (two batch phases every 12 h) and TN load of 135 mg L^{-1} . The IKEA® store and the Department of Agriculture, Food, and Environment of the University of Catania have been in charge of running and monitoring the HF-TW, respectively, from the time of the installation. Because of the high fluctuations of the flow and TN (Marzo et al., 2018), a hybrid TW was integrated with the SBR in 2014. The TW includes three in-series connected units: HF-TW, which allows for a reduction of organic matter and suspended solid (SS) concentrations, followed by two vertical subsurface flow (VF1-TW, VF2-TW), which are designed to remove the wastewater organic matter, SS, and to further nitrify ammonia to nitrate. The HF-TW unit has a surface area of about 400 m^2 (12 × 34 m), and is filled with 0.8–1.5 × 10^{-2} m of volcanic gravel to a depth of 0.60 m. The porosity and Ks values of the original clean gravel were 0.41 and 19,466 m day^{-1} , respectively (Licciardello et al., 2016). The HF-TW, planted with *Phragmites australis*, is fed discontinuously with a daily effluent from the SBR plus effluent from the screening unit, which does not include the SBR, when the wastewater produced in the IKEA® store exceeds a flow rate of 2.5 $m^3 h^{-1}$. Based on the total wastewater produced by IKEA, the annual volume of untreated wastewater feeding the HF-TW was, on average, around 30% of the total volume, while during weekends and holidays, the daily volume of untreated WW was up to 50% of the total daily volume amount. Due to the high volumes of WW produced at the IKEA® store at the end of 2016, the SBR was often bypassed, and a high organic load entered the hybrid TW system. Thus, it was already necessary to remove and replace the filter gravel close to the inlet area

after three years of operation (in April 2017). A CR-1000 automatic weather station (Campbell Scientific, Logan, UT, USA) was installed close to the experimental plant to measure the temperature, wind speed and direction, rainfall, global radiation, and relative humidity. The vegetation harvest was carried out every year (at the end of January or at the beginning of February). During the investigation campaign, the vegetation groundcover was about 85%. In particular, the plant density was low in the area close to the inlet and, in some regions, randomly distributed along the middle path. For more details on the hybrid TW, see (Marzo et al., 2018).

Figure 5.1 - Map of the location area and the hybrid treatment wetland (TW) at the IKEA® store, located in Catania, Sicily, Italy, showing the water flow routes (in blue).

5.2.2 Ks measurements in the full-scale HF-TW unit

The FH method was applied to determine the K_s values in the HF-TW unit in February 2019. In particular, four FH infiltration tests

were performed around each of the nine piezometers located in the HF system (Figure 5.2) at the same depth (see Table 4.1 and 4.2). Two open-ended tubes, one impervious (IMP) and one pervious (P), and the corresponding equations adapted from (NAVFAC, 1980) to various applicability conditions (Table 4.1 and 4.2) were used. In particular, the IMP permeameter (Table 4.1) also known as the Standpipe) allowed us to evaluate the vertical K_s values using Equation (4.8). For isotropic gravels (clean or not clogged), this would not be a problem. However, given that the clogging process is likely not to be isotropic, the vertical K_s values obtained using this method could be different from the horizontal K_s values. Instead, the P permeameter (Table 4.2) allowed us to evaluate both vertical and horizontal K_s, using Equation (4.9), as in Licciardello et al. (2016). Both schemes did not require drilling a borehole, as the pipe was merely pushed directly into the substrate. This saved time, compared to other schemes, and also minimized disturbance to the porous medium. A small hole was dug in the granular medium to reach the water table, and then the permeameter was inserted using a mallet. A plastic water reservoir (6.6 L volume) with measurement units was assembled together with a ball valve to add water in a single-pulse mode, as required. A pressure probe (Sensor Technik Sirnach (STS), AG, Sirnach, Switzerland), connected to a laptop by means of a CR200-R (Campbell Scientific) data logger, was used to measure the variation of the water levels (H) within the measurement unit. A driver was added to the device to allow for the insertion of the pressure probe inside the steel permeameter. The pressure value at atmospheric pressure was checked before each measurement started. Four water level data per second were recorded for a duration of 30 s. The decrease in the water height inside the permeameter was monitored until the water reached the static water table. The best fit between the simulated and measured water levels was obtained by summing and minimizing the squared differences between the theoretical curve and that obtained in the field, following Equation (4.10). This condition

allowed us to estimate the value of K_s using an iterative, nonlinear procedure that makes use of the Excel Solver spreadsheet plug-in (Frontline Systems, Incline Village, NV, USA)

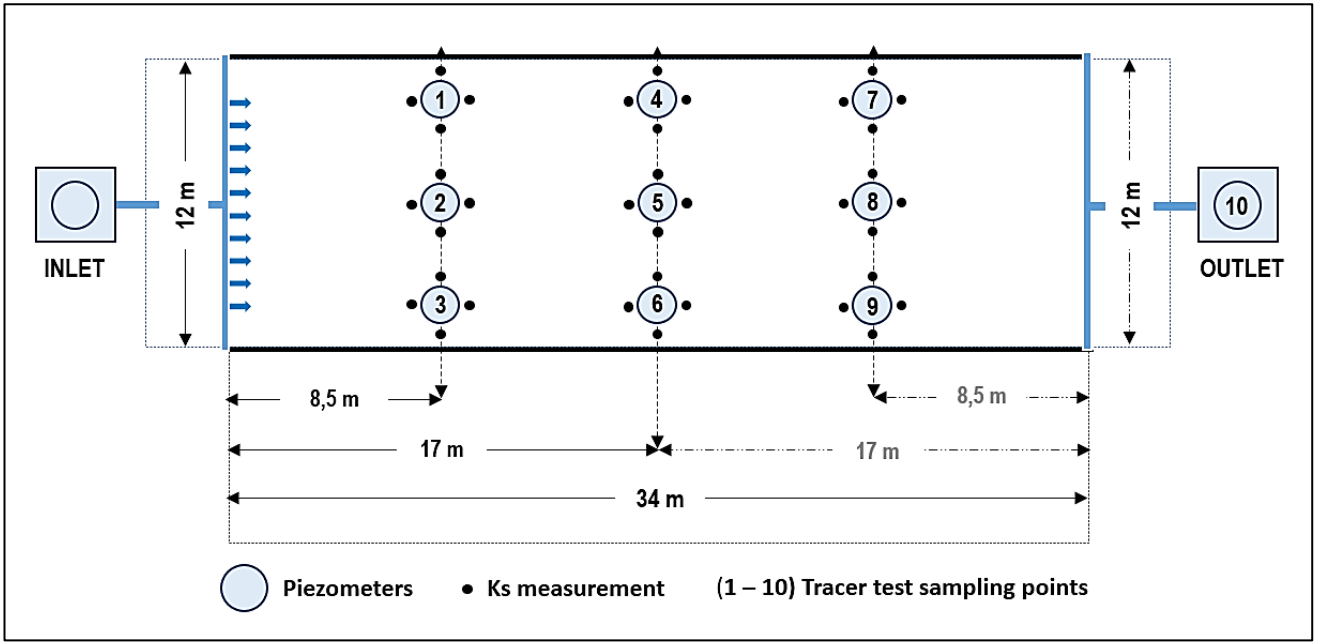

Figure 5.2 - Layout of the horizontal subsurface treatment wetlands (HF-TW) unit of the secondary wastewater treatment system of the IKEA® store, located in Catania (Sicily, Italy), showing the location of piezometers, saturated hydraulic conductivity (K_s) measurements and tracer test sampling point

The drainage equation (Eq. 4.11) proposed in Sanford et al. (1993) and applied to HF-TWs in (Sanford et al. (1995) was used to find a synthetic K_s for the whole HF-TW unit. The K_s (m min^{-1}) is the only unknown term in the above equation, when applied to the drainage experiments. Measured cumulative drainage volume data were obtained first by closing the inflow and outflow valves to produce a horizontal water table and then by opening the outlet valve and collecting the drainage volume in a tank. The inflow valve remained closed for the whole duration of the test. The variation of the water levels within the tank was measured by the pressure probe positioned in the tank and connected to a laptop, as described above. The water level data, recorded inside the tank every 5 min, were converted into drainage volumes. The drainage experiment was carried out once in February 2019. A range of conductivity values were applied to Equation (4.11), until the resulting outflow curve matched the measured outflow. The value of K_s that produced the closest fit and gave the simulated cumulated outflow closest to the measured one was taken as the hydraulic conductivity of the substrate for the particular drainage test.

5.2.3 Tracer Tests

A tracer test was conducted in February 2019 by introducing an impulse of NaCl into the HF-TW inlet at time zero. NaCl was chosen for its efficiency and low-cost characteristics, but also because it is not organic, and it was already successfully used in the same system (Marzo et al., 2018). The amount of tracer (32 kg 100 L^{-1} for a total volume of 200 L and a pulse duration of about 10 min) was chosen in order to reach an average benchmark concentration at least ten times that of the background concentration, as suggested in Keller and Bays (2000). The measured EC (µS cm^{-1}) values, after subtraction of the background value (between 1600 and 1800 µS cm^{-1}), were then converted into NaCl concentrations (mg L^{-1}) by a linear calibration

curve ($R^2 = 0.99$). The pumping discharge of the solution was the same as the normal water flow in the HF-TW system. The solution was prepared in a bucket, in which the tracer was added and mixed until a uniform concentration was reached. A pulse-inject of the tracer solution was then added with a pump into the inlet zone of the HF-TW system. The fluid electric conductivity (EC) was measured by ten conductivity probes (delta OHM–HD 2106.2, DeltaOhm, Padova, Italy). One of them was located at the outlet, and the others were located inside the nine piezometers in the HF-TW unit. The EC data were recorded by each probe every 15 min. The HF-TW outflow volumes were measured using a flow measurement device for the whole test. No rain occurred during the test. The NaCl injection into the HF-TW inlet provided information about the efficiency and detention times in the system. In fact, in ideal flow patterns, the water particles move at the same velocity, reaching the outlet together. In this case, a tracer impulse would also exit as an impulse (a sharp spike of concentration). It is clear from numerous studies that TWs are neither plug flow nor well mixed, and due to preferential flow channels, vertical stratification occurs in gravel systems, with more significant flows arising at lower levels in the system (Fisher P.J., 1990; Marsteiner, E.L., 1997; Drizo et al., 2000). Thus, also in the present case, the response to the impulse tracer input was a time-delayed, bell-shaped curve, called the retention time distribution (RTD). Thus, the analysis of this curve allowed for the derivation of critical parameters characterizing the hydraulic behavior of the system. First, it was necessary to evaluate the validity of the test, checking that the tracer was recovered nearly in its entirety at the wetland outlet. To achieve this, the relative tracer mass recovery (%) was calculated as Eq. 4.5. Then, the RTD, which represents the various time fractions of the water spent in the reactor and hence the contact time distribution for the system was analyzed. In general, the RTD is the probability density function for the residence times in a wetland. For an impulse input of a tracer into a steadily flowing system, the

time function is defined by Eq. 4.5. Then, RTD, which represents the various time fractions of the water spent in the reactor and hence the contact time distribution for the system was analyzed. In general, the RTD is the probability density function for the residence times in a wetland. For an impulse input of a tracer into a steadily flowing system, the time function is defined by:

$$E(t) = \frac{Q \cdot C(t)dt}{\int_0^\infty Q \cdot C(t)dt} \qquad \text{(Eq.5.1)}$$

The first numerator is the mass flow of the tracer in the wetland effluent at any time t, after the time of the impulse addition. The first denominator is the sum of all the tracers collected and should thus equal the total mass of the injected tracer. Thus, the actual residence time (*aRT*) is presumed to be the actual mean detention time and can be calculated as the first moment of the curve (the centroid of the C-curve) as Eq. 4.2. A wetland may have internal excluded zones that do not interact with the flow (Kadlec and Wallace, 2008) such as the volume occupied by biomass (roots, rhizomes, etc.). In a steady-state system without excluded zones, the *aRT* equals *nRT*, which is defined as Eq. 4.1. Following Whitmer et al. (2000) a parameter for evaluating the hydraulic efficiency of the system can be simply defined as Eq. 4.6. This measure has the advantage of being readily derived from the RTD, and it does not have the problem related to the calculation of *aRT* (Whitmer et al., 2000). The λ can be considered good if $\lambda > 0.75$; it is satisfactory if $0.5 < \lambda < 0.75$; and it is poor if $\lambda \leq 0.50$. A second parameter that can be determined directly from the RTD is the σ^2 or the square of the standard deviation (Eq. 4.3).

5.2.4 Wastewater quality characterization

Wastewater quality was monitored one/two times per month, from April 2016 to February 2019. The sampling points were located

at the hybrid TW inlet and at the three outlets of each TW unit (HF-TW, VF1-TW, and VF2-TW). Standard methods (APHA, 2005) were applied for WW quality analysis, which included TSS (mg L^{-1}) at 105 ◦C, BOD_5 (mg L^{-1}), COD (mg L^{-1}), PO_4 (mg L^{-1}), ammonia nitrogen (N-NH3, mg L^{-1}), TN (mg L^{-1}), nitrate nitrogen (N-NO3, mg L^{-1}), and *Escherichia coli* (*E. coli*, CFU 100 mL^{-1}). In order to characterize the HF-TW influent, the following parameters were calculated (Dotro et al., 2017). The maximum OLR (g BOD_5 m^{-2} day^{-1}) is defined as:

$$OLR = \frac{BOD_5}{A} \quad \text{(Eq.5.2)}$$

The HLR (mm day^{-1}) is defined as:

$$HLR = \frac{Q}{A} \quad \text{(Eq.5.3)}$$

The total suspended solids rate (TSSLR) (g TSS m^{-2} day^{-1}) is defined as:

$$TSSLR = \frac{TSS}{A} \quad \text{(Eq.5.4)}$$

Where: Q (m^3 day^{-1}) is the water inflow rate through the system; TSS (g day^{-1}) is the amount of TSS, based on the water inflow rate through the system; BOD5 (g day^{-1}) is the amount of BOD_5 based on the water inflow rate through the system; and A ($m^{2)}$ is the wetland surface area.

5.3 Results

5.3.1 K_s Measurements in the Full-Scale HF-TW

Table 5.2 and Figure 5.3 report the K_s mean values (indicated as K_s values below) around each of the nine piezometers inside the HF-TW unit and their standard deviation (±SD) observed in 2019 and

in the previous campaign (Licciardello et al., 2019). The K_s values measured in piezometer 1, 2, and 3, located in the first transect close to the inlet, were the lowest. A very low K_s value was also observed in piezometer 8 (Table 5.1 and 5.2). Consequently, in 2019 the lowest values of K_s were observed in the inlet transect (660 m day^{-1}, see Table 5.2) and along the middle path (3682 m day^{-1}, see Table 5.3). The K_s values found along the transects located in the middle part of the unit and close to the outlet were similar (Table 5.2).

5.3.2. Drainage Experiment

After the opening of the outlet valve, the outflow of the HF-TW, measurements were recorded every 5 min and ended after 1250 min. The K_s value that gave the best fit between the observed and simulated cumulative outflows was 3880 m day^{-1}, see Figure 5.4). The difference between the observed and simulated cumulative flows was 0.1 m^3. Figure 5.4 shows the observed and simulated cumulative outflow curves during the drainage experiment. Table 5.1. Spatial and temporal variation of the K_s (m day^{-1}) values for the nine piezometers inside the HF-TW unit in 2018 (Licciardello et al., 2019) and 2019.

Table 5.1 - Spatial and temporal variation of the K_s (m day^{-1}) values and relative standard deviation (SD) for the nine piezometers inside the HF-TW unit in 2018 (Licciardello et al., 2019) and 2019

		2018		2019		Reductions of K_s (%)		
Piezometers	**Distance from the Inlet**	**K_s**	**±SD**	**K_s**	**±SD**	**Relative to clean gravel[4]**		**In 2019 relative to 2018**
	m	**m·d^{-1}**		**m·d^{-1}**		**2018 (m·d^{-1})**	**2019 (m·d^{-1})**	**m·d^{-1}**
1	8.5	3072	±614	420	±420	84	98	86
4	17	6500	±2397	5008	±1505	67	74	23
7	25.5	7310	±584	7258	±584	62	63	1
2	8.5	4545	±961	225	±961	77	99	95
5	17	10217	±2937	7049	±2937	48	64	31
8	25.5	5301	±715	3770	±715	73	81	29
3	8.5	2045	±574	1335	±574	89	93	35
6	17	8449	±793	7468	±517	57	62	12
9	25.5	6309	±470	7285	±1223	68	63	15

[4] Note: K_s, hydraulic conductivity at saturation; SD standard deviation. 1 K_s = 19,466 m day^{-1}.

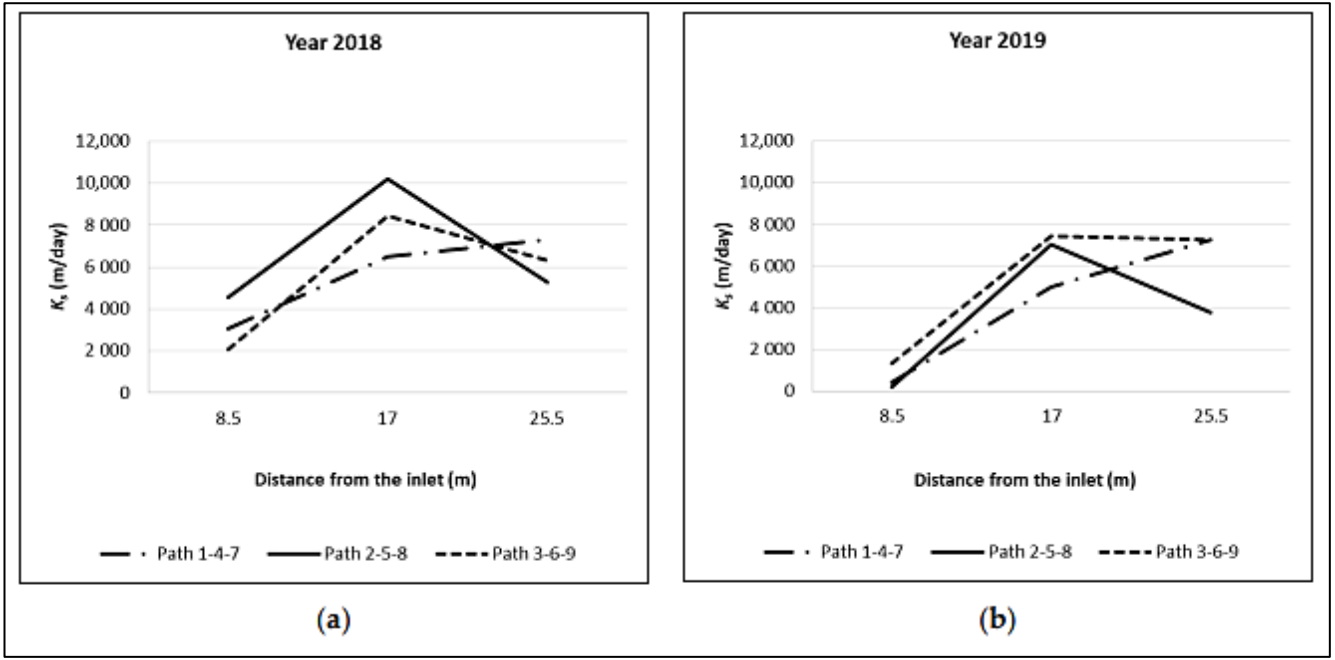

Figure 5.3 - Mean of hydraulic conductivity at saturation (K_s, m day^{-1}) values ($n=4$) for the nine piezometers inside the HF-TW unit (**a**) in 2018 (Licciardello et al., 2019) and 2019 (**b**).

Table 5.2 - Spatial and temporal variation of the K_s (m day^{-1}) values along the HF transects in 2018 (Licciardello et al., 2019) and 2019.

	K_s (m day^{-1})		Reductions of K_s (%)		
HF Transect	**2018**	**2019**	**Relative to clean gravel[4] (m day^{-1})**		**In 2019 relative to 2018 (m day^{-1})**
			2018	**2019**	
1-2-3	3221	660	83.5	96.7	79.5
4-5-6	8388	6508	59.6	66.6	22.4
7-8-9	6307	6104	67.6	68.6	3.2

Table 5.3 - Spatial and temporal variation of the K_s (m day^{-1}) values along the HF paths in 2018 (Licciardello et al., 2019) and 2019.

	K_s (m day^{-1})		Reductions of K_s (%)		
HF Path	**2018**	**2019**	**Relative to clean gravel[4] (m day^{-1})**		**In 2019 relative to 2018 (m day^{-1})**
			2018	**2019**	
1-4-7	5627	4229	71.1	78.3	24.8
2-5-8	6687	3681	65.6	81.1	45
3-6-9	5601	5363	71.2	72.4	4.2

5.3.3 Tracer Tests

The NaCl concentrations obtained at the outlet of the HF-TW during the tracer test experiment are shown in Figure 5.5. The overall percentage of tracer recovery was 94.5%, after a duration of 195 h. The high percentage of tracer recovery indicated that NaCl was marginally affected by the clogging matter. The mean residence time calculated using the moment analysis method was 88 h (with σ^2 = 46 h). During the tracer test, the average flow rate was 1.22 m^3 h^{-1}, corresponding to *nRT* of 78.4 h (based on an average depth of 0.60 m and a constant porosity of 0.4). The maximum NaCl concentration occurred at the outlet after 62.25 h from the beginning of the test (Figure 5.5), so λ was equal to 0.80. The maximum values of EC along the central path of the HF-TW unit were recorded after 11, 23, and 43 h at piezometer 2,5 and 8 respectively (Figure 5.6).

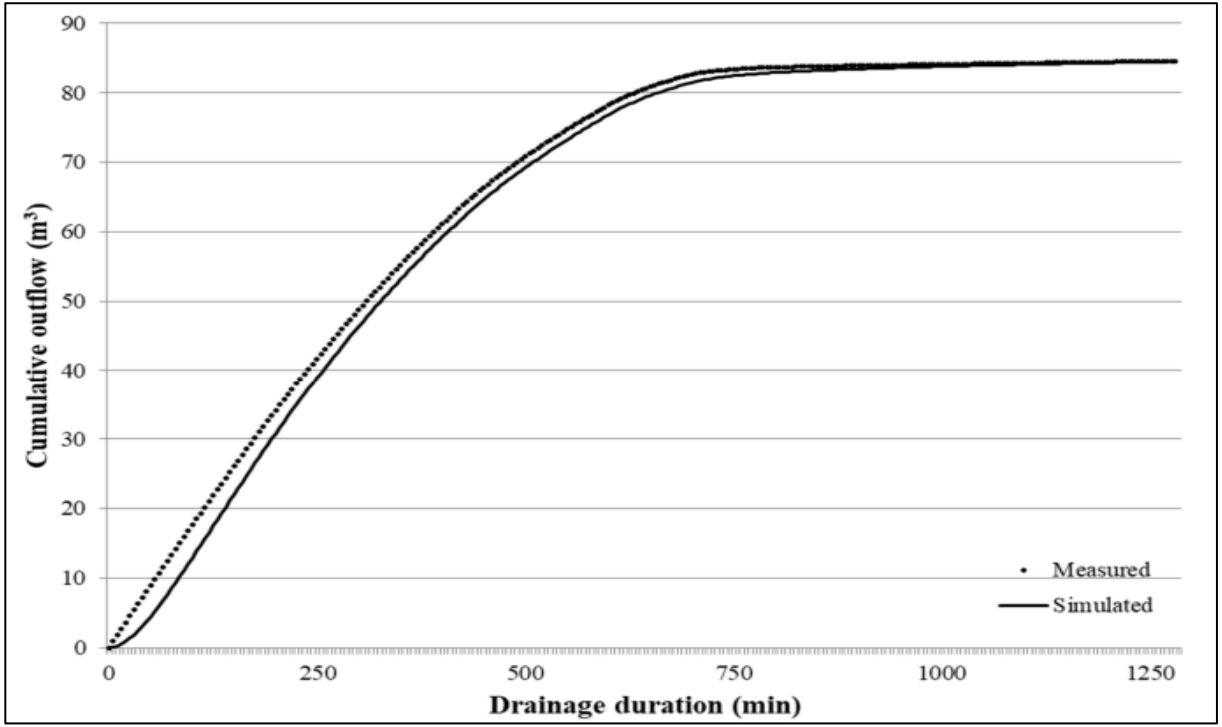

Figure 5.4 - Observed and simulated cumulative outflow curves during the drainage experiment.

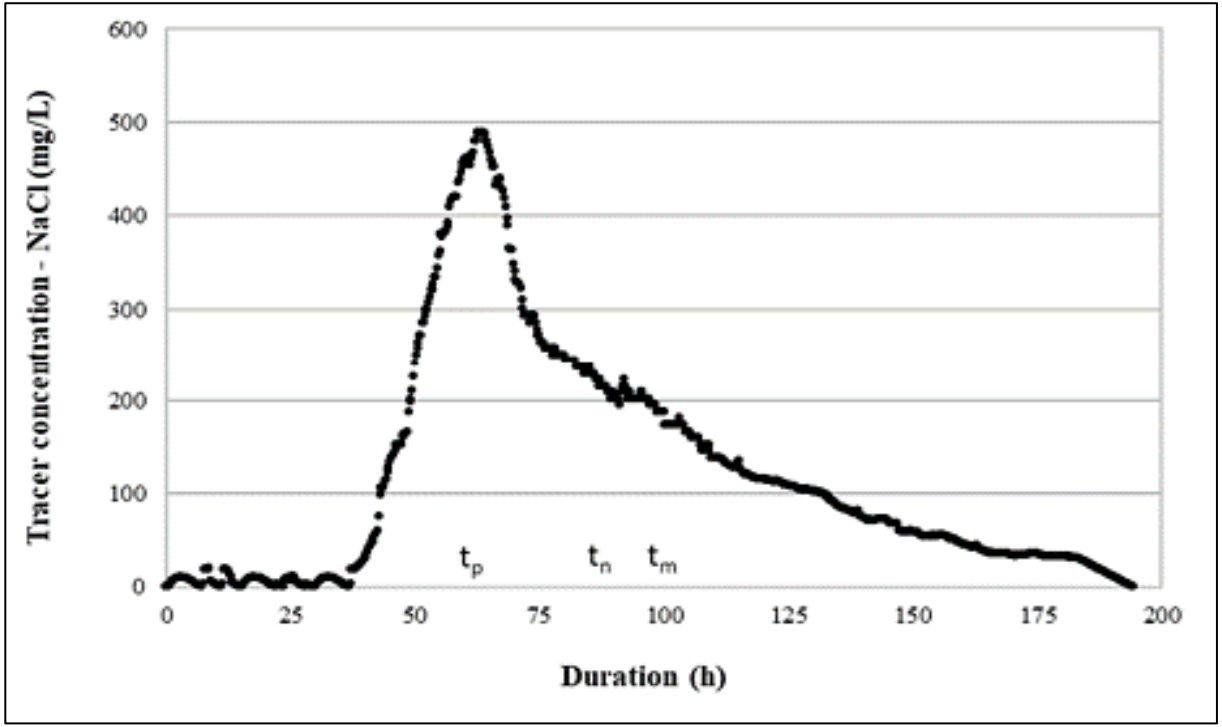

Figure 5.5 - Tracer (NaCl) concentration at the HF-TW outlet during the tracer test experiment.

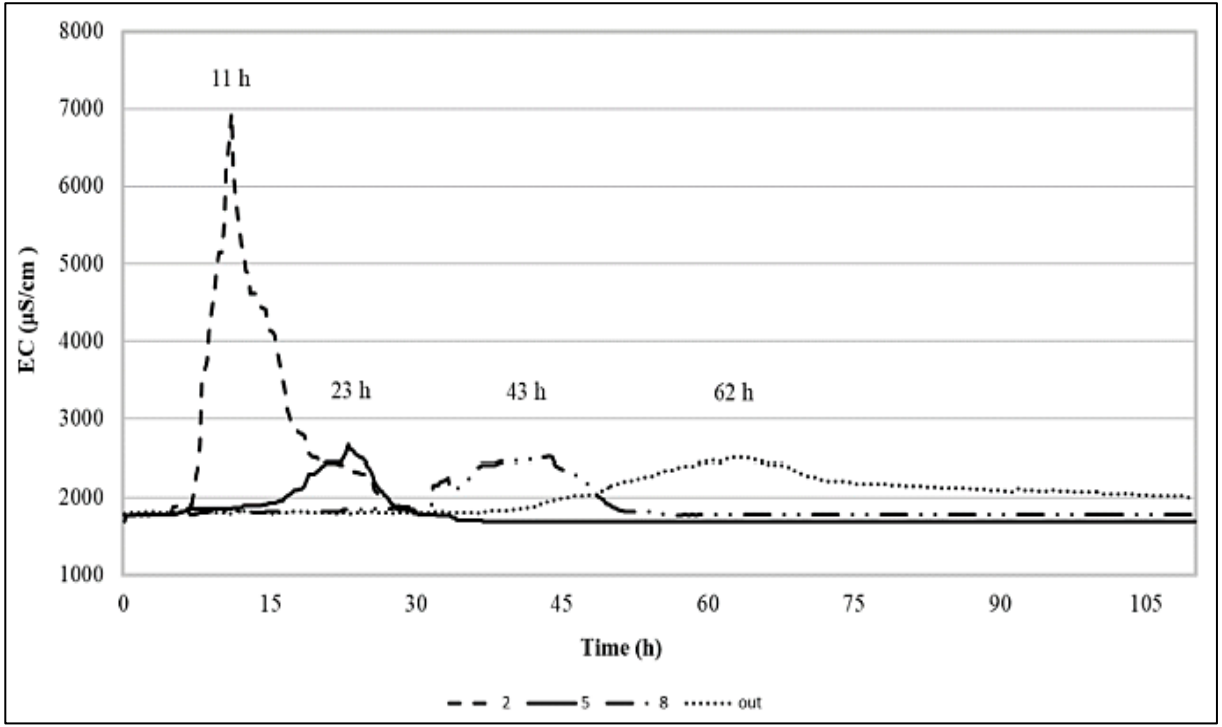

Figure 5.6 - Electrical conductivity (EC) variation (µS cm^{-1}) along the central path of the HF-TW unit (2-5-8) and at the outlet

5.3.4 Wastewater Quality Characterization

Table 5.4 shows the mean values of the physical–chemical parameters (and their standard deviations) evaluated by 26–38 samples for each parameter in different sections of the hybrid TW system from April 2016 to February 2019. The limits imposed by Italian regulations for wastewater discharge into water bodies are also shown (Table 3, annex 5, III part of the Italian Legislative Decree 152, 2006). A high variability of pollutant concentrations at the inlet of the hybrid TW evaluated by 26-38 samples for each parameter collected during the period from April 2016 to February 2019 (Table 5.4) confirmed that a large number of customers visit the IKEA® store during weekends and holidays. In particular, on these busy days, the hybrid TW often received wastewaters directly from the screening unit (up by 40–50% from the total daily HF-TW influent) and therefore had a lower quality. The hybrid TW units provided a very high mean efficient reduction of TSS, COD, and BOD_5 especially in the HF-TW, thus reducing the clogging problem in VF1-TWs and VF2-TWs and allowing for the limits fixed by the Italian law to be respected. The TN reduction was very high, confirming that both processes (nitrification and denitrification) were efficient. Moreover, because of the effluent recirculation to primary treatment, the nitrate at the hybrid TW outlet was lower than the Italian discharge threshold. Instead, the mean TP concentration was higher than the limit, which is probably due to the filter medium composition. A very significant mean reduction of E. coli was found at the hybrid TW (3 log unit). The mean annual values (and their standard deviations) for OLR, HLR, and TSSLR evaluated at the inlet of the HF-TW are reported in Table 5.5. The mean annual water flow rate varied from 24 to 32 m3 day^{-1}, with TSSLR, HLR, and OLR values in the range of those suggested for correct HF-TW design (Dotro et al., 2017). TSSLR and HLR increased from 2016 to 2018

5.4 Discussion

To better understand the hydraulic behavior of the HF-TW, K_s measurements were conducted in February 2019 using the newly implemented scheme (a pervious permeameter and calibrated equation) and were compared with data obtained in April 2018 (Licciardello et al., 2019) and with data obtained for clean gravel (K_s = 19,466 m day^{-1}, see Table 5.1). It is important to highlight that the WW characteristics (flow and quality), vegetation, and the main features of the K_s experimental campaigns of 2018 and 2019 were very similar. As expected, the spatial evolution of the clogging since the beginning of the operation period (2014) and during the observation period (2018–2019) was not uniform within the HF-TW unit. It was more severe in the area close to the inlet (Knowles and Davies, 2009; Pedescoll et al., 2012; Vymazal et al., 2018), and along the central path. Considering the temporal evolution of the phenomenon, very high reductions of K_s values (up to 89%) were already observed in 2018 after four years of operation for clean gravel. These reductions were generally more robust in 2019 (up to 99%) for the nine piezometers (Table 5.1). Only the Ks value for piezometer 9 did not increase in 2019 (K_s = 7285 m day^{-1}). Regardless, the variation in the year 2018 (976 m day^{-1}) was lower than that of the SD observed in 2019 (±1223 m day^{-1}). The lowest K_s value found in the inlet transect was also in 2018 (3221 m day^{-1}), but a very high reduction occurred in 2019 (Table 5.2). The K_s values along the central path 2-5-8 observed in 2019 were lower than those noted in 2018 (Table 5.3). The K_s values that occurred along the lateral paths in 2018 and 2019 were similar (Table 5.3). The slight K_s reduction found in the outlet zone in 2018 was also confirmed in 2019. The values of K_s that varied from a minimum of 225.8 m day^{-1} (±125.2) to a maximum of 7468.3 m day^{-1} (±517.1) at piezometer 2 and 6, respectively, in 2019, were in the range of those found by other authors for HF-TW gravels of a similar size and porosity (Knowles and Davies, 2009; Nivala et al., 2012).

Some studies (Caselles-Osorio et al., 2007; Pedescoll et al., 2009) reported lower K_s values (maximum values at the outlet area: 810 m day^{-1}) using the falling-head method with a pervious permeameter. Moreover, recent studies confirm the difficulty of measuring the hydraulic conductivity in HF-TWs (Knowles and Davies, 2000; Knowles et al., 2010; Matos et al., 2017), especially when the clogging is in the beginning phase and the growing vegetation makes the substrate non-isotropic. Notwithstanding the information acquired from punctual K_s measurements at nine points inside the HF-TW, it was difficult to evaluate the K_s value of the entire system, which cannot simply be the arithmetic mean, which, in this case, is 4425 m day^{-1}. Thus, for this evaluation, the drainage method proposed in Sanford W.E (1993) was used. The K_s value corresponding to 3880 m day^{-1} found for the HF-TW unit was similar to the arithmetic mean value of the K_s measurements obtained inside the unit. The K_s value was obtained after a calibration of Equation (4.11). The HF-TW was put out of service for the duration of the test (1250 min in this case). A K_s value of 3456 m day^{-1} was found in Sanford et al. (1995) study by applying the drainage equation method in a pea gravel unit with a thickness of 0.5×10^{-2} m, after a 2-year operation period. The drainage method also allowed for the evaluation of the porosity reduction of the gravel. In particular, the observed cumulative outflow revealed a porosity variation of the HF-TW gravel (with a size in the range from 0.8×10^{-2} to 1.5×10^{-2} m) from 0.41 to 0.28, which supports the reduction of the available water volume in the unit due to the clogging. A similar porosity reduction in HF-TW was observed in Sanford et al. (1995) study. In particular, a variation from 0.33 to 0.27 and 0.36 to 0.33 was found for pea gravel (with a size of 0.5×10^{-2} m) and coarse gravel (with a size in the range of 2×10^{-2} to 4×10^{-2} m), respectively, after a 2-year operation period

Table 5.4 - Mean values of the physical–chemical (mg L^{-1}) and bacteriological (CFU 100 mL^{-1}) parameters at the HF treatment wetland (TW) system inlet and outlet and at the hybrid -TW outlet during the operation period, April 2016–February 2019.

	Mean values (±SD) April 2016–February 2019			Italian WW discharge limits	N total samples	N samples lower than limits
	HF-TW Inlet	**HF-TW Outlet**	**Hybrid-TW Outlet**			
TSS	48.6 (±42.4)	13.3 (±9.0)	7.0 (±5.8)	80	34	34
BOD_5	106.1 (±104.9)	19.5 (±28.4)	15.8 (±26.6)	40	37	36
COD	209.4 (±203.5)	41.3 (±54.9)	29.8 (±47.9)	160	37	36
TN	79.5 (±26.2)	40.6 (±20.8)	27.6 (±11.3)	-	31	-
$N\text{-}NH_3^+$	17.6 (±21.3)	8.1 (±13.6)	0.7 (±1.4)	15[b]	38	38
$N\text{-}NO_3^-$	45.6 (±18.5)	14.5 (±16.2)	18.3 (±11.4)	20[b]	37	19
TP	14.6 (±7.8)	13.5 (±9.6)	11.2 (±7.4)	10	26	16
Escherichia coli	$7.1 \cdot 10^5$ ($\pm 1.1 \cdot 10^6$)	$1.3 \cdot 10^4$ ($\pm 3.7 \cdot 10^4$)	$6.6 \cdot 10$ ($\pm 1.1 \cdot 10^2$)	$5 \cdot 10^3$	26	26

Note: TSS, total suspended solids (mg L^{-1}); BOD_5, biological oxygen demand after five days (mg L^{-1}); COD, chemical oxygen demand (mg L^{-1}); PO_4, phosphate (mg L^{-1}); TN, total nitrogen (mg L^{-1}); $N\text{-}NH_3$, ammonia nitrogen (mg L^{-1}); $N\text{-}NO_3$, nitrate nitrogen (mg L^{-1}); *Escherichia coli* (CFU 100 mL^{-1}); ±SD, standard deviation. [a] Legislative Decree 152, 2006. Decreto Legislativo 3 Aprile 2006, n.152, "Norme in Materia Ambientale"; [b] Limit for discharge into surface water bodies.

Table 5.5. Mean annual values and relative standard deviation (±SD) of the water inflow rate (Q, m^3 day^{-1}), total suspended solids rate (TSSLR, g TSS m^{-2} ·day^{-1}), hydraulic loading rate (HLR, mm day^{-1}), and maximum areal organic loading rate (OLR, g BOD_5 m^{-2} day^{-1}) of the HF-TW unit during the period, 2016–2018. The values are based on the inflow rate through the system.

Mean Annual Values (Standard Deviations, ±SD)						
	2016		2017		2018	
Q	23.86	(±19.8)	31.5	(±19.1)	32.06	(±17.6)
TSSLR	4.6	(±2.9)	4.8	(±3.4)	6.5	(±3.1)
HLR	59.6	(±19.8)	79.0	(±19.1)	80.1	(±17.6)
OLR	11.8	(±6.9)	8.3	(±5.4)	13.3	(±5.6)

Note: Q, water inflow rate; TSSLR, total suspended solids rate; HLR, hydraulic loading rate; OLR, maximum areal organic loading rate, ±SD, standard deviation

As expected, the spatial evolution of clogging since the beginning of the operation period (2014) and during the observation period (2018–2019) was not uniform inside the HF-TW unit, and was more severe in the area close to the inlet (Knowles and Davies, 2009; Pedescoll et al., 2012; Vymazal J., 2018) and along the central path. Considering the temporal evolution of the phenomenon, very high reductions of the K_s values were observed already after four years of operation in 2018 (up to 89%) for clean gravel. These reductions were generally more robust in 2019 (up to 99%) for the nine piezometers (Table 5.1). Only the K_s value for piezometer 9 did not increase in 2019 (Ks = 7285 m day^{-1}). Regardless, the variation for the year 2018 (976 m day^{-1}) was lower than that of the SD observed in 2019 (±1223 m day^{-1}). The lowest K_s value found in the inlet transect was also in 2018 (3221 m day^{-1}), but a very high reduction occurred in 2019 (Table 5.2). The K_s values along the central path 2-5-8 observed in 2019 were lower than those noted in 2018 (Table 5.3). The K_s values that occurred along the lateral paths in 2018 and in 2019 were similar (Table 5.3). The slight K_s reduction found in the outlet zone during 2018 was confirmed in 2019. The values of K_s that varied from a minimum of 225.8 (±125.2) to a maximum of 7468.3 m day^{-1} (±517.1) at piezometer 2 and 6, respectively, in 2019 were in the range of those found in other research for HF-TW gravels of a similar size and porosity (Knowles and Davies, 2009; Nivala et al., 2012. Some studies (Caselles-Osorio et al., 2007; Pedescoll et al., 2009) reported lower K_s values (maximum values at the outlet area: 810 m day^{-1}) using the falling-head method with a pervious permeameter. Moreover, recent studies confirm the difficulty of measuring the hydraulic conductivity in HF-TWs (Knowles and Davies, 2000; Knowles et al., 2010; Matos et al., 2017), especially when clogging is in the beginning phase and the growing vegetation makes the substrate non isotropic. Several authors reported that a comparison of tracer tests performed during different periods is essential for understanding the spatial and temporal evolutions of clogging. Therefore, the results of the tracer test carried out in 2019

were analyzed in relation to those acquired for the same HF-TW system in the past (Marzo et al., 2018), along with the results of the K_s and drainage experiments carried out in 2019. The integrity of the tracer test results was guaranteed by the duration of the test, which lasted for 195 h in 2019 and is twice the *nRT* (Bodin et al., 2013). The *aRT* was higher than the *nRT* of about nine hours, thus confirming the presence of dead or stagnant zones (Chazarenc et al., 2003) and indicating that the flow may not include the entire volume of the HF-TW unit (Kadlec and Wallace, 2008; Seeger et al., 2013). In any case, the hydraulic efficiency observed in 2019 was good (λ = 0.80), following (Whitmer et al., 2000). The passage of the tracer monitored at the outlet revealed a uniform RTD, with a single peak of the NaCl concentration of about 480 mg L^{-1} occurring after 62.25 h from the beginning of the test, probably indicating a preferential path through the wetland [19]. Based on the K_s measurement results, the preferential path should be the central one (2-5-8), because the highest reductions of K_s were measured during the observation period. The preferential path inside the HF-TW unit seems to be also confirmed by the results of the tracer tests carried out in Marzo et al. (2018). The EC (mS cm^{-1}) values were higher along the central path than along the lateral paths during both tracer tests carried out in February and May 2017 (Marzo et al., 2018). Moreover, the EC maximum values observed at piezometers 2 and 5 in the present study (6950 and 2545 mS cm^{-1}, respectively) were lower (and the peak time was delayed) than those achieved in Marzo et al. (2018) before the restoration measurement in the inlet zone and higher (and the peak time was accelerated) than those observed after the restoration measurement. These differences can be explained by the fact that the clogging in the HF-TW unit is currently in an intermediate situation, in comparison to those reported in Marzo et al. (2018), indicating that it will soon require a restoration measure (i.e., removal and replacement of the filter gravel close to the inlet area). Thus, our findings support the idea that a comparison with previous tracer tests in the same system is fundamental for correctly

interpreting spatial and, obviously, temporal hydraulic changes in HF-TWs, as emphasized by several authors (Nivala et al., 2012). In Bowmer K.H. (1987), it was found that in an HF-TW unit, an area which exhibited a substantial preferential flow path had become a large dead zone after a 2-year operation period. Another important finding of the present study is that K_s values and the flow distribution obtained using widely applied methods, such us the FH method (with a newly implemented permeameter) and traditional tracer tests, are consistent with each other and with the K_s values obtained by using the drainage equation method proposed in (Sanford et al., 1993). The sensitivity in assessing the clogging phenomenon inside wetlands using different K_s measurements inside the unit and path flows (obtained by tracer tests) was already highlighted in several studies (Nivala et al., 2012; Marzo et al., 2018). The use of a drainage equation method that can provide an estimate of the hydraulic behavior of an entire system by determining a single value of K_s can further help in the analysis of the complex hydrology of HF-TW units. Unfortunately, in the latter case, it is necessary to put the HF-TW out of service. This limits the feasibility of the test for large HF-TWs. Moreover, considering the qualitative aspects of WW, the hybrid TW (SBR and TW) treating up to 50 m3 day−1 water flow and characterized by the TSSLR, HLR, and OLR design parameters, as suggested in the literature on HF-TWs, was able to function within Italian law standards, with only partial clogging of the HF-TW unit.

5.5 Conclusion

The clogging of HF-TWs is a complex phenomenon that must be continuously monitored, especially in systems that have already been affected with clogging during their lifetime, in order to apply restorative measurements and prevent negative effects on treatment efficiency. In the HF-TW of the hybrid TW system functioning as a secondary wastewater treatment system of the IKEA® store, it was

already necessary to remove and replace the filter gravel close to the inlet area after three years of operation (in April 2017). The application of traditional and innovative methods to assess the clogging allowed for the quantification of the phenomenon in the HF-TW, as well as the identification of the most time-efficient and easily repeatable way to quantify the phenomenon. First, it must be noted that the K_s measurement (obtained by a newly implemented scheme), tracer test, and drainage equation results were consistent with each other in highlighting a partial clogging in the inlet area of the HF-TW unit of the hybrid TW system after 5 years of operation, despite the fact that the filter gravel was replaced in 2017. The K_s values were very low (< 1000 m ·day^{-1}) in the transect close to the inlet and along the central flow path. The drainage method revealed a high reduction of porosity in the HF-TW gravel during the operation period. The RTD was uniform, with a single peak of the NaCl concentration, and the mean residence time was higher than the nominal time. This confirmed that there was nonuniform flow through the HF-TW and the presence of stagnant zones. Moreover, the comparison of the results with tests carried out previously for the same system suggests the need to perform these measurements at least once a year and to plan HF-TW restorative measures soon. Moreover, considering the main advantages and disadvantages of the methods applied, it must be noted that the newly implemented scheme (with the pervious permeameter) reduces the number of K_s measurement points along the vertical dimension, and only measurements along the paths and transects are needed to characterize K_s. On the other hand, the drainage equation method, allowing for the identification of one K_s value for the whole HF unit at once, requires the system to be out of service for the entire duration of the test. Finally, tracer tests allow for an understanding of the effect of the clog matter on the flow through a porous medium, rather than assessing the clogging severity. In conclusion, the results highlighted that, especially for large systems, the combination of the newly implemented scheme with traditional

tracer tests is the most efficient approach for more thoroughly understanding clogging development in HF-TWs. Despite the partial clogging of HF-TW, the hybrid TW was able to meet the Italian law standards for wastewater discharge into water bodies.

6. Metal removal processes in a pilot hybrid constructed wetland for the treatment of semi-synthetic stormwater [5]

Abstract

This study investigates the reliability of a pilot hybrid TW located in Eastern Sicily (Italy). To address the uncertainty associated with implementing representative monitoring during highly variable storm events, unique to Mediterranean conditions, a recipe for semi-synthetic stormwater was used to evaluate the removal efficiency of the system. This was characterized by metals (Cd, Cr, Fe, Pb, Cu, Zn) and relative concentrations typically found in urban stormwater runoff. Approximately one month of intensive monitoring activities were carried out and quality analyses were conducted on three matrices comprising the pilot H-W: water, biomass (*Canna indica*, *Typha latifolia*), and volcanic gravel substrate. Metal retention in early clogging matter (SS) was also examined. The results showed a significantly high H-TW efficiency for the removal of all metals (70–98%) already at the horizontal flow unit outflow, confirming its strategic role. A metal mass balance analysis was also conducted to describe the retention capacity and influence of each system component on the overall efficiency (ranging from 87.8% for Cr to 99.2% for Pb). Metal removal was mostly related to sediment and substrate processes, while plants exhibited root bioaccumulation and phytostabilisation capacity even with a limited impact on overall system retention. The pilot H-TW exhibits characteristics suitable for the treatment of metal-enriched stormwater runoff and validates the

A modified version of this chapter was published as [5] D. Ventura, M. Ferrante; C. Copat; A. Grasso; M. Milani; A. Sacco; F. Licciardello; G.L. Cirelli. Metal removal processes in a pilot hybrid constructed wetland for the treatment of semi-synthetic stormwater in Sc. of total environment Volume 754, 1 Feb 21 https://doi.org/10.1016/j.scitotenv.2020.142221

useful application of decentralised natural systems for water resource management.

Keywords: Substrate processes; Root stabilisation; Metals; Macrophyte; Sediment; Sicily

6.1 Introduction

Wastewater (WW) management is promoted in the 6th Sustainable Development Goal (SDG) of 17 SDGs adopted by all United Nations (UN) Member States, as part of the 2030 Agenda for Sustainable Development (UN, 2015). The SDG 6 sets out to "ensure availability and sustainable management of water and sanitation for all" by covering the entire hydrologic cycle, including the management of WW and ecosystem resources. A UN report (UN, 2017) states that it is likely that in excess of 80% of WW worldwide is still discharged without adequate treatment, holding open discussions on the best approach to adopt; centralized or decentralized systems. Currently, in several countries' WW management is a norm; however, the major issues are related to the progressive aging of water infrastructure constructed during old economies and the highly expensive investment required to build or adapt new infrastructure. Treatment wetlands (TWs) are recognized as resilient, economic and extensive decentralized eco-technologies capable of meeting the challenges related to wastewater management. They integrate water service management and reduce the resource demands for freshwater through the reuse of unconventional valuable resources, such as stormwater (Malaviya and Singh, 2012). In the last few years, TWs have become increasingly common as a treatment system to remove contaminants in urban stormwater that are potentially detrimental to the receiving water ecosystems (Walaszek et al., 2017). Chemical contamination of water resources is recognized as an ever-increasing issue across the world (Richir and Gobert, 2016; Al-Akeel, 2017). In particular, the presence of metals in the environment may be due to

natural geochemical processes (e.g., weathering of ultramafic rocks), and human activities (e.g., mining, smelting, combustion of fossil fuels) (Dhote and Dixit, 2009). Various authors have reported on the performance of TWs for urban stormwater treatment (e.g., Schmitt et al., 2015; Adyel et al., 2016), and the removal efficiency of various metals (Gill et al., 2014). The accumulative and non-biodegradable nature of metals implies that these elements are potentially hazardous above specific tolerable limits to natural ecosystems, and ultimately to all living organisms (Tchounwou et al., 2012). Macrophytes play a fundamental role in wetland geochemistry due to their capacity to collect and transport micro- and macro-elements such as metals (Vodyanitskii and Shoba, 2015). Indeed, wetland plants can generally accumulate high levels of heavy metals from water and sediments owing to their extended root system, highly productive biomass, static nature, and tolerance to toxicity (Milošković et al., 2013). As a result, the use of macrophytes for phytoremediation is considered an effective strategy to remove metals from wastewater (Rezania et al., 2016). Some metals are important micronutrients for living organisms (e.g., Cu, Mn, Zn), despite producing toxic effects at higher concentrations (Kabata-Pendias, 2011). Other metals (e.g., Cd, Cr and Pb), have unknown biological functions and may prove to be highly toxic to organisms even at low concentrations (Nagajyoti et al., 2010). Greater knowledge on stormwater treatment systems and the performance of these systems is required for application in modern cities. Stormwater quality is strictly dependent on climatic variables; the highly stochastic nature of rainfall events is currently complicated by extreme climate phenomena. The Mediterranean area is characterized by long drought periods and increasing short and intense precipitation. As such, the design phase and performance assessment of TWs can become quite difficult. This study has two major aims: (i) Evaluating the overall efficiency of a pilot hybrid TW (H-TW), with free water surface (FWS) and horizontal subsurface flows (HF), in reducing metals added in a semi-synthetic stormwater runoff (SSR)

drained from the parking area of an IKEA® retail store in Eastern Sicily (Italy); (ii) observing the specific role of macrophytes, filtering medium and sediments during the treatment train. This study also analyses the concentrations of Cd, Cr, Cu, Fe, Pb and Zn in roots, rhizomes, and stems of *Canna indica* and *Typha latifolia* to shed further light on bio-stabilization capability and the occurrence of translocation paths.

6.2 Materials and methods

6.2.1 Pilot hybrid-TW

The pilot H-TW is located in the parking lot of a large IKEA® store of Catania (Eastern Sicily, Italy; latitude 37°26′ N, longitude 15°01′ E, altitude 11 m a.s.l.) (Figure 6.1). It was installed at the end of 2016 and used for the treatment of road runoff that had been drained and collected from this area. In a semi-arid climate, such as the Southern Mediterranean regions, stormwater treatment poses a challenge due to the prolonged dry periods and short and intense precipitation events; there is a potential for rainfall shortage to cause a system blockage. WW generated at the parking lot was conveyed into the system following conventional SBR treatment, during the dry period (Apr–Sept). As reported by Ventura et al. (2019), the system consists of a unique inlet tank (pond), followed by two identical parallel lines, each including a horizontal subsurface treatment wetland with HF and a FWS unit in series (see, Figure 4.1). All units were made up of fiberglass tanks. In the pond, the initial treatment is comprised of floating solid settlement and flow WW equalization, especially when the system feeding has switched from stormwater to SBR effluent treatment. The HF units, consisted of *C. indica*, at a density of 74 plants per m^2, and volcanic gravel (grain size 10–25 mm, porosity of 0.4) as a filtering medium. Note that the plant density measurements were conducted in July 2018, following 1.5 years of operation; the initial planting density was 5 plants per m^2. These units

mainly reduce organic matter (biochemical oxygen demand, BOD_5 and chemical oxygen demand, COD), and suspended solids (SS) from the WW. The FWS units exposed WW to solar radiation, facilitating a disinfection process, reducing nitrogen and phosphorous concentrations and providing further retention capacity through the massive root system of *Typha latifolia* placed on a floating support in the tank (density of 70 plants · m^{-2}). The influent was carried through the fiberglass tanks of the system via submersible pumps. These were equipped with a water level sensor, located at the outlet of each stage (where a flow meter is present), and had a maximum flow rate of 1 $m^3 \cdot d^{-1}$ for line, and a nominal hydraulic retention time (*nRT*) of 96 h. The selected macrophytes, *C. indica* (Indian shot), a rhizomatous species native to America, and *T. latifolia* (broadleaf cattail), a cosmopolitan rhizomatous species, are well known and increasingly used in TWs for their relative metal phytoremediation capacity (Calheiros et al., 2015; Cule et al., 2016; Carranza-Álvarez et al., 2008; Bonanno and Cirelli, 2017). Detailed information on the SBR wastewater treatment is provided in Marzo et al. (2018), and a preliminary evaluation of the pilot H-TW design and performance is detailed in Ventura et al. (2019)

Figure 6.1 - General overview of a pilot hybrid-TW system at the IKEA® store of Catania (Eastern Sicily).

6.2.2 *Set-up of semi-synthetic stormwater runoff*

As previously observed by studies on the same system (Ventura et al., 2019), monitoring activities were highly challenging due to the absence of precipitation, the unpredictability of heavy rainfall events, and the low metal concentrations in natural stormwater runoff drained and collected from the surrounding parking lot (reported in Table 6.2 as C*). For this reason, a semi-synthetic stormwater runoff (SSR) was produced, based on reference concentrations for stormwater runoff quality from different contexts, as per Ciaponi et al. (2014) (see, Table 6.1). This enabled the simulation of natural stormwater quality and allowed the implementation of the entire H-TW treatment process to be as realistic as possible. SSR was defined as semi-synthetic as metals (Cu, Cd, Cr, Zn, Pb, Fe) were added into the stormwater regularly drained and collected from the parking lot, following metal dissolution in a bucket (Fig. 3). In late December 2018 and January 2019, the SSR was produced on a weekly basis in the inlet (pond) and then pumped throughout the system. This task did not modify the nominal incoming flow rate and five loading tests (each one for each of the five weeks), were conducted.

6.2.3 *Pilot hybrid-TW sampling campaigns*

SSR quality at the H-TW system was monitored three times per week in the pond and at the outlet of each stage (HF1–HF2, FWS1– FWS2; see, Figure 4.1). The SSR sampling frequency was fixed according based on the actual hydraulic retention time (*aRT*). The *aRT* was determined through experimental observation in the system at each treatment stage using tracer test measurements (data not reported), according to the methodology described by Marzo et al. (2018). The *aRT* was found to be 32 and 80 h at the HF and FWS units, respectively, after the loading time (0 h) (in Figure 6.3, named as

Pond_h0, HF_h32, FWS_h80). The H-TW removal efficiency (RE) was calculated using Equation (Eq., 6.1):

$$RE = \frac{C_{in} - C_{out}}{C_{in}} \cdot 100 \quad \text{(Eq. 6.1)}$$

where C_{in} (mg · L^{-1}) and C_{out} (mg · L^{-1}) are the pollutant concentrations at the inlet and outlet, respectively. Biomass sampling consisted of collecting four specimens of *C. indica* and *T. latifolia* at each sampling point (corresponding to a surface area of 0.06 m^2) at the HF and FWS units (see, Figure 4.1), for a total of 24 and 16 samples in total, respectively. Prior to the first SSR input (Pre), samples of stems (above-ground biomass, AGB), roots and rhizomes (below-ground biomass, BGB) were collected. Only BGB samples were collected at the end of the five SSR treatment tests (*Post*) as the epigeal organs of the plants were already senescent in early February. In the laboratory, samples were cleaned and dissected. Volcanic filtering medium sampling was undertaken for each HF unit collecting point at the inlet, middle part and outlet of the system; it consisted of three replicates (a plastic cup ≈ 0.12 L used for each sample) (see, Figure 4.1). The volcanic gravel (geographical originating from the Etna valley district), was then powdered through a mortar. Clean samples (T_0) and at *Pre* and *Post* SSR treatment were subsequently analyzed. Metal content in SS was also analyzed and samples (monitoring points, see Figure 4.1) were collected *Pre* and *Post* SSR treatment in the pond (single sample per point) and HF units (three samples per point). SS are recognized to be largely responsible for clogging in the H-TW system. Plants and sludge dry weight (DW) and suspended solids (SS) were measured after samples were dried in a thermo-ventilated oven at 65 °C to constant weight. Filtering media and sludge samples were collected in 0.12 L volume plastic cups. Sludge DW was estimated in the pond during the *Pre* and *Post* phase and not the HF units as the complete extraction of sediments and filtering media would have caused a system blockage.

Table 6.1 - Quality of stormwater runoff from literature data (Ciaponi et al., 2014).

Metals	Unit	Residential area[a] (local traffic)	Commercial area[a] (low traffic roads)	Commercial area[b] (*NSQD)
Cd_{total}	$\mu g \cdot L^{-1}$	0.5	1.8	0.89
CV		--	--	2.7
Cr_{total}	$\mu g \cdot L^{-1}$	2	16	6
CV		--	--	0.9
Cu_{total}	$\mu g \cdot L^{-1}$	17	46	17
CV		--	--	1.5
Pb_{total}	$\mu g \cdot L^{-1}$	17	50	18
CV		--	--	1.6
Zn_{total}	$\mu g \cdot L^{-1}$	107	508	150
CV		--	--	1.2

Statistical variability for each pollutant concentration is expressed as coefficient of variation "CV".

[a] Bannerman et al. (1993) from Medison and Wisconsin.

[b] Mestre and Pitt (2005) from *NSQD database (mean values, 503 samples).

*The National Stormwater Quality Database (developed by the University of Alabama and the Centre for Watershed Protection under support from the U.S. Environmental Protection Agency).

Figure 6.2 - Pilot hybrid-TW system (Catania, Italy): the addition of metals to produce semi-synthetic stormwater runoff (SSR) for the experimental set-up.

Collected sludge covered a roughly 1 m^2 surface, where each sampling point of the six in the pond unit ≈ 0.16 m^2. Table 6.3 presents the metal Mass Balance (*MB*, %) calculated for each treatment component (macrophytes, filtering medium and SS) to underline the role played by each of these components in the Total Metal Retention (*TMR*) of the system (Eq., 6.2). The *TMR* is the mass of metals loaded in the system (mg) and that calculated at the end of the experiment. The MB parameter was determined as the ratio (Eq., 6.3) between the metals retained by each component (in mg and equal to the difference between *Post* and *Pre* content (mg $\cdot L^{-1}$) related to the total DW of the component considered (kg) and the *TMR*:

$$TMR = C_{Post} \cdot V_{Post} - C_{Pre} \cdot V_{Pre} \quad \text{(Eq. 6.2)}$$

This ratio was calculated by Eq. (6.3):

$$MB = \frac{MR}{TMR} \cdot 100 \quad \text{(Eq. 6.3)}$$

6.2.4 Chemical analysis

For metal extraction, the acid digestion of water was conducted in a microwave open system (DIGI-PREP SCP SCIENCE) with a digestion solution of 5 mL of 65% nitric acid (HNO_3) at 120 °C for a 120 min operation cycle. Samples of volcanic gravel, sediments and plants were mineralized in an Ethos Touch Control microwave system (Milestone S.r.l., Italy) equipped with pressurized vessels (N. 12), using a heated mixture of strong acids. Acid digestion was conducted with 9 mL of 65% HNO_3 and 3 mL di hydrochloric acid (HCl) for sediments and 6 mL of HNO_3 and 2 mL of 30% peroxide hydrogen (H_2O_2) at 200 °C for a 50 min operation cycle. Inductively coupled plasma-mass spectrometry (ICP-MS) Elan-DRC-e (Perkin-Elmer, USA) was used for metal quantification. Analytical blanks were processed in the same way as samples, and concentrations were determined using standard solutions prepared in the same acid matrix.

Standards for instrument calibration were prepared with a multi-elements certified reference solution ICP Standard.

6.2.5 Statistical analysis

The Student's t-test were used to quantify the differences in water quality and treatment lines (HF1-FWS1 and HF2-FWS2) for the *Pre* and *Post* metal loading in the system. One-way analysis of variance (ANOVA) was implemented to evaluate the eventual filter media retention and to ascertain whether the three organs of *C. indica and T. latifolia* (roots, rhizomes, stems) accumulate significantly different metal concentrations. Post hoc analysis was conducted using a Tukey test to identify the specific mean pairs that differ in a significant way. Following SSR treatment, given the lack of available stem samples, differing concentrations between roots and rhizomes were checked using the Student's test. This was also applied to analyze metal content differences between the same hypogeal organs and in SS for the *Pre* and *Post* phases. A $p < 0.05$ result was considered significant, and all statistical analyses was conducted using the R software (R Core Team, 2014).

6.3 Results and discussion

The C* from previous results (Ventura et al., 2019) and metal concentrations measured in this study (observed SSR) are reported in Table 6.2. The forecasted metal concentrations have been reported as the Expected SSR; these are the concentrations due to chemical weighing, and are preliminary to each of the five loading tests. These levels were slightly higher than reference ones (Table 6.1) due to an initial intent to better underline removal during the treatment train. In some cases (i.e., Cd, Pb, Cu), the expected concentrations were not fully met; this is likely due to field operations. A small volume of incoming stormwater was collected in a bucket, where metals were added and shaken and this concentrated volume of water was stirred

using a pump directly in the pond for a time period to homogenize the entire volume of water. The highly acidic pH (< 4) would have properly encouraged metal dissolution (Karathanasis and Johnson, 2003; Chubaka et al., 2018), which may have been inhibited by observed pH in the pond (8.5 ± 0.3). Despite these considerations, the quality of the SSR was completely in line with values from literature (Table 6.1) and comparable to natural stormwater runoff. This confirmed the reliability of using SSR to evaluate the effectiveness of H-TW applications for stormwater treatment without any particular limitation. Figure 6.3 shows that the HF units played a key role in H-TW removal efficiency, with Fe, Cu and Cd removal efficiency being the lowest (70%, 78%, 86%) and Cr, Zn and Pb removal efficiency being the highest (93%, 93%, 98%). Mean values of outlet metal concentrations were far below Italian standard limits for wastewater discharge (Legislative Decree 152/2006, 2006) and reuse (Ministerial Decree 185/2003, 2003). Figure 6.3, clearly confirms an improvement in SSR quality during treatment, and demonstrates the overall system retention capability in terms of the mass balance of metals (Figure 6.4). This allowed further analysis of the role of all components traditionally characterizing TW systems in harnessing natural processes for contaminant abatement. The overall system removal efficiency was 95.6% for Cd, 93.6% for Cr, 87.8% for Fe, 91.9% for Cu, 97.6% for Zn, and 99.2% for Pb. Table 6.3 reports on the overall metal retention in the pilot H-TW, together with the metal content in each component (plants, filtering medium and SS) for the *Pre* and *Post* treatment phases. The DW of *C. indica* was on average 11.7 ± 2.6 kg · m^{-2} for AGB and 5 ± 1.11 kg · m^{-2} for BGB, with a ratio of 2.3. The measured BGB DW of *T. latifolia* was 2.03 kg · m^{-2}; previously, Ben Salem et al. (2017) had observed the highest BGB DW in *T. latifolia* at 1.24 kg · m^{-2}. The total SS weight in the bottom of the pond was approximately 4.5 kg, with an average of 750 ± 32 g·m^{-1}. Sludge DW in the HFs was not determined due to technical drawbacks and metal content retained in these units was also not measured. Metal

concentrations (mg · kg^{-1}) in SS were analyzed for preliminary evaluation in the pond and HF units. Concentrations were generally higher in the pond than in the HF units, with the exception of Fe, as reported in Table 6.4. In terms of stormwater quality, Ventura et al. (2019) reported that the mean SS concentration at the inlet of the pond and at the HFs was 120 ± 112 and 69 ± 47 mg · L^{-1}, respectively. Additionally, they reported an SS removal efficiency of 46% (±34.4) and 45.4% (±17.2), respectively. The filtering medium did not play an active role in metal retention or release, and was considered an inert component of the system. Differences in metal concentrations (mg · kg^{-1}) at T_0 (clean volcanic gravel), *Pre* and *Pos*t treatment (Table 6.4) were not statistically significant ($p < 0.05$).

6.3.1 Metal content in plants organs

The highest metal concentrations were generally found in the roots, even in the Pre phase (when stems were also analyzed). The concentration of Zn was uniform in all organs of *C. indica* and in the below-ground organs of *T. latifolia.* The Cu content in the latter was the same in all organs. The content of Cr, Fe, Cd and Pb were equally lower in the rhizomes and stems with respect to the roots, for both plants; this highlights that there are more differences between belowground organs than between rhizomes and stems. It also suggests the absence of translocation processes directing metals toward aerial plant biomass. In the *Post* treatment (Table 6.6), Zn content was uniform in the below-ground organs of both plants, while Cu and Pb were only in *C. indica*. In both plants, Cd was observed in the lowest concentrations in the roots, while it was under detectable limits in other organs for the *Pre* and *Post* treatment phases. As observed by Ben Salem et al. (2017), in a domestic landfill site (France), *T. latifolia* organs contain Fe as the metal with the highest average concentrations, followed by Mn, As, Zn, Cr, Cu, Ni and Cd, without seasonal influence. According to the analyzed metals, this study also found that Fe was present in the highest concentration, with

the following trend in descending order: Fe > Zn > Cu > Pb ≥ Cr > Cd (Tables 6.5 and 6.6). Note that climatic variations were not considered relevant due to the month-long experimental period, with an average temperature of 10.9 ± 3.9 °C. Although *C. indica* also contained the same metal content trend, the *Post* phase Cr concentration was slightly higher than Pb in the roots.

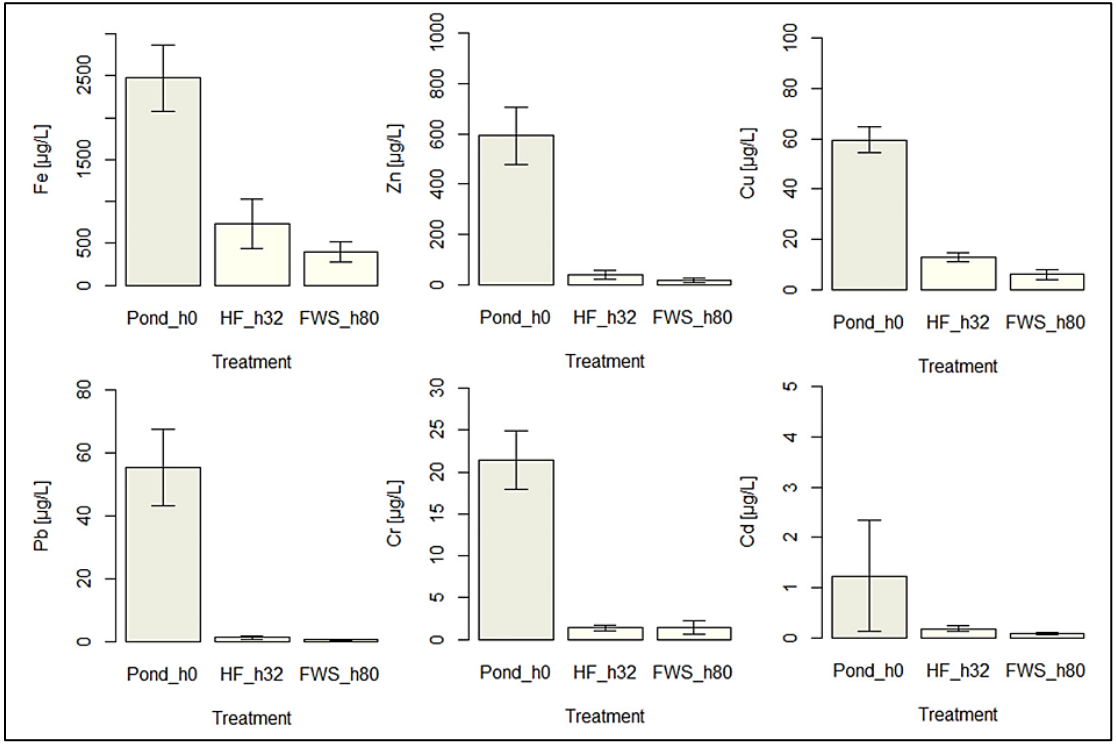

Figure 6.3 - Mean metal concentrations (µg · L^{-1}) and standard error for semi-synthetic stormwater runoff treatment at the pilot hybrid-TW system (Catania, Italy) from December 2018 to January 2019

Table 6.2 - Mean metal concentrations and standard deviations (±), denoted by C*, as reported by a previous investigation (Ventura et al., 2019) on stormwater runoff conveyed into the hybrid-TW. The Expected SSR is the forecasted metal concentrations in the semi-synthetic stormwater due to preliminary chemicals weighing conducted in a laboratory. The observed SSR are the metal concentrations detected in the semi-synthetic stormwater in the pond in Catania, Italy

SSR	Unit	Cr	Fe	Cu	Zn	Cd	Pb
Expected SSR	$\mu g \cdot L^{-1}$	30	3000	80	500	5	100
C*	$\mu g \cdot L^{-1}$	2.55 (±0.01)[a]	1422 (±68.25)[a]	11.22 (±0.23)[a]	32.01 (±0.19)[a]	0.1 (±0.01)[a]	1.91 (±0.33)[a]
Observed SSR	$\mu g \cdot L^{-1}$	21.50 (±3.49)[b]	2473.37 (±399.48)[b]	59.56 (±5.25)[b]	591.45 (±113.84)[b]	1.22 (±1.1)[b]	55.26 (±12.11)[b]

Note: different letters indicate significant differences between C* and Observed SSR for the same metal (t-test, $p < 0.05$).

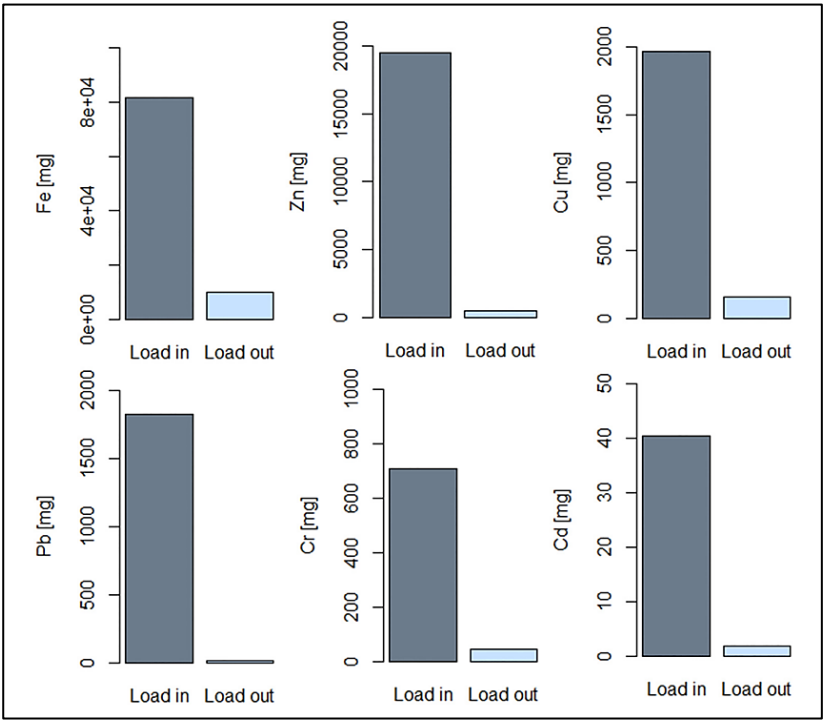

Figure 6.4 - Metal mass balance calculated as the sum of all five loading steps at the inlet (Load in) and outlet (Load out) during semi-synthetic stormwater (SR) treatment in the pilot hybrid TW system (Catania, Italy).

Table 6.3 - Metal content (mg) analyzed in macrophytes and SS prior to (*Pre*) and after (*Post*) semi-synthetic stormwater runoff treatment in the pilot hybrid-TW system (Catania, Italy). Proportional influence (%) of macrophytes, SS and filtering media on overall system metal retention.

Component		Unit	Cr	Fe	Cu	Zn	Cd	Pb
TMR		mg	663.73	71687.17	1806.19	19045.95	36.68	1809.17
Canna indica	Content, *Pre*	mg	12.90	9366.12	423.04	837.67	0.34	7.35
	Content, *Post*	mg	26.96	6239.17	488.98	2428.88	0.64	15.71
	MB	%	2.12	-4.36	3.65	8.35	0.76	0.46
Typha latifolia	Content, *Pre*	mg	1.94	6750.41	42.34	146.84	0.48	1.74
	Content, *Post*	mg	2.05	15978.67	45.14	276.78	0.19	3.37
	MB	%	0.02	12.87	0.16	0.68	-0.75	0.09
Macrophyte MB		%	2.14	8.51	3.81	9.04	0.01	0.55
HF filtering medium [(b)]		--	Inert	Inert	Inert	Inert	Inert	Inert
	Content, *Post*	mg	1.00	695.18	6.20	21.18	0.11	1.49
SS	Content, *Post*	mg	205.16	74761.36	957.84	6461.92	3.20	364.98
SSMB		%	30.76	103.32	52.69	33.82	7.98	20.09

[a] Total metal retention in the system.

[b] Horizontal flow units.

[c] Pond; MB: partial metal mass balance indicates the relative influence of each component to overall removal.

Table 6.4 - Mean metal concentrations (mg ·kg^{-1}) and standard deviation (±SD) in SS (*Post)* and filtering medium (T0; *Pre* and *Post* treatment) in the pond and HF units during semi-synthetic stormwater runoff treatment in the pilot hybrid-TW system (Catania, Italy).

Component		Unit	Cr	Fe	Cu	Zn	Cd	Pb
SS	Pond, *Post* (±SD)	mg ·kg^{-1}	45.59 (± 18.45)	16613.64 (± 6012.31)	212.85 (± 81.59)	1435.98 (± 553.16)	0.71 (± 0.28)	8.11 (± 33.63)
	HF, *Post* (±SD)	mg ·kg^{-1}	14.12 (± 1.18)	3061.51 (± 1.18)	122.94 (± 13.59)	267.17 (± 44.96)	0.04 (± 0.01)	2.62 (± 0.62)
Filtering medium	T0 (±SD)	mg ·kg^{-1}	19.70 (± 4.20)	45820.00 (± 3096.00)	80.65 (± 4.15)	44.88 (± 5.46)	0.05 (± 0.00)	2.06 (± 0.20)
	HF, *Pre* (±SD)	mg ·kg^{-1}	20.93 (± 1.20)	46472.00 (± 1419.00)	75.11 (± 1.30)	43.71 (± 1.84)	0.05 (± 0.00)	1.36 (± 0.15)
	HF, *Post* (±SD)	mg ·kg^{-1}	22.79 (± 1.60)	46336.00 (± 1394.00)	84.58 (± 3.86)	37.68 (± 1.58)	0.13 (± 0.08)	1.94 (± 0.27)

Note: T0 = clean gravel

6.3.2 Bioaccumulation paths

Metals were mostly retained by SS in the pond, as supported by the data for the dry matter content analyses. Bioaccumulation observed in both macrophytes was limited, with values lower than 1% (for Cd, Pb) or ranging between 2% and 4% (for Cr, Cu) (Table 6.3). *T. latifolia* and *C. indica* exhibited positive rate of retention, respectively for Fe and Zn, contributing almost 10% of the total retention of these metals. However, as indicated in Table 6.3, the total percentual Fe retention was higher than 100% as the system has been accumulating metals since its early stages of operation (see C*, Table 6.2). Karathanasis and Johnson (2003) had observed that the Fe uptake by different plant species was the highest among the metals studied in an acid mine drainage wetland; this was particularly when Fe was by far the most concentrated in the wetland. The same authors also recognized that the formation of Fe plaques on the root epidermis of macrophytes signified that Fe uptake was more likely a result of Fe sequestration as opposed to bioaccumulation. Karathanasis and Johnson (2003) also found further evidence suggesting a direct correlation between lower Fe bioaccumulation and lower soluble metal concentrations (due to pH gradient: 3.2 to 6.4) in *T. latifolia*, compared to other species present. In this study, despite the use of a considerably different wetland environment, and much lower Fe levels, both macrophytes exhibited the opposing behaviours as *T. latifolia* demonstrated high Fe uptake while *C. indica* clearly released its Fe. In this sense, it appears that the *T. latifolia* was unaffected by a higher pH and an eventual decrease in the soluble metal concentrations, being more efficient in Fe retention compared to *C. indica*. The latter may explain the higher levels of Fe in HF sediments then those in the pond (data reported in Table 6.4). In conjunction with pH, many factors may account for metal distribution in sediment, their translocation paths, and their release (for example, wetlands may be a sink or source of toxic metals). These factors are able to influence the solubility and speciation of metals and thus, their

bioavailability and uptake process by plants (e.g., in the case of Fe uptake relay on reduction form Fe^{3+} to Fe^{2+} or the chelation strategy for the direct absorption of Fe^{3+}). Depending on the plant physiology, environmental conditions and the metal type, various phenomena can occur. Ventura et al. (2019) reported a mean dissolved oxygen of 1.6 ± 0.6 mg · L^{-1} in the HF units of the same H-TW, during the same fall-winter season of the previous year. They also measured high dissolved oxygen levels in the FWS units (8.4 ± 2.3 mg · L^{-1}). These differences in dissolved oxygen concentrations may be attributable to the opposing behaviour of Fe uptake by *T. latifolia* and *C. indica*. Weis and Weis (2004) described the strong correlation between anoxic sediment and extremely high metal concentrations in a reduced chemical status, which corresponds to lower bioavailability in comparison with oxidised soils and environments. Similarly, the release of Fe observed in *C. indica*, may have been encouraged by the anoxic conditions in the saturated filtering layer of HF units, which may have been a source of Fe. Consideration should also be given to the further reduction of oxygen movement from the aerenchyma tissue to the rhizosphere of *C. indica*, due to the occurrence of senescence. The suitability of *T. latifolia* in terms of Fe retention may have been encouraged by its larger root system for the eventual constitution of plaques for Fe sorption, promoting the rhizofiltration process. Metal concentrations that were significantly different ($p < 0.05$) due to bioaccumulation or release in roots and rhizomes of both plants for the *Pre* and *Post* treatment phases are reported in Figure 6.5. In particular, *C. indica* presented higher levels of Cr and Zn and lower Fe levels in the roots, and higher levels of Pb and Cr in the rhizomes in *Post* than *Pre* treatment. Similarly, by comparing the metal content in the same organs of *T. latifolia*, Fe concentrations had increased in the roots and Pb concentrations had increased in the rhizomes at the end of the treatment. In both plants, there was always a significant increase in the Pb concentration in the rhizomes from undetectable levels, while the Pb content in the roots remained largely unchanged. Although *C.*

indica and *T. latifolia* are widely recognized as plants with a capacity for phytoremediation, there is a lack of research on the application of live *C. indica* plants for the heavy metal treatment of wastewater in contaminated sites. Many researchers have analyzed its potential and performance in metal adsorption and removal through dry biomass and derived biochar, as described by the Langmuir model (Dixit et al., 2014; Cui et al., 2016; Gopkar et al., 2017). Other researchers have reported on successful applications of *C. indica*-based TWs for conventional WW treatment and pollution control (Cui et al., 2010; Calheiros et al., 2015; Samal et al., 2017). This study confirms the relatively small impact of plant bioaccumulation of metals compared to overall wetland retention capability, as previously observed by Karathanasis and Johnson (2003). This is despite the huge difference in the metal concentrations in acid mine drainage wetlands and in the plants analyzed. Roots generally played the key role in metal bioaccumulation, acting as a soil stabilizing filter, typical of tolerant species, as previously observed by Ahmad et al. (2010) and Klink et al. (2013) on *T. latifolia*. Root accumulation in vascular macrophytes is mainly due to the presence of the lacunar system in cortex parenchyma, facilitating unselective metal passage (Sawidis et al., 1995). Ben Salem et al. (2017) has reported on the efficient absorption of micronutrients in plant root systems and their aptitude to highly select their transfer from the roots to the rhizome. In this study, the highest root metal content was for metals that are also plant micronutrients, such as Fe and Zn. The accumulation (i.e., *T. latifolia*) or release (i.e., *C. indica*) of Fe may be associated to an eventual luxury uptake process. This phenomenon, as coined by Mitsch and Wise (1998), may occur when plants are exposed to high metal concentrations. This may justify the release of metals in instances when the plants micronutrient needs are reduced, as influenced by specific environmental and climatic conditions. The Zn content in the sediment and its accumulation in *C. indica* roots was lower than 125 ppm and the DW of 0.2 mg $\cdot$ g^{-1} limits reported for unpolluted soils

and potential phytotoxicity in leaf tissue (Tsonev and Cebola Lidon, 2012). This study has indirectly confirmed the complexity of metal bioavailability paths, as it is strongly influenced by chemical-physical conditions (e.g., temperature, pH and salinity) of water and substrate (e.g., organic complexation, precipitation, oxidoreductive potential, hydrolysis) (Ben Salem et al., 2017). It has also focused on the probable and important contribution that plants play through a variety of soil processes, such as substrate stabilisation, microbial attachment, and rhizosphere oxidation (Karathanasis and Johnson, 2003). In terms of the environmental conditions, the H-TW was characterized by pH fluctuations among the units (pH of pond 8.5 ± 0.3, HF 7.3 ± 0.05, and FWS 7.6 ± 0.09), while an acid gradient was absent, suggesting more favourable and uniform conditions for limited metal solubility and bioavailability

Table 6.5 - Metal content (mg · kg^{-1}), and relative standard deviation (±SD) in the organs (root, rhizome, stem) of *Canna indica* and *Typha latifolia*, prior to (*Pre*) the addition of semi-synthetic stormwater runoff in the pilot hybrid-TW system (Catania, Italy), and statistical analysis.

Sample	Organs	Unit	Cr	Fe	Cu	Zn	Cd	Pb
Canna indica	root	mg · kg^{-1}	0.13	144.12	4.11	6.64	0.01	0.12
		(±SD)	(±0.04)a	(±45.50)a	(±0.40)a	(±1.97)a	(±0.01)	(±0.07)
	rhizome	mg · kg^{-1}	0.07	12.02	2.97	7.16	<0.01	<0.01
		(±SD)	(±0.05)b	(±7.74)b	(±0.96)b	(±2.99)a	--	--
	stem	mg · kg^{-1}	0.08	10.02	0.92	4.36	<0.01	<0.01
		(±SD)	(±0.01)b	(±5.17)b	(±0.23)c	(±0.70)a	--	--
Typha latifolia	root	mg · kg^{-1}	0.25	1057.75	3.61	11.91	0.08	0.27
		(±SD)	(±0.18)a	(±470.13)a	(±4.24)a	(±7.07)a	(±0.10)a	(±0.18)
	rhizome	mg · kg^{-1}	0.06	48.87	3.33	11.44	<0.01	<0.01
		(±SD)	(±0.03)b	(±30.19)b	(±3.73)a	(±10.30)a	--	--
	stem	mg · kg^{-1}	0.08	7.38	0.29	3.27	<0.01	<0.01
		(±SD)	(±0.03)b	(±5.32)b	(±0.10)a	(±0.73)b	--	--

Note: statistical analysis was conducted (one-way ANOVA, with significance shaped as $p < 0.05$) except for concentrations considered too low (< 0.01). Different letters (*a*, *b*, *c*) describe for the same metal significant differences among the organs of the same plant species (Post-hoc Tukey test).

Table 6.6 - Metal content (mg · kg^{-1}), and relative standard deviation (±SD) in the organs (root, rhizome, stem) of *Canna indica* and *Typha latifolia*, post to (*Post*) the addition of semi-synthetic stormwater runoff in the pilot hybrid-TW system (Catania, Italy), and statistical analysis.

Sample	Organs	Unit	Cr	Fe	Cu	Zn	Cd	Pb
Canna indica	root	mg · kg^{-1} (±SD)	0.27 (±0.05)a	76.14 (±53.98)a	4.79 (±2.39)a	14.99 (±7.00)a	0.01 (±0.02)	0.13 (±0.02)
	rhizome	mg · kg^{-1} (±SD)	0.20 (±0.06)b	9.92 (±3.60)b	3.49 (±1.51)a	25.79 (±19.74)a	<0.01 --	0.13 (±0.00)a
Typha latifolia	root	mg · kg^{-1} (±SD)	0.28 (±0.07)a	2588.34 (±1490.39)a	5.27 (±3.13)a	30.24 (±24.03)a	0.02 (±0.02)	0.43 (±0.15)a
	rhizome	mg · kg^{-1} (±SD)	0.05 (±0.03)b	31.30 (±18.90)b	1.62 (±0.89)a	14.39 (±9.83)a	<0.01 --	0.13 (±0.00)b

Note: different letters indicate significant differences in the concentration of a metal between the two kinds of organs of the same plant species (t-test, $p < 0.05$); stem samples were not included because they were not available during sample collection; statistical analysis was not conducted for concentrations below <0.01.

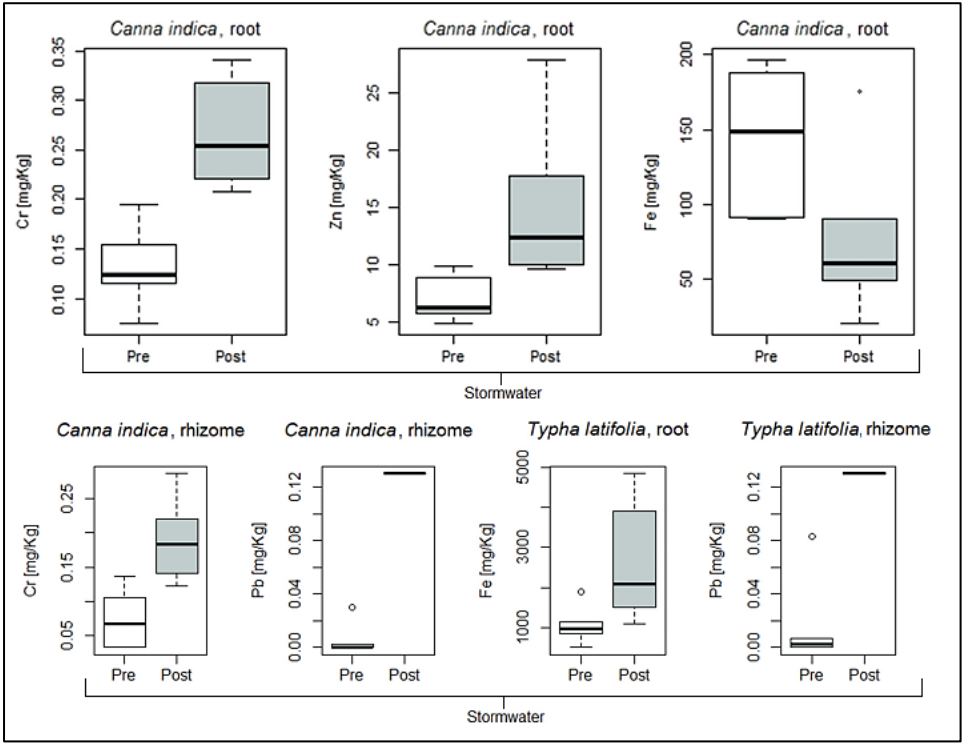

Figure 6.5 - Metal bioaccumulation in macrophytes hypogeal organs Pre and Post semi-synthetic stormwater runoff treatment in the pilot hybrid-TW system from December 2018 to January 2019, in Catania, Italy

6.4 Conclusion

A semi-synthetic stormwater was produced and treated in a pilot H-TW at an IKEA® store parking lot in Catania, Italy. The analysis of metal concentrations in water, macrophytes, and sediments, before, during, and after treatment, enabled the implementation of a general qualitative evaluation in terms of mass balance and the forecast of metal retention pathways. The overall metal retention capability of the system was extremely high (87–99%) and major removal was likely due to substrate-related processes, as the highest accumulations were observed in the sediment and there was partial removal in the root biomass. Substrate metal adsorption is likely to have been encouraged by an alkaline pH, and the sedimentation and rhizo-filtration processes. This was confirmed by positive trends for SS removal performance in the pond and HF units, alongside the highest removal efficiency of metals observed in the water at the HF outlets (70–98%). However, it was not possible to determine the quantitative difference between the pond and the HFs. There was minimal metal bioaccumulation in the roots with respect to the overall system retention capability, representing a stabilization factor. Phytoextraction processes, typical of hyperaccumulator plants, were not observed; this should be a consideration when selecting macrophytes for a TW system. The capacity for heavy metal tolerance is variable for different plant species and should be a guide to achieve the most favorable substrate conditions (e.g., rhizosphere surface area extent) to confine and better manage environmental pollution. The eventual toxic effects of metals on plant growth should also be considered and further research is required to understand these effects. The findings of this study indicate that the confinement of pollutants in the substrate and root systems may be beneficial in the control and management of TWs for stormwater runoff treatment applications. Regular maintenance of these systems, such as the disposal of vegetation cuttings (uncontaminated by translocated metals), is

possible without any necessary landfilling. However, landfilling will be required for sediments and hypogeal plant biomass management during the final disposal of the system or for high level maintenance operations (e.g., cleaning or substitution of clogged filter media). In conclusion, this case study confirms the reliability of TW systems in stormwater runoff treatment for metal pollution control (through the use of a semi-synthetic stormwater runoff). Additionally, the findings suggest the application of TWs for safe stormwater discharge practices, for decentralized water sources and the application of water reuse, particularly when freshwater resources are limited.

7. Electrical resistivity imaging for monitoring soil water motion patterns under different drip irrigation scenarios[6]

Abstract

The use of hydro-geophysical methods provides insights for supporting optimal irrigation design and management. In the present study, the electrical resistivity imaging (ERI) was applied for monitoring the soil water motion patterns resulting from the adoption of water deficit scenarios in a micro-irrigated orange orchard (Eastern Sicily, Italy). The relationship of ERI with independent ancillary data of soil water content (SWC), plant transpiration (T) and in situ measurements of hydraulic conductivity at saturation (K_s, i.e., using the falling head method, FH) was evaluated. The soil water motion patterns and the maximum wet depths in the soil profile identified by ERI were quite dependent on SWC (R^2 = 0.79 and 0.82, respectively). Moreover, ERI was able to detect T in the severe deficit irrigation treatment (electrical resistivity increases of about 20%), whereas this phenomenon was masked at higher SWC conditions. K_s rates derived from ERI and FH approaches revealed different patterns and magnitudes among the irrigation treatments, as consequence of their different measurement scales and the methodological specificity. Finally, ERI has been proved suitable for identifying the soil wetting/drying patterns and the geometrical characteristics of wet bulbs, which represent some of the most influential variables for the optimal design and management of micro-irrigation systems.

A modified version of this chapter was published as [6]D. Vanella, J. M. Ramírez-Cuesta; A. Sacco; G. Longo Minnolo; G. L. Cirelli; S. Consoli Electrical resistivity imaging for monitoring soil water motion patterns under different drip irrigation scenarios in Springer - Irrigation Science Volume 39, 12 Sep 20 https://doi.org/10.1007/s00271-020-00699-8

7.1 Introduction

In semi-arid and arid regions, irrigation management practices depend on the accurate characterization of temporal and spatial soil water content (SWC) dynamics (Vereecken et al. 2008). In general, the soil texture and the soil hydraulic characteristics represent the two main drivers of SWC changes and soil water infiltration (Campbell and Norman 1998). Nowadays, the most common methods adopted to measure SWC distribution at the root-zone level (e.g., time domain and/or frequency domain sensors, neutron probes) present several limitations (Robinson et al. 2008). The main drawback of these SWC methods concerns their point-based nature and specifically the non-representativeness and restricted sampling volume (i.e., 10–100 cm^3). In addition, these measurements strongly depend on sensors location in the soil profile (Bogena et al. 2015; Robinson et al. 2008). Furthermore, their installation requires drilling that may cause disturbance of soil structure and water flow regime. However, even if the SWC variation is recognized as a proxy of soil water infiltration (Brindt et al. 2019), identifying water flow pathways due to irrigation in the unsaturated soil profile where plant roots are mainly distributed is a complex challenge (Guo et al. 2019; Zhang et al. 2017). In fact, very large variations in SWC exist throughout the root zone especially under localized irrigation (García-Tejera et al. 2017), mainly due to the preferential root growth in the wetted bulbs (Klepper 1991). Several methods have been developed and applied for the infiltration rates characterization. Specifically, the soil hydraulic conductivity at saturation (*Ks*) can be obtained by field and laboratory methods. In situ *Ks* measurements, based on constant head (CH) or falling head (FH) methods, are generally preferred instead of laboratory determinations. In fact, the small-sized soil samples handled in laboratory may not be representative of the field conditions (Ibrahim and Aliyu 2016). The high spatial and temporal variability of *Ks* requires, however, a huge number of field measurements for a

comprehensive understanding of the infiltration process. Moreover, it is known that the different in situ K_s methods provide distinct infiltration rates even under the same soil conditions (Guo et al. 2019). The use of hydro geophysical methods may contribute to solve some of the above-mentioned limitations for capturing lateral SWC changes and potentially for determining the relative soil water motion. It has been demonstrated how especially electrical resistivity (ER) methods, such as electrical resistivity tomography (ERT) or electrical resistivity imaging (ERI), can successfully image the SWC dynamics, as a derived soil property (e.g., Bertermann and Schwarz 2018; Binley et al. 2015; Robinson et al. 2012; Schwartz et al. 2008). Moreover, ER surveys involve the use of several electrodes in galvanic contact with the soil surface and/or subsurface, which allows significant flexibility for the configuration of ER acquisitions at the field scale (Binley et al. 2015). Even though, the most suitable ER configuration needs to be tailored as function of the target problem, and in terms of sensitivity (e.g., horizontal and vertical scales) that can be practically achieved (Ronczka et al. 2015). In this sense, recent ER applications have been conducted in micro-irrigated field conditions for evaluating the wetted fraction area and the irrigation fronts (Cassiani et al. 2015; Hardie et al. 2018; Moreno et al. 2015; Vanella et al. 2018, 2019). Moreover, the rapid development of time-lapse ER measurement systems permits to explore the time domain of eco-hydrological dynamics processes with high accuracy (Jayawickreme et al. 2014; Singha et al. 2015; Williams et al. 2017). However, the use of these approaches for determining the K_s have not yet been exploited, despite it may contribute for better defining the geometry of the wet bulbs, which represents one of the most influential variables for the design and management of drip irrigation systems (Arbat et al. 2013). In this study, time-lapse ERI

surveys were performed to identify the drying/wetting patters of the unsaturated soil profile following the application of deficit irrigation (DI). Strategies integrated with drip irrigation systems. ERI surveys have provided important insights to describe the characteristics of the subsoil in terms of SWC, exploring the ER sensitivity at the different levels of SWC. Therefore, the aims of the study were (1) to identify and characterize the water flow paths occurring during micro-irrigation events, (2) to individuate the mechanisms of mass exchange in the subsoil (i.e., wetting and drying patterns) due to irrigation and plant transpiration (T), and (3) to assess the potentiality of ERI for the soil water motion identification. The general objectives have been achieved by: (a) identifying ER distribution as function of the different SWC conditions during the irrigation season; (b) tracking and assessing the soil drying and wetting patterns through the ER changes during irrigation events supplied at different crop evapotranspiration (ET_c) rates (100, 75 and 50% of ET_c); and (c) evaluating the potential use of ERI in determining K_s by assessing the temporal evolution of the wet bulbs under different irrigation scenarios (full and DI).

7.2 Material and methods

7.2.1 Irrigation set-up and ancillary data

The experimental trial was conducted in an orange orchard planted with 12-year-old trees (*Citrus sinensis* (L.) Osbeck) cv '*Tarocco Sciara*' C1882 grafted on Carrizo citrange root-stock [*Poncirus trifoliata* (L.) Raf. × C. *sinensis* (L.) Osbeck], located in Southern Italy (Sicily) and managed by CREA-OFA (Centro di Ricerca Olivicoltura, Frutticoltura e Agricoltura of the Italian Council for Agricultural Research and Agricultural Economics Analyses). This area presents semi-arid climate conditions, with mean air temperature and relative humidity values of 18.2 °C and 77%, respectively; and annual rainfall and reference evapotranspiration (ET0) values of 1300.7 and 656.6 mm, respectively, for the year 2019. At the orchard

under study, trees were trained with a rounded shape with plant density of 380 trees per hectare for 4 × 6 m spacing. The effective rooting depth ranged between 30 and 40 cm (Cassiani et al. 2015; Vanella et al. 2018). The effects of DI strategies on the soil drying/wetting patterns of the subsoil were compared with a control treatment (T1), which receives 100% of ET_c by two surface drip lines, located directly close to the trunk, each characterized by a flow rate of 4 $L \cdot h^{-1}$ per single-emitter (spaced 0.6 m on each drip line) with a total number of 12 emitters per tree (48 $L \cdot h^{-1}$). The FAO-56 approach (Allen et al. 1998) was implemented for estimating the daily ET_c. Reference ET_0, estimates using "the Penman Monteith equation", was multiplied by the FAO-56 Kc for citrus adjusted by a localized coefficient (i.e., 0.7) calculated as ratio between the canopy cover size (m^2) and the area pertaining to each tree (24 m^2) (Consoli et al. 2006, 2014, 2017; Fereres et al. 1981; Longo-Minnolo et al. 2020; Saitta et al. 2020). The ET_0 values were obtained using hourly and daily meteorological data provided by a weather station located 2-km far from the field site and managed by the "Servizio Informativo Agrometeoro-logico Siciliano (SIAS)". The experimental design consists in a randomized block scheme with 4 irrigation treatments replicate in 3 times; each replica contains 24 trees (e.g., details are given in Consoli et al. 2014, 2017; Puglisi et al. 2019). The adopted DI strategies have the following characteristics: (a) sustained deficit irrigation (T2), receiving 75% of ET_c by two dripper lines buried at 0.35 m from the soil surface, characterized by a flow rate of the single-emitter of 4 and 2 $L \cdot h^{-1}$ (spaced 0.6 m on each drip line), emitting a total of 36 $L \cdot h^{-1}$. This strategy allowed to neglect the evaporation losses (e.g., about 25%, according to Consoli and Papa 2013), being the irrigation doses similar to those provided in T1; (b) regulated deficit irrigation (T3), receiving an irrigation amount of 100% ET_c until DOY (day-of-the-year) 217 in 2019, and 50% ET_c. from DOY 218 till the end of the of the irrigation season, emitting a total of 36

or 24 L · h^{-1} per tree. The irrigation systems specifics are the same as in T1; (c) partial root-zone drying (T4), receiving 50% of ET_c by two surface drip lines located 0.35 m from the trunk line, each characterized by a flow rate of the single-emitter of 4 L · h^{-1} (spaced 0.6 m on each drip line); the drip lines are activated alternatively every week, thus wetting only half of the orange tree root system, emitting a total of 24 L · h^{-1} per tree. The soil texture at the field site is sandy loam, with 65, 12 and 23% of sand, clay and silt, respectively, and average bulk density of 1.25 g · cm^{-3} (Aiello et al. 2014; D'Emilio et al 2018). SWC for field capacity (FC, log of the pressure in h Pa, pF = 2) and wilting point (WP, pF = 4.2) were determined using a sandbox and a pressure plate apparatus as described in Consoli et al. (2017). Ancillary data of SWC (Decagon, Inc., Pullman, WA, USA) and T (Tranzflo NZ Ltd., Palmerston North, NZ) were used for monitoring at hourly scale the soil–water–plant exchanges processes occurring at each irrigation treatment (i.e., full and DI). In particular, 5 SWC probes were installed at the field at 0.3 m below the soil surface, i.e., one for T1–T3 and 2 at both sides of T4 (West and East). Additionally, two trees per treatment (8 in total) were instrumented with a sap flow sensor, located at a height of 0.4 m on the tree trunks, adopting the heat pulse (HP) method and an hoc corrections for wounding effects were applied using 0.48 and 0.33 as fractions of wood and water in the sapwood, respectively (Saitta et al. 2020). Details on sensors installed at the field site are reported in Mary et al. (2019), Vanella and Consoli (2018), and Vanella et al. (2018, 2019).

7.2.2 Electrical resistivity imaging surveys

7.2.2.1 ERI data acquisition

ERI surveys were carried out during the 2019 irrigation season (DOY, 168–278) using 2 ERI arrays (a and b, shown in Figure

7.1). The ERI arrays (with length of 10.65 m) covered simultaneously two irrigation treatments (i.e., T1–T2 in (a) and T3–T4 (b) in Figure 7.1). The ERI arrays consisted of 72 electrodes (stainless steel rods of about 0.15 m, with diameter of 0.03 m) buried for 2/3 of their length into the soil surface with a spacing of 0.15 m. ERI dataset were acquired by a ten-channel Syscal Pro resistivity meter (IRIS Instruments, Orleans, France). The electrode acquisition scheme was a full dipole–dipole skip-2 (with 5,000 direct and reciprocal measurements), because of its inherent strength in solving ER lateral changes (Samoüelian et al. 2005). The high spatial coverage of the adopted ERI configuration permitted to reach depths of investigation of about 1m (Figure 7.1). The average time for each ERI dataset acquisition was about 25 min (Table 7.1). A pulse duration of 250 ms for each measurement cycle and a target of 50 mV for potential readings were set as criteria for current injection. ERI monitoring was performed on different temporal scale: seasonal term and short term. The seasonal-term ERI monitoring allowed the evaluation of the background ER (i.e., at t_0, initial condition, no irrigation) during three periods of the irrigation season (June, July and September; Table 7.1). The short-term ERI monitoring was performed for assessing the temporal evolution of wet bulbs through the acquisition of ERI dataset, with high temporal resolution (time-lapse mode), specifically during (t_1–t_5) and after (t_6–t_7) the irrigation event. Details on ERI acquisitions duration and irrigation timing are reported in Table 7.1.

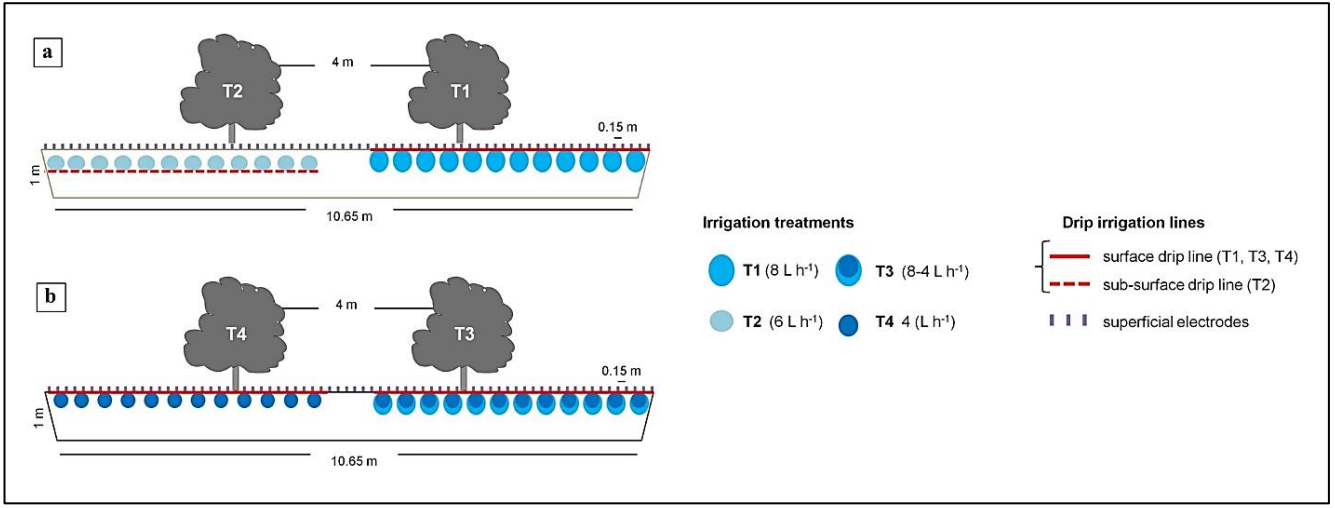

Figure 7.1 - Electrical resistivity imaging (ERI) arrays at the field site: a refers to acquisitions performed at T1 (full irrigation) and T2 (sustained deficit irrigation); and b at T3 (regulated deficit irrigation) and T4 (partial root-zone drying).

Table 7.1 - Time schedule of the seasonal and short-term electrical resistivity imaging (ERI) acquisitions carried out at the field site during irrigation timing (t) for the different day-of-the-year (DOY): t0, denotes the initial condition with no irrigation; t_1–t_5, refer to the irrigation phase and; t_6–t_7 refer to after the end of the irrigation

Irrigation period	Irrigation timing (t)	T1 and T2		T3 and T4	
		Starting (hh:mm)	Ending (hh:mm)	Starting (hh:mm)	Ending (hh:mm)
June (177-179)	t_0	09:04	09:33	08:47	09:16
	t_1	09:04	10:08	09:33	10:01
	t_2	10:01	10:38	10:03	10:31
	t_3	10:42	11:09	10:33	11:01
	t_4	11:11	11:34	11:06	11:35
	t_5	11:46	12:14	11:37	12:05
	t_6	12:02	12:48	12:11	12:39
	t_7	12:51	13:19	12:41	13:01
July (198-200)	t_0	09:06	09:35	08:22	08:51
	t_1	09:38	10:06	08:58	09:27
	t_2	10:08	10:36	09:28	09:57
	t_3	10:38	11:06	10:00	10:29
	t_4	11:08	11:35	10:32	11:01
	t_5	11:38	12:05	11:04	11:33
	t_6	12:01	12:37	11:37	12:06
	t_7	12:39	13.06	12:08	12:37
September (273-275)	t_0	09:00	09:30	08:40	09:10
	t_1	09:34	10:03	09:18	09:47
	t_2	10:05	10:33	09:48	10:17
	t_3	10:35	11:03	10:18	10:51
	t_4	11:06	11:34	10:53	11:23
	t_5	11:38	12:07	11:24	12:00
	t_6	12:12	12:40	12:02	12:31
	t_7	12:42	13.01	12:33	13:02

Note: Starting and ending times (hh:mm) are given in local time. T1–T4 refer to full irrigation, sustained deficit irrigation, regulated deficit irrigation and partial root-zone drying strategies, respectively.

7.2.2.2 ERI data processing

The ERI background and time-lapse dataset were processed with the freeware R2 code (v3.1) (Binley 2016) to obtain forward/inverse solution for two-dimensional (2D) current flow in a finite element mesh. As defined by Binley and Kemna (2005) and Binley (2015), the inverse solution is based on a regularized objective function combined with weighted least squares (an 'Occams' type solution). A 2D triangular mesh generated in Gmsh software (Geuzaine and Remacle 2009), consisting of 5,085 elements and 2,621 nodes, was adopted for the ERI background and time-lapse inversions. They were performed at 10 and 5% error level, respectively (Vanella et al. 2018). The reconstruction of the 2D ERI imagery was performed using Para-View software (v3.8.1).ER changes (in percentage terms, %) were assessed by running the inversion of the ratio between the ERI dataset referred to selected time periods (e.g., t_1, ..., t_7, during and after irrigation, Table 7.1) and the background ERI dataset (t_0, Table 7.1), as follows (Eq. 7.1):

$$d_r = \frac{d_r}{d_0} \times F\left(\sigma_{ohm}\right) \tag{7.1}$$

where d_r is the resistance ratio (Ω), dt e d_0 (Ω) are the resistance dataset of selected time periods (t_1–t_7) and of the initial condition (t_0), and F (ρohm) is the resistance value (Ω) obtained by running the forward model for an arbitrarily chosen ER (i.e., 100 Ωm). This procedure allowed to identifying the ER changes (%) compared to the initial condition (t_0, no irrigation) and, thus, to evidence wetting or drying soil patterns (e.g., the threshold corresponding to a decline/increase in ER was set equal to or greater than 10%). ER changes (%) were mainly related to variations in SWC occurring in T1–T4, assuming that further variables including soil temperature, salinity, and composition and arrangement of soil particles, vary minimally during the ERI short-term monitoring (Samoüelian et al. 2005).

7.2.3 Soil water motion rate measurements

7.2.3.1 ERI-based K_s

The soil water motion rate derived by ERI imagery (K_s, ERI) was calculated as the ratio between the maximum ERI-based wetting depth (d_{ERI}) and the time between two consecutive instants within an irrigation event (t_1–t_5, Table 7.1), as follow (Eq. 7.2):

$$K_{s,ERI} = \frac{\Delta d_{ERI}}{\Delta_t} \quad (7.2)$$

where, Δd_{ERI} (cm) is the difference between the maximum depths reached by the wet bulb at time ti and ti-1, and Δt (s) is the difference between ti and ti−1 during the irrigation event (t_1–t_5).

7.2.3.2 Hydraulic conductivity at saturation measurements

The falling head method (FH) was used to measure the soil saturated hydraulic conductivity ($K_{s, FH}$) at the irrigation treatments (NAVFAC 1986). The $K_{s, FH}$ values were retrieved according to the procedure described by Caselles-Osorio and García (2006) and Pedescoll et al. (2009), consisting in the measurement of the travel time of a water column that moved vertically along an impervious permeameter driven into the soil. The $K_{s, FH}$ apparatus was a steel tube with height equals to 0.65 m and an internal diameter of 0.10 m. To supply a water pulse mode through the tube, a ball valve was connected with another 0.65 m polyethylene terephthalate tube with a capacity of 6.6 L (Figure 7.2). At each treatment, the tube was placed at a distance of 0.5 m from the tree trunk, in a hole pre-drilled into the soil surface (0.3 m depth); and then it was filled with water. A pressure probe (STS–Sensor Technik Sirnach, AG) was inserted inside the tube to measure the pressure (or water heights) variation in time during the soil water motion. The pressure probe

worked through a data logger system (CR 200-R, Campbell Scientific), connected to a laptop, that recorded pressure data every minute up to the entire duration of each $K_{s, FH}$ measurement (set at 60 min).

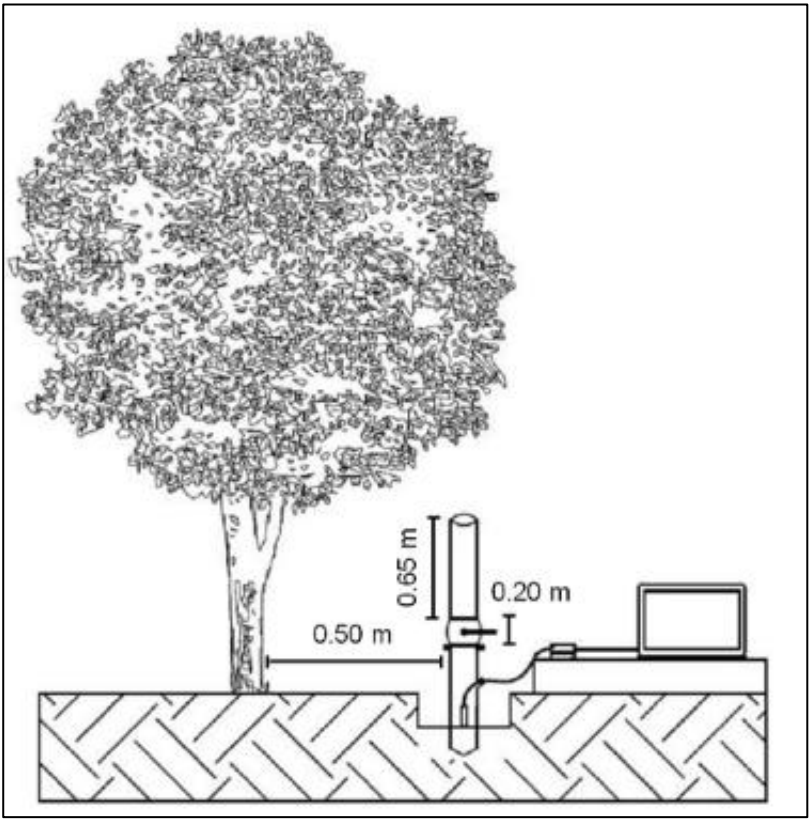

Figure 7.2 - Layout of the in situ saturated hydraulic conductivity measurements using the falling head procedure (Ks, FH)

A total of 5 repetitions per treatment unit (T1–T4) were collected during the 2019 irrigation season. Measurements of $K_{s, FH}$ were performed in the tree row adjacent to the one where ERI surveys were carried out. The relationship between water level into the tube

and time is represented by a negative exponential curve, and its slope is related to the $K_{s,\,FH}$ ($m \cdot s^{-1}$), as follows:

$$K_s = d^2 \frac{\ln(2L \cdot d^{-1})}{8Lt} ln\left(\frac{h_1}{h_2}\right) \quad (7.3)$$

where, d is the diameter of the tube (m); L is the buried length of the tube (m); t is time (s); h_1 and h_2 are the heights of the water level (m) inside the tube at time 1 and time 2 (s), respectively. To derive the $K_{s,\,FH}$ values, the best fit between the observed (h_{obs}) and modeled (h_{mod}) heights of the water level was solved using the ordinary last square method, through an iterative non-linear procedure implemented in Excel solver (Frontline Systems, Incline Village, NV, see Eq. 4.10).

7.2.4 Statistical analyses

The goodness of the relationships between the mean SWC and ER decreasing (%) observed at T1–T4, as well as those retrieved between the mean SWC and the ERI-derived-wet bulb depths, was identified on the basis of the coefficient of determination (R^2). Discrepancies in Ks values among T1–T4 were assessed by performing one-way analyses of variance (ANOVA) (for both $K_{s,\,ERI}$ and $K_{s,\,FH}$) and the treatment mean values were compared each other adopting the Fisher's least significant difference test (LSD) at 0.05 significance level ($p \leq 0.05$)

7.3 Results

7.3.1 General weather patterns, transpiration, irrigation and SWC

During the 2019 irrigation season, the cumulative ET_0 and rainfall values were 643 and 91 mm, respectively (Figure 7.3, a and c);

whereas, the cumulative irrigation amounts were 317, 238, 237 and 159 mm for T1, T2, T3 and T4, respectively. The daily ET_0 and ET_c values observed during the seasonal ERI campaigns in June, July and September, 2019 (see, Table 7.1) were 6.79, 6.51-, and 3.83-mm day^{-1} and 3.32, 3.18- and 1.87-mm day^{-1}, respectively (Figure 7.3, a). As for daily ET_0 and ET_c, a similar decreasing temporal trend throughout the 2019 irrigation season was observed in terms of daily T rates (Figure 7.3, b). At the irrigation treatment level, daily T rates shown average values of 1.55 (± 0.19), 1.10 (± 0.18), 0.86 (± 0.12) and 1.18 (± 0.18) mm day^{-1} in T1, T2, T3 and T4, respectively. In general, the SWC conditions during the irrigation period ranged between the FC (0.28 $m^3 m^{-3}$) and the WP (0.14 $m^3 m^{-3}$) values for the soil under study (showing a water-holding capacity of 0.14 $m^3 m^{-3}$) (Figure 7.3, c). During the seasonal ERI campaigns, hourly SWC values at the initial condition (t_0), ranged from 0.17 to 0.25 $m^3 m^{-3}$ in June, from 0.21 to 0.25 $m^3 m^{-3}$ in July, and from 0.20 to 0.25 $m^3 m^{-3}$ in September, showing SWC higher in T1 and T2 (0.24 ± 0.01 $m^3 m^{-3}$) than that in T3 and T4 (0.20 ± 0.02 $m^3 m^{-3}$)

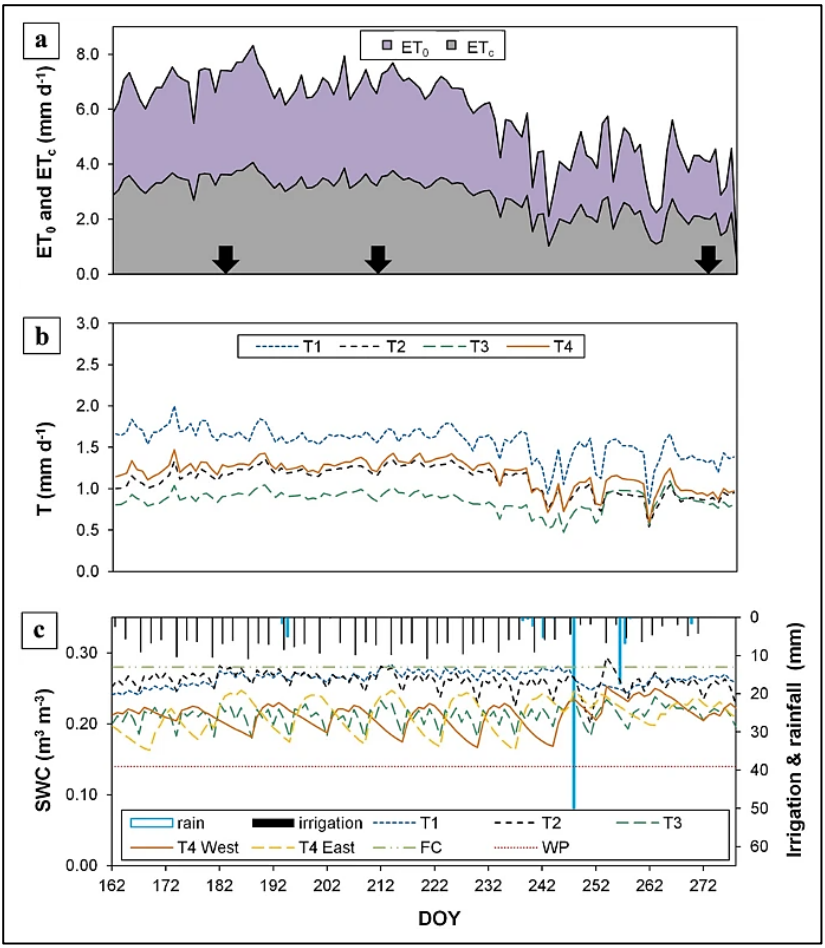

Figure 7.3 - Daily temporal patterns of (**a**) reference (ET_0) and crop (ET_c) evapotranspiration rates (mm day^{-1}); (**b**) transpiration (*T*) (mm day^{-1}), and (**c**) soil water content (SWC) conditions (m^3 m^{-3}), irrigation and rainfall (mm) at the field site from day-of-the-year (DOY) 162–278 (2019). The arrows indicate the periods of the seasonal electrical resistivity imaging (ERI) monitoring. T1–T4 refer to full irrigation, sustained deficit irrigation, regulated deficit irrigation and partial root-zone drying strategies, respectively; FC and WP stand for field capacity and wilting point, respectively

7.3.2 Background ERI images

The Figure 7.4 shows the background ER tomograms at the initial condition (t_0, i.e., no irrigation) in T1–T4, within the seasonal-term ERI monitoring (Table 7.1). Mean ER values (Ω m) showed a decreasing trend of about 16% at all the treatments from the beginning (June) to the end (September) of the 2019 irrigation season (Figure 7.5, a–d). This ER decreasing pattern was higher in T1 (Figure 7.5) and T2 (Figure 7.5) (19% and 20%, respectively) and lower in T3 (Figure 7.5) and T4 (Figure 7.5) (10% and 14%, respectively).

7.3.3 Time-lapse monitoring by ERI

Figures 7.6, 7.7 and 7.8 show the time-lapse inversions of the short-term ERI dataset acquired during (t_1–t_5) and after (t_6–t_7) the irrigation events, compared to the initial condition (t0, Figure 7.4). The mean ER changes (%) observed in T1–T4 during the short-term ERI campaigns are reported in Figure 7.9. Evident contrasts in ER changes (%) became readily apparent for the different irrigation events during the 2019 irrigation season, representing ER increasing (yellow areas) and decreasing (blue areas) patterns. The ER increasing pattern was detected mainly in the deeper soil layers of T4 in June (Figure 7.6 and 7.9), reaching ER increases of about 20% and involving in average 28% of the entire ERI transect. However, the ER decreasing trends represent the most predominant phenomenon, acting especially in the shallow soil layers due to irrigation (Figure 7.6, 7.7, 7.8, 7.9). Generally, irrigation resulted in the formation of individual rounded wet bulbs that became elliptical with time and formed a continuous "wet band" by their overlapping. However, the shape of the wet bulbs identified by ERI (Figure 7.6, 7.7, 7.8) was dependent on the background SWC (t_0) in T1–T4, and on the different flow rates emitted (i.e., 8 L· h^{-1} in T1; 6 L· h^{-1} in T2; 8 L· h^{-1} in T3 until DOY 217 and then 4 L· h^{-1}, 4 L· h^{-1} for T4).

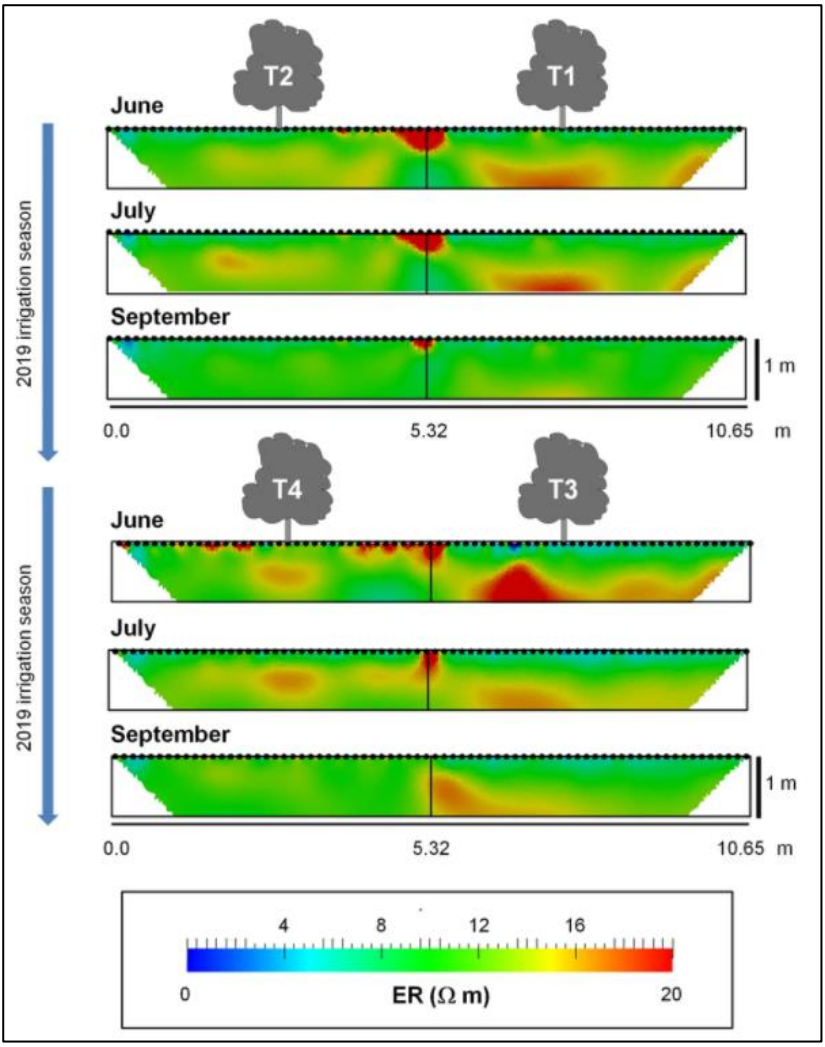

Figure 7.4 – The background electrical resistivity (ER) tomograms at T1–T4 (values are in Ω m) for the field surveys (June, July and September, 2019). T1–T4 refer to full irrigation, sustained deficit irrigation, regulated deficit irrigation and partial root-zone drying strategies, respectively

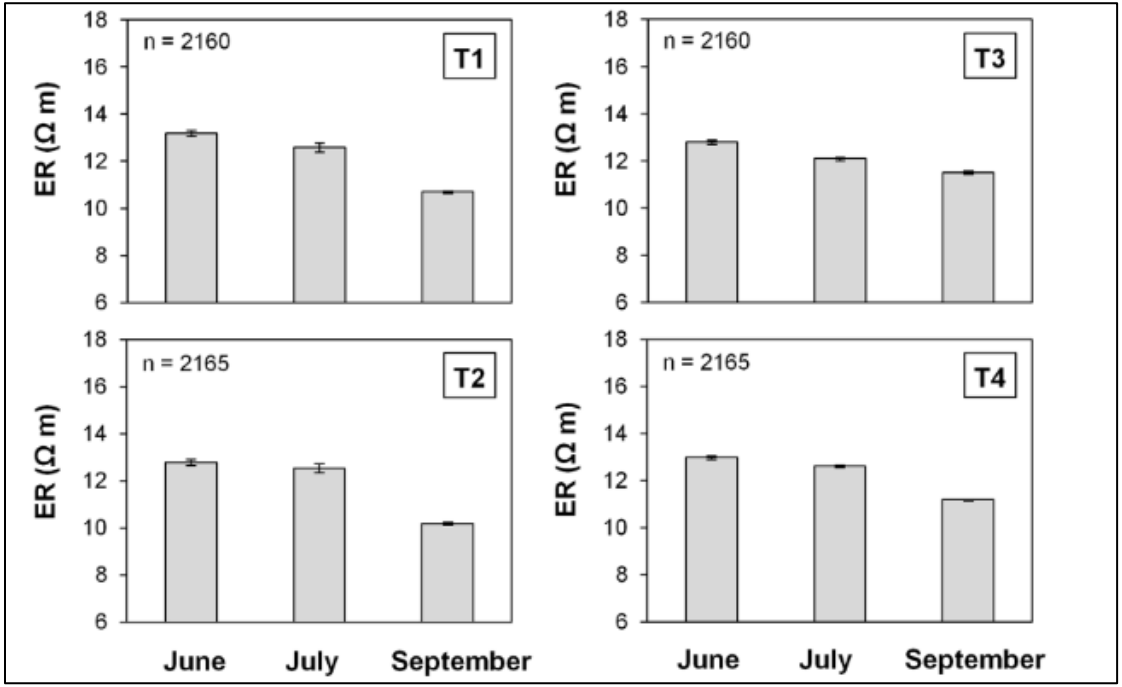

Figure 7.5 - Mean values (and standard error) of electrical resistivity (ER) tomograms (Ω m) at background (t0) for T1 (full irrigation), T2 (sustained deficit irrigation), T3 (regulated deficit irrigation) and T4 (partial root-zone drying); n corresponds to the number of cells of each tomogram

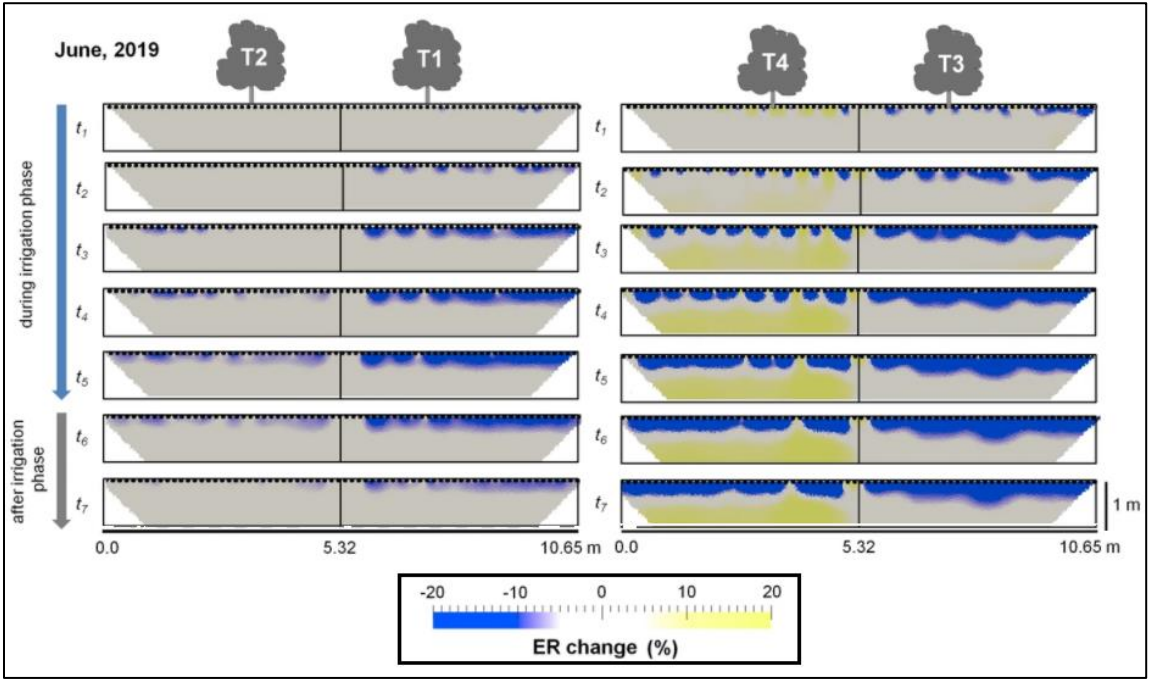

Figure 7.6 - Electrical resistivity (ER) change (%) observed during the irrigation phases and after the irrigation event (t1–t7) compared to the initial condition (t_0) in June, 2019. T1–T4 refer to full irrigation, sustained deficit irrigation, regulated deficit irrigation and partial root-zone drying strategies, respectively

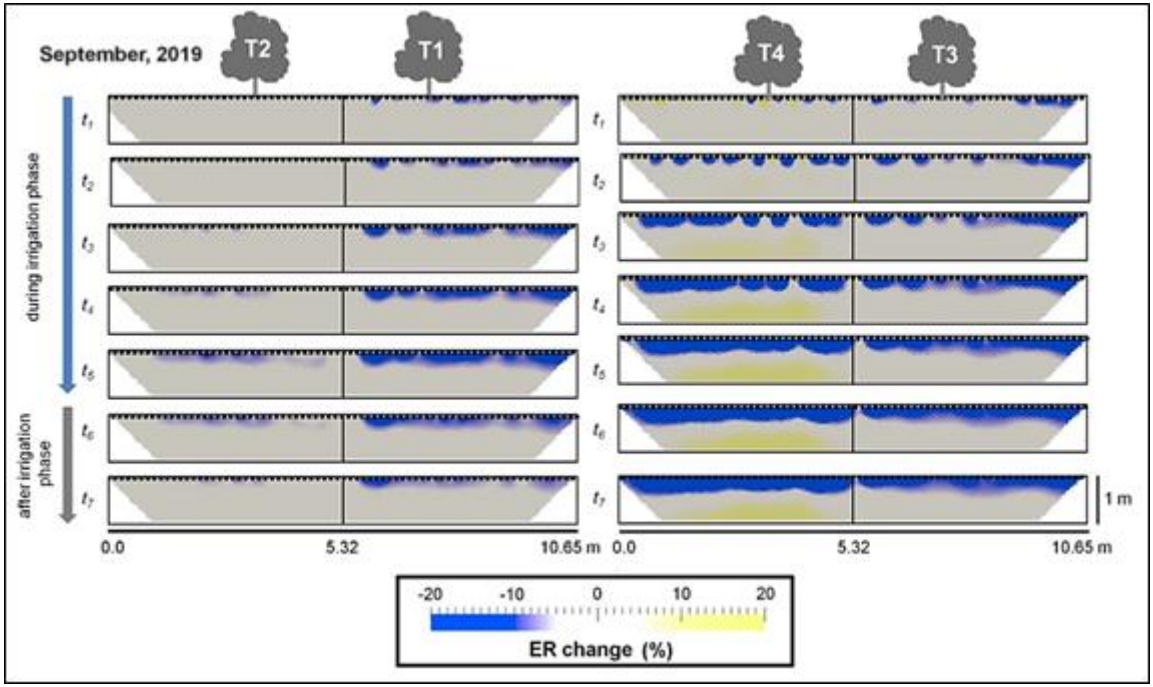

Figure 7.7 - Electrical resistivity (ER) change (%) observed during the irrigation phases and after the irrigation event (t1–t7) compared to the initial condition (t0) in July, 2019. T1–T4 refer to full irrigation, sustained deficit irrigation, regulated deficit irrigation and partial root-zone drying strategies, respectively

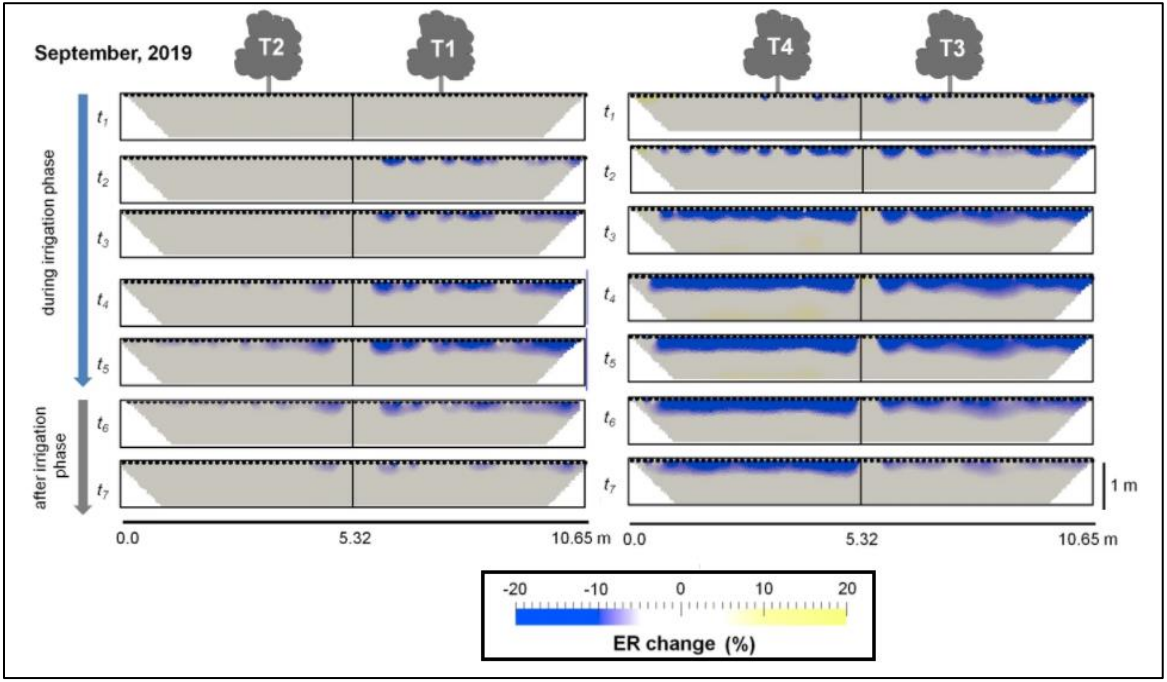

Figure 7.8 - Electrical resistivity (ER) change (%) observed during the irrigation phases and after the irrigation event (t1–t7) compared to the initial condition (t0) in September, 2019. T1–T4 refer to full irrigation, sustained deficit irrigation, regulated deficit irrigation and partial root-zone drying strategies, respectively

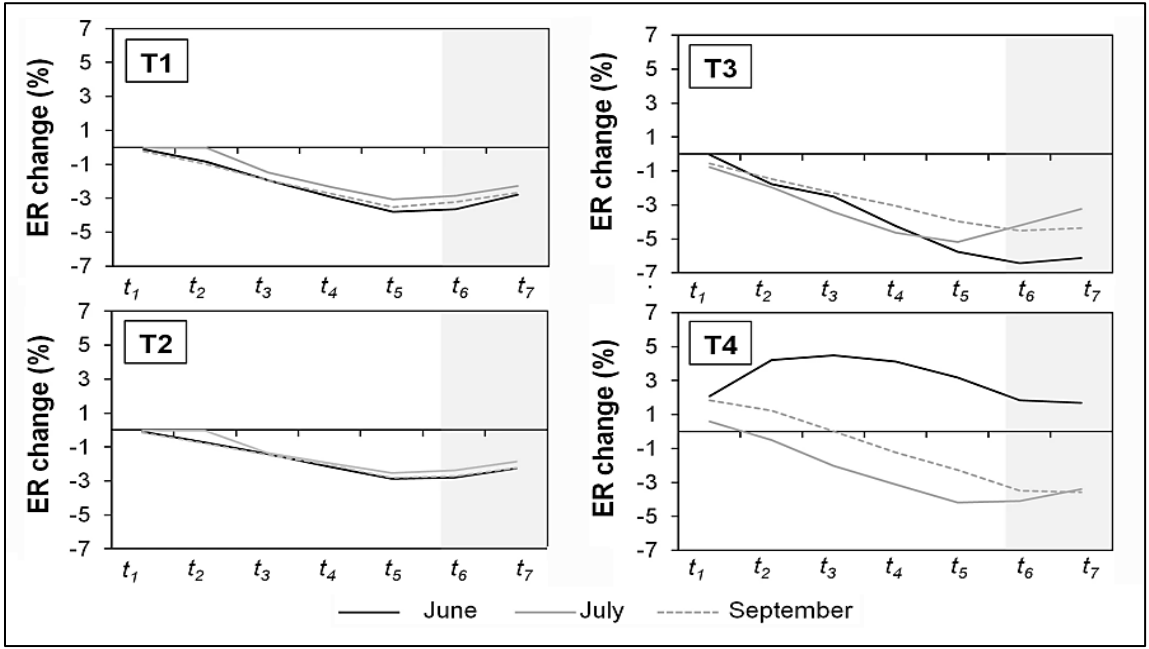

Figure 7.9 - Mean electrical resistivity (ER) change (%) observed during the irrigation phases (t1–t5) and after the irrigation event (shaded area; t6–t7) in comparison to the initial condition (t0, no irrigation period) for the ERI monitoring period (June, July and September, 2019). T1–T4 refer to full irrigation, sustained deficit irrigation, regulated deficit irrigation and partial root-zone drying strategies, respectively.

7.3.4 Emitting rates–wet bulbs relationship

The increasing of the emitter flow rate raised the horizontal radius of the wet bulbs (T1–T3 versus T4). In fact, when the same flow rate was supplied in T1 and T3 (i.e., 8 L · h^{-1}), the horizontal radius was similar in June and July, reaching nearly half of the distance between the emitters (i.e., 0.6 m) at time t2 (Figure 7.6 and 7.7). Such treatments were, thus, characterized by a continuous horizontal band of SWC along the irrigation lines. On September, when T3 was supplied as T4 (4 L · h^{-1}), the wetting fronts of T3–T4 showed smaller horizontal radius (Figure 7.8). On the other hand, increasing the emitter flow rate did not raise the vertical radius of the wet bulbs. In fact, it was quite similar and oscillating around 0.3 m depth from the soil surface in T1, T3 and T4. After the time t3, a prevalent lateral water movement was observed in the irrigation treatments. A stationary pattern was observed at the end of irrigation events (t6–t7), with a decline of magnitude of ER decreasing in average 5% less negative than in t5 (Figure 7.9). No vertical preferential flow patterns were detected.

7.3.5 The SWC–wet bulbs relationship

The Figure 7.10 a, b shows that wet bulbs were identified better when the initial SWC was lower, i.e., in T3 and T4; whereas, their identification was less clear during wetter initial conditions (as in T1 and T2). This behavior was also observed when comparing the decreasing patterns during the seasonal ERI monitoring, being the degree of definition of these decreases less detectable from June to September, 2019. Specifically, a good relationship was observed between the mean hourly SWC measured during the ERI acquisitions and the observed average ER % decrease, with R^2 of 0.79 (Figure10, a). A good relationship was also observed between the mean hourly SWC and the ERI-derived maximum depth of the wet bulbs with R^2 of 0.82 (Figure 10, b).

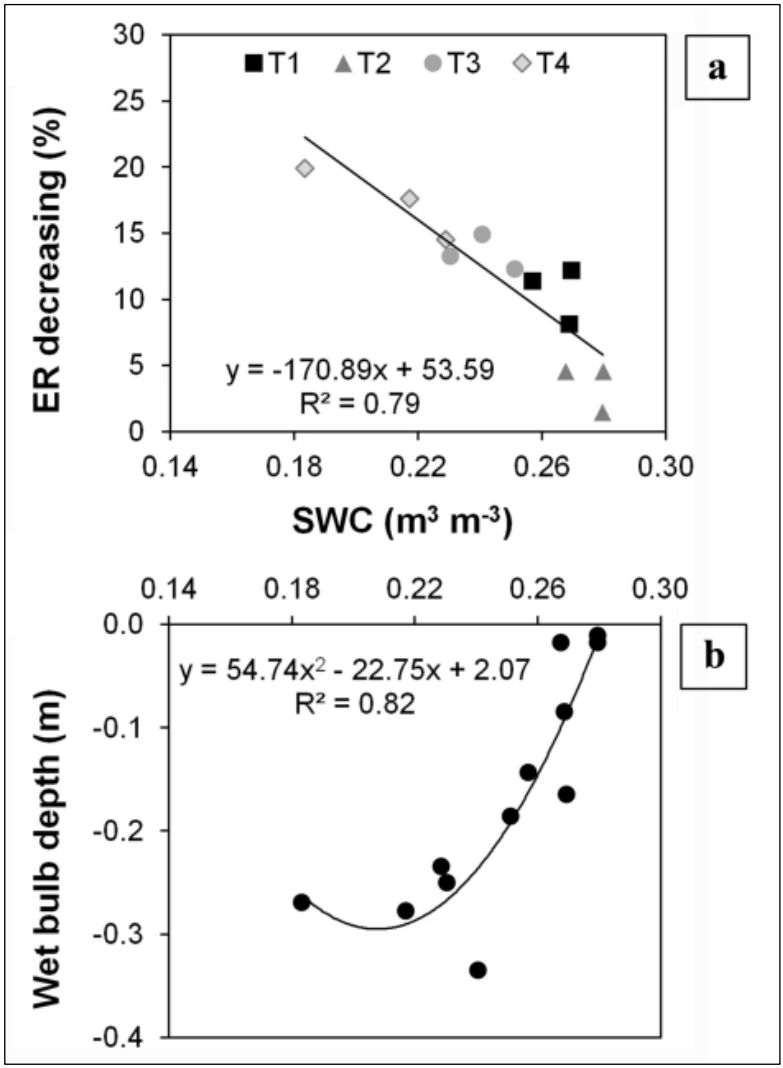

Figure 7.10 - Relationships between the mean soil water content (SWC; $m^3\ m^{-3}$) and an electrical resistivity (ER) decreasing (%); and b the electrical resistivity imaging (ERI)-derived wet bulbs depths (m). T1–T4 refer to full irrigation, sustained deficit irrigation, regulated deficit irrigation and partial root-zone drying strategies, respectively

7.3.5 Hydraulic conductivity at saturation results

The Figure 7.11, shows the mean (± standard error) K_s values (μm s^{-1}) obtained from ERI ($K_{s,\ ERI}$) and FH ($K_{s,\ ERI}$) approaches. In Figure 7.11, a, it is inferred that T2 had the lowest $K_{s,\ ERI}$ value (6.43 μm s^{-1}) showing significant differences with T1 (25.03 μm s^{-1}). The highest $Ks_{,\ ERI}$ values were found in the surface DI treatments (T3–T4) with mean $K_{s,\ ERI}$ values of 36.33 μm s^{-1}, not showing significant differences among them. Different patterns were observed for $K_{s,\ FH}$ values (Figure 7.11, b). Significant differences were found between T4 and T2–T3, with $K_{s,\ FH}$ values of 194.23 μm s^{-1} and 140.38–132.96 μm s^{-1}, respectively. Contrarily, no significant differences were observed between T1 (177.22 μm s^{-1}) and the other treatments. Nevertheless, the magnitudes of $K_{s,\ ERI}$ and $K_{s,\ FH}$ were quite different, presenting the FH measurements one order of magnitude higher than the ERI approach.

7.4 Discussion

In this study, the ERI technique was applied to identify the drying/wetting patters of the unsaturated soil profile following the application of DI strategies integrated with drip irrigation systems. The 2D-ERI surveys provided important insights to describe the characteristics of the subsoil in terms of SWC, exploring the ER sensitivity at the different levels of SWC; this aspect has been scarcely investigated in previous studies (Mary et al. 2019). Following the homogeneous structure of the soil and the climatic conditions at the field site (Figure 7.3), it was shown that the driving factor explaining the decreasing trend in ER is closely related to SWC changes induced by drip irrigation. This consideration is confirmed by independent SWC measurements that showed a transition pattern from drier soil conditions (higher ER values) to wetter conditions (lower ER values), going from June to September during the 2019 irrigation season.

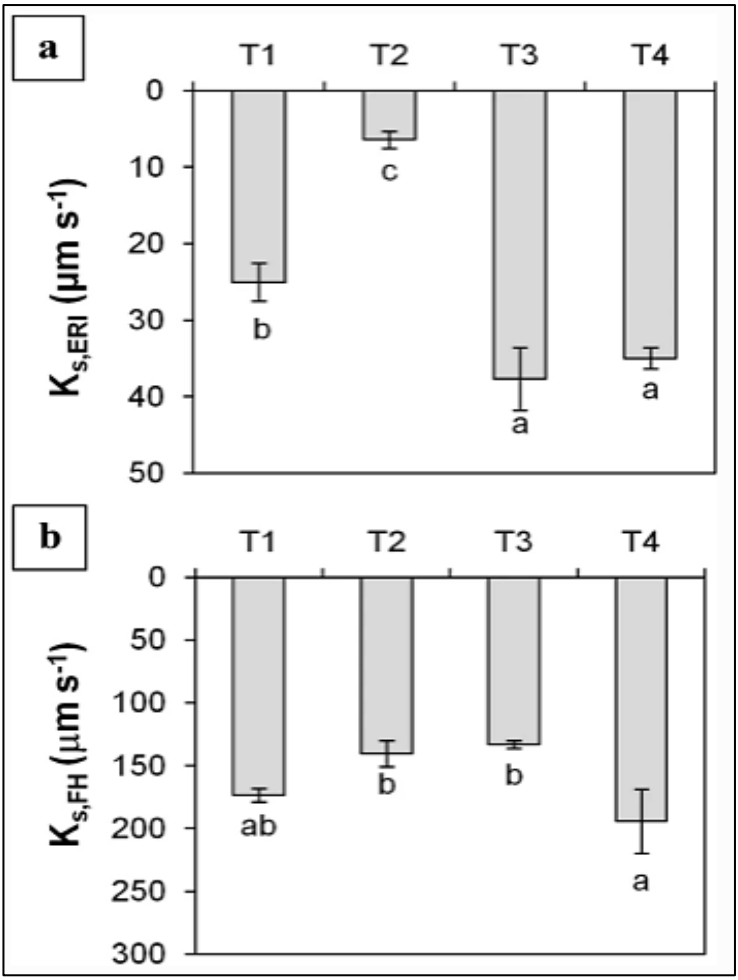

Figure 7.11 - Mean (± standard error) hydraulic conductivity at saturation (K_s) values (µm s^{-1}) derived by (a) electrical resistivity imaging (ERI), Ks, ERI); and (b) falling head (FH) method (Ks, FH). T1–T4 refer to full irrigation, sustained deficit irrigation, regulated deficit irrigation and partial root-zone drying strategies, respectively. Different letters indicate *Ks* significant differences among treatments according to Fisher's least significant difference test (LSD) ($p \leq 0.05$)

It was also confirmed, comparing the seasonal ERI images, that those treatments that received more water (T1 and T2) showed lower ER values than those subjected to more severe DI strategies (T3 and T4) (Figure 7.3 and 7.4). This observation is in line with the results of Cassiani et al. (2015) and Bertermann and Schwarz (2018), which have achieved robust relationships between the ER and the different levels of SWC at the laboratory scale, recognizing the SWC as the most influential soil property. This points out the need of using ancillary data for characterizing the field condition for a realistic interpretation of ERI data (Vanella et al. 2019). The SWC deficit, detected by the increase in ER that occurs in the deeper soil layers of T4 especially in June, was attributed to the combination of higher T rates (Figure 7.3, b) and lower SWC (Figure 7.3, c) recorded in this treatment in com-parison with the other DI treatments. This ER increasing pattern (up to 20%) was not observed in the other DI treatments, since they received more irrigation and, therefore, root-water uptake (RWU) process was partially masked by the higher initial SWC conditions. Similar observations were obtained by other authors (Mares et al. 2016; Mary et al. 2019; Vanella et al. 2018), who detected a strictly alignment between the high T rates derived by sap flow measurements and the decline of SWC retrieved by ERI due to the RWU. However, uncertainties in the estimation of T rates cannot be excluded and need to be addressed (Flo et al. 2019; Motisi et al. 2012). In this regard, a meta-analysis carried out by Flo et al. (2019), using data of 16 studies and 21 species, evidenced that the average accuracy deviation for sap flow. The HP method was about 14%. Probes installation, wounding, scaling sap flow variability and variation in wood parameters were highlighted as the main uncertain sources influencing sap flow HP method accuracies (Flo et al. 2019; Intrigliolo and Castel 2007; Intrigliolo et al. 2009;

Motisi et al. 2012). On the other hand, ER decreasing patterns obtained by the short-term ERI analysis allowed delineating the wet bulbs in different irrigation scenarios (full irrigation versus DI). Small differences were observed between the vertical extent of the wet bulbs formed as a result of the different flow rates (8–4 $L \cdot h^{-1}$), reaching average depths ranging from 0.16 to 0.46 m from the soil surface. This confirmed that the vertical flow component depends mainly on the soil texture (i.e., sandy loam). On the contrary, increasing the flow rate from 4 to 8 $L \cdot h^{-1}$ had a more evident influence on the horizontal component, raising the horizontal radius of the wet bulbs. These findings were in agreement with those reached by Elaiuy et al. (2015), who suggested the use of a wider spacing among drippers when the emitting rates increased from 1.0 to 1.6 $L \cdot h^{-1}$. Moreover, the absence of preferential vertical flow detected by ERI demonstrates the efficiency of the microrotation system and the appropriate irrigation scheduling operating at the field (i.e., no percolation flow means that the whole SWC is available for the RWU). In this scenario, ERI may be considered as a valid tool for evaluating the irrigation system emission uniformity, aiming at monitoring the discharged flow rates of several drippers at the same time (Rossi et al. 2013). Furthermore, the study demonstrates the ability of ERI to detect wet bulbs for SWC between 0.18 and 0.27 $m^3\ m^{-3}$, providing useful information on the DI regime. For example, the SWC observed in T2 did not allow identifying well-defined wet bulbs due to the high initial SWC. The approaches applied to determine Ks in the different irrigation scenarios ($K_{s,\ ERI}$ and $K_{s,\ FH)}$ have revealed different patterns, which also vary in their magnitude, mainly due to the different measurement scales and methodologies adopted. More specifically, $K_{s,\ ERI}$ presented significantly lower values for those treatments with higher SWC (T1 and T2 vs T3 and T4; Figure

7.11), whereas no significant differences were observed in $K_{s,\,FH}$. This could be due to the FH method that started measuring from 30 cm above the soil surface, thus neglecting the upper layer where, as identified by the ERI technique, most of the SWC is present, unifying the effect of the irrigation strategies on $K_{s,\,FH}$. Thus, the soil sampled with FH may not satisfied the saturated conditions at the base of the HF method, which could explain the higher order of magnitude of $K_{s,\,FH}$ compared to $K_{s,\,ERI}$. Additionally, $K_{s,\,ERI}$ (Eq. 7.2) performance mainly depends on the ability of ERI in detecting the wet bulbs which in this study seems to be strictly influenced by the degree of soil saturation. Otherwise, FH approach determines $K_{s,\,FH}$ from the difference of water heights in the permeameter with time, which can be the result not only of a prevalent vertical flow but also of a horizontal one. Even if no preferential vertical flow were individuated by ERI, it is not possible to exclude the presence of preferential horizontally flow due to the roots distribution in T1–T4, that could explain the higher order of magnitude of $K_{s,\,FH}$ values compared to $K_{s,\,ERI}$. Several authors have related the higher infiltration capacity of irrigated soils to the formation of macro-pores due to roots activity, which can contribute almost 85% of the total infiltration variation (Bronick and Lal 2005; Cameira et al. 2003; Wu et al. 2017). However, some authors have pointed out some limitations in the *in-situ* K_s determination, as the necessity of a high number of measurements in order to accurately characterize and represent the wide K_s variability in space and time (Zhang et al. 2019). In particular, $K_{s,\,FH}$ estimates depend on the initial SWC, on the height of the water released in the soil and on the duration of the soil water motion process (Alagna et al. 2016). Furthermore, the FH methodology provides point-based K_s estimations that may not be representative of the entire system, which is partially solved with the use of the ERI technique. However, despite the limitations above-mentioned, the results of this study indicate the potential use of the FH

methodology to evaluate the K_s on the least disturbed layers of the soil (depth > 0.3 m) while the ERI surveys proved to be more useful to determine the effect of irrigation treatments on K_s estimates in unsaturated soils.

7.5 Conclusion

The study herein presented highlighted that hydro geophysical techniques can play an important role in supporting irrigation management strategies for giving insights on the efficiency of the irrigation systems as well as for characterizing the soil water dynamics. On the one hand, ERI has permitted to identify the water flow paths under different drip irrigation scenarios by delineating the wet soil bulbs. The resulting ERI-derived wet soil bulbs have reached similar depths in all irrigation treatments, regardless of flow rates, suggesting that the vertical component of the flow is prevalent and depends mainly on the soil structure. In addition, ERI technique has allowed to evaluate the efficiency of the micro-irrigation through the simultaneous monitoring of the flow supplied by the different drippers, enabling the identification of potential failures in the irrigation system. Furthermore, the absence of preferential vertical flows detected by ERI indicates that the irrigation schedule is appropriate. On the other hand, the identification of subsoil ER patterns has permitted to capture the soil drying effect related to the RWU process, especially in the irrigation strategy characterized by the most severe deficit. Finally, ERI resulted more useful for determining the K_s in unsaturated soils than FH methodology, which provided K_s information mainly referable to the less disturbed soil layers.

8. Conclusions

This work explored different aspects and issues related to the complex matter of water resource management, with a special emphasis on WW treatment by TW. The thesis ranges from theoretical considerations to the analysis of technical aspects related to design, operative modalities, treatment and hydraulic performance. Notwithstanding, in general, TWs have been confirmed to be a reliable and resilient solution for WW treatment and unconventional water recovery and reuse; they are frequently approached as a "black box" in terms of process understanding and evaluation. Still, there is no standardized TW design and operation approach, but they are determined mainly on the basis of the previous results or by long-term experiences. The case studies depicted in this thesis are set in the Sicilian context and suggest inductive methodological approaches, allowing to achieve new levels of comprehension of the related problems with a local insight (Mediterranean climate) for wide-ranging modalities and future prospective. The thesis highlighted that system design and operative options must be carefully planned case-by-case, considering goals, requirements and management needs. In this sense, monitoring activities for treatment and hydraulic performance require optimization and enhanced knowledge to ensure their success in a range of applications. The investigation on TW hydraulics should be performed since the start-up phase emphasizing a multicriterial approach that involves different monitoring methodologies (traditional and innovative) can provide valuable information for TW performance enhancement and design improvement. This could be very useful to apply restorative measurements and prevent negative effects on treatment efficiency, reduce O&M costs, optimize their management, and maximize their longevity.

Specific conclusions have been drawn from study cases depicts

in this thesis: (1) The H-TW system exhibited positive performance even if treating two types of WW, different in terms of nutrient-richness. However, there is still a severe incongruity between the Italian legislation for water reuse and the guidelines proposed by the EU. In fact, at the light of EU guidelines proposed, the water quality reported in this case study would fulfil the minimum requirements for reuse in green area. irrigation, in contrast with the stringent Italian standard limits, which would not be fully accomplished. Therefore, the overcoming of this gap probably remains the crucial point to make effective the WW reuse practice in Italy. (2) The hydraulic behaviour of the HF units of the same system cited in point (1) has evaluated by mean of K_s evaluation and RTD analysis. All the investigations demonstrated that clogging remained in the initial stages of development. The RTD analysis highlighted the good hydraulic performance of HF systems. the K_s values obtained using the FH method and the drainage equation were statistically similar to those obtained during the initial stages of operation under similar conditions. The study demonstrates the collective reliability of these measurements to assess the evolution of the clogging phenomenon in HF-TWs. The study made it possible to extrapolate important information that appears to have delayed the development of the clogging highlighting the strategic role of the settling pond at the beginning stage of the system. A pre-treatment step could be crucial to improve H-TW efficiency and cope with WW variability (particularly in case of nutrient rich effluents during spring/summer season), addressing a feasible option among the intended uses considered. (3) In the HF-TW of a full-scale hybrid TW system functioning as a secondary wastewater treatment system of the IKEA® store, the application of traditional and innovative methods to assess the clogging allowed for the quantification of the phenomenon in the HF-TW, as well as the identification of the most time-efficient and repeatable way to quantify the phenomenon in order to apply restorative measurements and prevent negative effects on treatment

efficiency. Moreover, considering the main advantages and disadvantages of the methods applied, the results highlighted that, especially for large systems, the combination of the newly and traditional approaches is the most efficient way for more thoroughly understanding clogging development in HF-TWs. Despite the partial clogging of HF-TW, the hybrid TW was able to meet the Italian law standards for WW discharge into water bodies. (4) This study investigated the reliability of the pilot H-TW for the metal pollution control in variable storm events unique to Mediterranean conditions. The overall metal retention capability is extremely high and major removal process was due to substrate-related mechanisms. The results showed a significantly high H-TW efficiency for the removal of all studied metals already at the horizontal flow unit outflow, confirming its crucial role. The study indicates that the confinement of pollutants in the substrate and root systems may be beneficial in the control and management of TWs for stormwater runoff treatment applications suggesting the application of TWs for safe stormwater discharge practices and the application of water recovery and reuse, principally when water resources are limited. (5) The hydro-geophysical surveys play a central role in supporting irrigation strategy and its efficiency evaluation, as well as an important tool for understanding the soil water dynamics. ERI and FH as consequence of their different measurement scales and their methodological specificity revealed different patterns and magnitudes among the irrigation treatments. In particular, ERI resulted more useful for determining the K_s in unsaturated soil condition than FH methodology, which provided K_s information mainly referable to the less disturbed soil layers.

References

Adyel, T.M., Oldham, C.E., Hipsey, M.R. (2016) "Stormwater nutrient attenuation in a constructed wetland with alternating surface and subsurface flow pathways: event to annual dynamics" *Water Res*. 107, 66–82.

Ahmad, A., Diwan, H., Abrol, Y.P., Parek, A. (2010) "Global climate change. Stress and plant productivity". In: Sopory, S.K., Bohnert, S.S., Govindjee, H.J. (Eds.), Abiotic Stress Adaption in Plants: Physiological, Molecular and Genome Foundation. Springer Science + Business Media B.V. Springer, Netherlands, pp. 503–521.

Aiello R., Bagarello V., Barbagallo S., Consoli S., Di Prima S., Giordano G., Iovino M. (2014) "An assessment of the Beerkan method for determining the hydraulic properties of a sandy loam soil". *Geoderma* 235:300–307

Aiello R., Bagarello V., Barbagallo S., Iovino M., Marzo A., Toscano A. (2016). Evaluation of clogging in full-scale subsurface flow constructed wetlands. Ecol. Eng. 95, 505–513,

Alagna V., Bagarello V., Di Prima S., Giordano G., Iovino M. (2016) "Testing infiltration run effects on the estimated water transmission properties of a sandy-loam soil". *Geoderma* 267:24–33

Al-Akeel, K. (2017). "The Pollution of Water by Trace Elements Research Trends, Advances in Bioremediation and Phytoremediation" Naofumi Shiomi. IntechOpen - Available from:

Al-Isawi, R.H.K.; Scholz, M.; Wang, Y.; Sani, A. (2015) "Clogging of vertical-flow constructed wetlands treating urban wastewater contaminated with a diesel spill" *Environ. Sci. Pollut. Res*. 2015, 22, 12779–12803,

American Public Health Association (APHA, 2005) Standard Methods for the Examination of Water and Wastewater, 21th ed.; American Public Health

Association (APHA): Washington, DC, USA, 2005.

ANZECC (2000) Australian and New Zealand guidelines for fresh and marine water quality. (Australian Water Association).

APHA (American Public Health Association), AWWA (American Water Works Association), and WPFC (Water Pollution Control Federation), Standard Methods for the Examination of Water and Waste Water, American Public Health Association, Wash, USA, 19th edition, 1998

APHA, 2001. AWWA, WEF, Standard Methods for the Examination of Water and Wastewater, twentieth ed. Washington, DC.

Arbat G., Puig-Bargués J., Duran-Ros M., Barragán J., De Cartagena F.R. (2013) "Drip-irriwater: computer software to simulate soil wetting patterns under surface drip irrigation". *Comput Electron Agric* 98:183–192

Ayaz, S. C., Aktas, Ö., Fındık, N., Akca, L., & Kınacı, C. (2012). "Effect of recirculation on nitrogen removal in a hybrid constructed wetland system". *Ecological Engineering*, 40, 1–5.

Bannerman, R.T., Owens, D.W., Dodds, R.B., Hornewer, N.J. (1993). Sources of pollutants in Wisconsin stormwater. *Water Sci. Technol.* 28 (3–5), 241–259.

Barbagallo S., Cirelli G.L., Marzo A., Milani M., Toscano A. (2011). "Hydraulic behavior and removal efficiencies of two H-SSF constructed wetlands for wastewater reuse with different operational life". *Water Sci. Technol*. 64, 1032-1039.

Beharrell M. (2004), Chapter 19, "Operation and Maintenance for Constructed Wetlands", Editor(s): M.H. Wong, In Developments in Ecosystems, Wetlands Ecosystems in Asia, Elsevier, Vol. 1, 347-359.

Begum S., Mohammad R., Brown R.J. (2008) "A comparative review of stormwater treatment and reuse techniques with a new approach: Green Gully". *WSEAS Transactions on environment and development*, 4(11), pp. 1002-1013

Ben Salem, Z., Laffray, X., Al-Ashoor, A., Ayadi, H., Aleya, L. (2017). "Metals and metalloid bioconcentrations in the tissues of Typha latifolia

grown in the four interconnected ponds of a domestic landfill site". *J. Environ. Sci.* 54, 56-68

Bertermann D. and Schwarz H. (2018) "Bulk density and water content-dependent electrical resistivity analyses of different soil classes on a laboratory scale". *Environ Earth Sci* 77(16):570.

Binley A. (2016) R2 version 3.1 Lancaster University website: http://www.es.lancs.ac.uk/people/amb/Freeware/R2/R2.htm. Accessed 1 Jun 2019.

Binley A. (2015) Tools and techniques: DC electrical methods. In: Schubert G (ed) Treatise on geophysics, 2nd edn, vol 11. Elsevier, Amsterdam, pp 233–259.

Binley A., Hubbard S.S., Huisman J.A., Revil A., Robinson D.A., Singha K., Slater L.D. (2015) "The emergence of hydrogeophysics for improved understanding of subsurface processes over multiple scales". *Water Resour Res* 51(6):3837–3866.

Binley A. and Kemna A. (2005) "DC Resistivity and Induced Polarization Methods. In: Rubin Y, Hubbard SS (eds) Hydrogeophysics". *Water Science and Technology* Library, vol 50. Springer, Dordrecht.

Birch, G.F., Matthai C., Fazeli M.S. (2004). Efficiency of a constructed wetland in removing contaminants from storm water. Wetlands 24,459.

Birch, G.F., Matthai C., Fazeli M.S. (2004). Efficiency of a constructed wetland in removing contaminants from storm water. Wetlands 24,459.

Bodin, H., Persson, J., Englund, J.E., Milberg, P. (2013) "Influence of residence time analyses on estimates of wetland hydraulics and pollutant removal". *J. Hydrol*., 501, 1–12.

Bogena H.R., Huisman J.A., Güntner A., Hübner C., Kusche J., Jonard F., Vey J., Vereecken H. (2015) "Emerging methods for noninvasive sensing of soil moisture dynamics from field to catchment scale: A review". *Wiley Interdiscip Rev Water* 2(6):635–647.

Bolton L., Joseph S., Greenway M., Donne S., Munroe P., Christopher Marjo C. E. (2019) "Phosphorus adsorption onto an enriched biochar substrate in

constructed wetlands treating wastewater", *Ecological Engineering: X*, Volume 1, 100005.

Bonadonna L., Briancesco R., D'Angelo A.M, Marini, R. (2002). "Clostridium perfringens as an environmental pollution indicator and its hygienic role". Istituto Superiore di Sanità, 39 p. Rapporti ISTISAN 02/8.

Bonanno, G., Cirelli, G.L. (2017). "Comparative analysis of element concentrations and translocation in three wetland congener plants: Typha domingensis, Typha latifolia and Typha angustifolia". *Ecotoxicol. Environ.* Saf. 143, 92–101.

Boog J., Nivala J., Aubron T., Mothes S., van Afferden M., Müller R.A., (2018) "Resilience of carbon and nitrogen removal due to aeration interruption in aerated treatment wetlands",
Sc. of The Tot. Environ., Vol. 621, 960-969.

Boretti, A. and Rosa, L. (2019) "Reassessing the projections of the World Water Development Report", *Clean Water* 2, 15.

Bresciani and Masi (2013) "Manuale pratico di Fitodepurazione" Terra Nuova eds. Città di Castello, Italy.

Brindt N., Rahav M., Wallach R. (2019) "ERT and salinity a method to determine whether ERT-detected preferential pathways in brackish water-irrigated soils are water-induced or an artifact of salinity". *J Hydrol* 574:35–45

Brix H. (1994) "Functions of macrophytes in constructed wetlands". *Water Science and Technology, Vol.* 29 (4), 71–78.

Cameira M.R., Fernando R.M., Pereira L.S. (2003) "Soil macropore dynamics affected by tillage and irrigation for a silty loam alluvial soil in southern Portugal". *Soil Tillage Res.* 70(2):131–140.

Campbell G.S., Norman J.M. (1998) "Water flow in soil. In: An introduc-tion to environmental biophysics". *Springer,* New York

Carranza-Álvarez, C., Alonso-Castro, A.J., Alfaro-De La Torre, M.C., García-De La Cruz, R.F. (2008). "Accumulation and distribution of heavy

metals in Scirpus americanus and Typha latifolia from an artificial lagoon in San Luis Potosí, México. *Water Air Soil Pollut*. 188, 297–309.

Carrasco-Acosta P., Garcia-Jimenez P., Herrera-Melián J.A., Peñate-Castellano N., Rivero-Rosales A. (2019) "The effects of plants on pollutant removal, clogging, and bacterial community structure in palm mulch-based vertical flow constructed wetlands" *Sustainability*, Vol. 11, 632.

Carvalho, P.N.; Araújo, J.L.; Mucha, A.P.; Basto, M.C.P.; Almeida, C.M.R. (2013) "Potential of constructed wetlands microcosms for the removal of veterinary pharmaceuticals from livestock wastewater". *Bioresource. Technol*. Vol. 134, 412–416.

Caselles-Osorio A, Garcia J (2007) "Effect of physico-chemical pre-treatment on the removal efficiency of horizontal subsurface-flow constructed wetlands" *Environ. Pollut.* 146, 55–63.

Caselles-Osorio A, Puigagut J, Segù E, Vaello N, Granès F, Garcia D, Garcia J (2007), "Solids accumulation in six full-scale subsurface flow constructed wetlands". *Water Research*, Vol. 41, 1388-1398.

Cassiani G., Boaga J., Vanella D., Perri M.T., Consoli S. (2015) "Monitoring and modelling of soil–plant interactions: the joint use of ERT, sap flow and eddy covariance data to characterize the volume of an orange tree root zone". *Hydrol Earth Syst Sci* 19(5):2213–2225

Chazarenc, F.; Gérard, M.; Gontheir, Y. (2003) "Hydrodynamics of horizontal subsurface flow constructed wetlands". *Ecol. Eng*., 21, 165–173.

Chen, H (2011) Surface-Flow Constructed Treatment Wetlands for Pollutant Removal: Applications and Perspectives. *Wetlands* Vol. 31, 805–814.

Chubaka, E.C., Whiley, H., Edwards, J.W., Ross, K.E. (2018). "Lead, zinc, copper, and cadmium content of water from South Australian rainwater tanks". Int. *J. Environ. Res. Public Health* 15 (7), 1551.

Ciaponi, C., Papiri, S., Sanfilippo, U., Todeschini, S. (2014). "Acque di prima pioggia nei sistemi di fognatura". Manuale di progettazione. Centro Studi Idraulica Urbana (CSDU)©, Hoepli S.p.A (ISBN 978-88-203-6322-2).

Cirelli, G.L., Consoli S., Di Grande V., Milani M., Toscano A. (2007) "Subsurface constructed wetlands for wastewater treatment and reuse in

agriculture: five years of experiences in Sicily, Italy". *Water Sci Technol.* Vol. 56, (3), 183–191.

Cohen-Shacham, E., Walters, G., Janzen, C. and Maginnis, S. (eds.) (2016) "Nature-based Solutions to address global societal challenges. Gland, Switzerland: IUCN.

Consoli S., O'Connell N., Snyder R. (2006) "Measurement of light interception by navel orange orchard canopies: case study of Lindsay", California. *J Irrig Drain* E ASCE 132(1):9–20

Consoli S. and Papa R. (2013) Corrected surface energy balance to measure and model the evapotranspiration of irrigated orange orchards in semi-arid Mediterranean conditions. *Irrig Sci* 31:1159–1171.

Consoli S., Stagno F., Roccuzzo G., Cirelli G.L., Intrigliolo F. (2014) "Sustainable management of limited water resources in a young orange orchard". *Agric Water Manag* 132:60–68

Consoli S., Stagno F., Vanella D., Boaga J., Cassiani G., Roccuzzo G. (2017) "Partial root-zone drying irrigation in orange orchards: effects on water use and crop production characteristics". *Eur J Agron* 82:190–202

Cooper P. "The performance of vertical flow constructed wetland systems with special reference to the significance of oxygen transfer and hydraulic loading rates". *Water Sci. Technol.* 1 May 2005; 51 (9): 81–90.

Corbella C, García J., Puigagut J. (2016) "Microbial fuel cells for clogging assessment in constructed wetlands" *Science of The Total Environment*, Vol. 569–570: 1060-1063.

Cui, L., Ouyang, Y., Lou, Q., Yang, F., Chen, Y., Zhu, W., Luo, S. (2010). Removal of nutrients from wastewater with Canna indica L. under different vertical-flow constructed wetland conditions. *Ecol. Eng.* 36, 1083–1088.

Cui, X., Fang, S., Yao, Y., Li, T., Ni, Q., Yang, X., He, Z. (2016). "Potential mechanisms of cadmium removal from aqueous solution by Canna indica derived biochar". *Sci. Total Environ*. 562, 517–525.

Cule, N., Vilotic, D., Nesic, M., Veselinovic, M., Drazic, D., Mitrovic, S. (2016) "Phytoremediation potential of Canna indica L. in water contaminated

with lead. *Fresenius Environ. Bull*. 25 (9), 3728–3733.

De Feo G., De Antoniou, G., Fardin H. F., El-gohary F., Zheng X. Y., Reklaityte I., Butler D., Yannopoulos, S., Angelakis, A.N. (2014). "The Historical Development of Sewers Worldwide (June)", Sustainability, 3936–3974.

Debarati G.S., Hoyois P., Wallemacq P., Below R. (2016) Annual Disaster Statistical Review 2017 The numbers and trends – Technical report - Université Catholique de Louvain, Institut de Recherche Santé et Société

D'Emilio A., Aiello R., Consoli S., Vanella D., Iovino M. (2018) "Artificial neural networks for predicting the water retention curve of Sicilian agricultural soils". *Water* 10(10):1431

Dhote, S. and Dixit, S. (2009) "Water quality improvement through macrophytes—a review". *Environ. Monit. Assess*. 152, 149–153.

Dixit, A., Dixit, S., Goswami, C.S. (2014) "Study on the assessment of adsorption potential of dry biomass of Canna indica with reference to heavy metal ions from aqueous solutions". *J. Chem. Eng. Process. Technol.* 5, 189.

Dotro, G., Langergraber G., Molle P., Nivala J., Puigagut J., Stein O., Von Sperling M. (2017). *Treatment wetlands*. IWA publishing.

Drizo, A., Frost, C.A., Grace, J., Smith, K.A. (2000) "Phosphate and ammonium distribution in a pilot-scale constructed wetland with horizontal subsurface flow using shale as a substrate". *Water Res*. 2000, 34, 2483–2490.

EC, European Commission (2019)
http://europa.eu/rapid/press-release_IP-19-1475_en.htm

Elaiuy M.L., Santos L.N.D., Sousa A., Souza C.F. (2015) "Wet bulbs from the subsurface drip irrigation with water supply and treated sewage effluent". *Engenharia Agríc* 35(2):242–253

European Union EU (2018)
http://ec.europa.eu/environment/water/pdf/water_reuse_regulation.pdf 448

Ergaieg, K., Msaddek, M.H., Kallel, A. (2021) "Monitoring of horizontal subsurface flow constructed wetlands for tertiary treatment of municipal

wastewater". *Arab J Geosci* **14,** 2045

FAO (1994) http://www.fao.org/3/T0234e/T0234E04.htm

Fernandez-Fernandez, M.I., Vega P.T.M., Jaramillo-Morán, M.A., Garrido M. (2020) "Hybrid Constructed Wetland to Improve Organic Matter and Nutrient Removal". *Water* Vol. 12, 2023.

Fereres E., Pruitt W.O., Beutel J.A., Henderson D.W., Holzapfel E., Schulbach H., Uriu K. (1981) "Evapotranspiration and drip irrigation scheduling. In: *Drip irrigation management*. University of California, Leaflet, pp. 8–13.

Fisher, P.J (1990) "Hydraulic characteristics of constructed wetlands at Richmond, New South Wales, Australia. *In Constructed Wetlands in Water Pollution Control*; Cooper, P.F., Findlater, B.C., Eds.; Pergamon Press: Oxford, UK, 1990; pp. 21–32

Flo V., Martinez-Vilalta J., Steppe K., Schuldt B., Poyatos R. (2019) "A synthesis of bias and uncertainty in sap flow methods. *Agr. For.t Met.* 271:362–374

Foladori P., Ruaben J., Ortigara A.R.C. (2013) "Recirculation or artificial aeration in vertical flow constructed wetlands: A comparative study for treating high load wastewater", *Bioresource Technology*, Vol. 149, 398-405,

Frumin G.T., Gildeeva I.M. (2014) "Eutrophication of water bodies — A global environmental problem". *Russ J Gen Chem* Vol. 84, 2483–2488.

García J., Diederik P., Rousseau L., Morató J., Lesage E., Matamoros V., Bayona J.M. (2010) "Contaminant Removal Processes in Subsurface-Flow Constructed Wetlands: A Review, Critical Reviews" *Environmental Science and Technology*, Vol. 40 (7), 561-661.

Garcia-Artigas, R.; Himi, M.; Revil, A.; Lovera, R.; Sendrós, A.; Casas, A.; Rivero, L. (2020 "Time-domain induced polarization as a tool to image clogging in treatment wetlands". *Sci. Total Environ*. 2020, 724, 138189.

García-Tejera O., López-Bernal Á., Orgaz F., Testi L., Villalobos F.J. (2017) "Analysing the combined effect of wetted area and irrigation volume on olive tree transpiration using a SPAC model with a multi-compartment soil solution". *Irrig Sci* 35(5):409–423

Gerke S., Baker L.A., Xu Y. (2001). Nitrogen Transformations in a Wetland Receiving Lagoon Effluent: Sequential Model and Implications for Water Reuse". Water Res. 35, 3857-3856.

Geuzaine C. and Remacle J.F. (2009) "Gmsh: a three-dimensional finite element mesh generator with built-in pre- and post-processing facilities". *Int J Numer Methods. Eng*. 79(11):1309–1331

Ghrabi A., Bousselmi L., Masi F., Regelsberger M. (2011) "Constructed wetland as a low cost and sustainable solution for wastewater treatment adapted to rural settlements: the Chorfech wastewater treatment pilot plant". *Water Sci Technol*. Vol. 63 (12), 3006–3012.

Gill, L.W., Ring, P., Higgings, N.M.P., Johnston, P.M. (2014). Accumulation of heavy metals in a constructed wetland treating road runoff. *Ecol. Eng.* 70, 133–139.

Gopkar, N.S., Sahare, A.B., Patil, U.S., 2017. Bio-sorption of heavy metal ions from aqueous solutions using dry biomass of Canna indica. *Int. J. Appl. Res.* 3 (3S), 43–46.

Guo L., Liu Y., Wu G.L., Huang Z, Cui Z., Cheng Z., Zhang R.Q., Tian F.P., He H. (2019) "Preferential water flow: influence of alfalfa (*Medicago sativa* L.) decayed root channels on soil water infiltration". *J. Hydrol* 578:124019

Kabata-Pendias, A., 2011. Trace Elements in Soils and Plants. Fourth edition. Taylor & Francis Group, Boca Raton, FL, USA (534 pp.).

Karathanasis, A. and Johnson, C., 2003 "Metal removal potential by three aquatic plants in an acid mine drainage wetland mine". *Water Environ*. 22, 22.

Klink, A., Macioł, A., Wisłocka, M., Krawczyk, J. (2013) "Metal accumulation and distribution in the organs of Typha latifolia for heavy metal removal from wastewater". *Ecotoxicol. Environ. Saf*. 112, 80–86.

Goonetilleke, A., Liu, A., Managi, S., Wilson, C., Gardner, T., Bandala, E. R., Holden, J. (2017) "Stormwater reuse, a viable option: Fact or fiction?" *Economic Analysis and Policy*, 56, 14–17.

Gorgoglione A. and Torretta V. (2018) "Sustainable Management and

Successful Application of Constructed Wetlands: A Critical Review". *Sustainability* Vol. 10, 3910.

Guo Y., Cui, Y., Dong B., Liu. F (2017) "Tracer study of the hydraulic performance of constructed wetlands planted with three different aquatic plant species". *Ecol. Eng*. 102, 433-442.

Haddis A., Van der Bruggen B., Smets I. (2020) "Constructed wetlands as nature-based solutions in removing organic pollutants from wastewater under irregular flow conditions in a tropical climate, *Ecohydrology & Hydrobiology*, Vol. 20 (1), 38-47.

Hansson A., Pedersen E., Weisner S.E.B. (2012) "Landowners' incentives for constructing wetlands in an agricultural area in south Sweden" *J. Environ. Manag*., Vol. 113 (2012), 271-278.

Hardie M., Ridges J., Swarts N., Close D. (2018) "Drip irrigation wet-ting patterns and nitrate distribution: comparison between electrical resistivity (ERI), dye tracer, and 2D soil–water modelling approaches". *Irrig Sci* 36(2):97–110

Hua G.F., Zhao Z.W., Kong J. (2014) "Effects of plant roots on the hydraulic performance during the clogging process in mesocosm vertical flow constructed wetlands". *Environ. Sci. Pollut. Res*. 21**,** 13017–13026.

Hua T. and Hynes R.J. (2016) "Constructed wetlands: fundamental processes and mechanisms for heavy metal removal from wastewater streams" Inter. Journal of Env. Eng., Vol.8 (2/3), 148 – 178.

Holland J.F., Martin J.F., Granata T., Bouchard V., Quigley M., Brown L.C. (2004). Effects of wetland depth and flow rate on residence time distribution characteristics. Ecol. Eng. 23, 189 –203.

Ibrahim M.M and Aliyu J. (2016) "Comparison of methods for saturated hydraulic conductivity determination: field, laboratory and empirical measurements (a preview). *J Appl Sci Technol* 15(3):1–8.

Intrigliolo D.S., Castel J.R. (2007) "Evaluation of grapevine water status from trunk diameter variations". *Irrig Sci* 26:49–59.

Intrigliolo D.S., Lakso A.N., Piccioni R.M. (2009) "Grapevine cv. 'Riesling' water use in the northeastern United States. *Irrig Sci* 27:253–262.

Ioannidou, V.G., Pearson, J.M. (2018) “Hydraulic and Design Parameters in Full-Scale Constructed Wetlands and Treatment Units: Six Case Studies”. *Environ. Process*. Vol. 5, 5–22.

Jayawickreme D.H., Jobbágy E.G., Jackson R.B. (2014) “Geophysical subsurface imaging for ecological applications. *New Phytol* 201(4):1170–117

Justin M.Z., Zupančič M. (2009) “Combined purification and reuse of landfill leachate by constructed wetland and irrigation of grass and willows” *Desalination*, Vol. 246 (1–3), 157-168.
Kadlec R.H. (2009) “Comparison of free water and horizontal subsurface treatment wetlands” *Ecological Engineering*, Vol. 35, (2), 159-174.

Kadlec R.H., Knight R.L. (1996) “Treatment Wetlands, First Edition”. Boca Raton, Florida: CRC Press.

Kadlec R.H., Wallace S.D. (2008) Treatment Wetlands, Second Edition. Boca Raton, Florida: CRC Press.

Kandra H., McCarthy D., Deletic A. (2015). Assessment of the impact of stormwater characteristics on clogging in stormwater filters. Water Resour. Manag. 29, 1031–1048.

Karathanasis, A.D., Potter C.L., Coyne M.S. (2003) “Vegetation effects on fecal bacteria, BOD, and suspended solid removal in constructed wetlands treating domestic wastewater”, *Ecol. Eng.*, Vol. 20 (2) 157-169,

Keller C.H. and Bays J.S. (2000). Tracer studies for treatment wetlands. In Treatment Wetlands for Water Quality Improvement, Quebec, Canada, 2000; CH2MHILL.

Khan S., Ahmad I., Tahir Shah M.., Rehman S., Khaliq A. (2009) “Use of constructed wetland for the removal of heavy metals from industrial wastewater”. *Journal of Environmental Management*. Vol. 90, (11), 3451-3457.

Klepper B. (1991) “Crop root system response to irrigation”. *Irrig. Sci* 12(3):105–108.

König M., Escher B.I., Neale P.A., Krauss, M., Hilscherová K., Novák J., Teodorovìc I., Schulze T.; Seidensticker S., Hashmi M.A.K (2017) “Impact of untreated wastewater on a major European river evaluated with a combination of In Vitro bioassays and chemical analysis”. *Environ. Pollut*. 220, 1220–1230.

Knowles P.R. and Davies P.A. (2012) “A method for the in-situ determination of the hydraulic conductivity of gravels as used in constructed wetlands for wastewater treatment”. Desalination and Water Treat. 1, 257–266.

Knowles P., Dotro G., Nivala J., Garcia J. (2011) “Clogging in subsurface-flow treatment wetlands: occurrence and contributing factors”. *Ecol Eng*. 37, 99–112.

Knowles, P.R.; Griffin, P.; Davies, P.A. (2010) “Complementary methods to investigate the development of clogging within a horizontal subsurface flow tertiary treatment wetland”. *Water Res.*, 44, 320–330.

Lavrnić S., Zapater-Pereyra M., Cristino S., Cupido, D., Lucchese, G., Pascale M.R., Toscano, A., Mancini, M. (2020) “The Potential Role of Hybrid Constructed Wetlands Treating University Wastewater—Experience from Northern Italy” *Sustainability* 2020, Vol. 12, 10604.

Langergraber G. and Haberl R. (2001) "Constructed wetlands for water treatment." *Minerva Biotecnologica* Vol. 13 (2) 123.
Lee C., Fletcher T.D., Sun G. (2009) “Nitrogen removal in constructed wetland systems” *Eng. Life Sci*., Vol. 9, 11-22

Legislative Decree 152 (2006) “Decreto Legislativo 3 aprile 2006, n.152”, 'Normative requirements on the environment’, GU n. 88, April 14th 2006.

Le Coustumer S., Fletcher T.D., Deletic A., Barraud S., Poelsma P. (2012). The influence of design parameters on clogging of stormwater biofilters: a large-scale column study. Water Res. 46, 6743–6752,

Li Y., Guibing Zhu G., Jern Ng W., Keat Tan S. (2014) “A review on removing pharmaceutical contaminants from wastewater by constructed wetlands: Design, performance and mechanism”. Sc. of The Tot. Envir. Vol. 468-469, 908-932.

Li D., Zheng B., Liu Y., Chu Z., He Y., Huang M. (2018) "Use of multiple water surface flow constructed wetlands for non-point source water pollution control". *Appl Microbiol Biotechnol* 102, 5355–5368.
Licciardello F., Aiello R., Alagna V., Iovino, M., Ventura, D., Cirelli G.L. (2019) Assessment of clogging in constructed wetlands by saturated hydraulic conductivity measurements. Water Sci. Technol. 79, 314-322,

Licciardello F., Milani M., Consoli S., Pappalardo N., Barbagallo S., Cirelli G.L. (2018). Wastewater tertiary treatment options to match reuse standards in agriculture. Agricultural Water Management. 210, 232-242,

Licciardello F., Sacco A., Barbagallo S., Ventura D., Cirelli G.L. (2020) Evaluation of Different Methods to Assess the Hydraulic Behavior in Horizontal Treatment Wetlands. Water 2020, 12, 2286.

Liu H., Hu Z., Song S., Zhang J., Nie L., Hu H., Li F., Liu Z. (2018) "Quantitative detection of clogging in horizontal subsurface flow constructed wetland using the resistivity method". *Water* 10:1334.

Longo-Minnolo G., Vanella D., Consoli S., Intrigliolo D.S., Ramírez-Cuesta J.M. (2020) "Integrating forecast meteorological data into the ArcDualKc model for estimating spatially distributed evapotranspiration rates of a C*itrus orchard*. *Agric Water Manag* 231:105967

Malaviya, P., Singh, A. (2012) "Constructed wetlands for management of urban stormwater runoff. Crit. Rev." *Environ. Sci. Technol.* 42 (20), 2153–2214.

Maloszewski, P.; Wachniew, P.; Czuprynski, P. (2006) "Study of hydraulic parameters in heterogeneous gravel units: Constructed wetland in Nowa Slupia (Poland)". *J. Hydrol*. 331, 630–642.

Marsteiner, E.L. (1997)" Subsurface Flow Constructed Wetland Hydraulics". Master's Thesis, Clarkson University, Potsdam, NY, USA, 1997

Martinez C.J. and Wise W.R. (2003) "Hydraulic analysis of Orlando easterly wetland" *Environ. Eng.* 129, 553–560.

Mary B., Vanella D., Consoli S., Cassiani G. (2019) “Assessing the extent of citrus tree root apparatus under deficit irrigation via multi-method geo-electrical imaging”. *Sci rep* 9(1):1–10

Marzec, M.; Jóźwiakowski, K.; Dębska, A.; Gizińska-Górna, M.; Pytka-Woszczyło, A.; Kowalczyk-Juśko, A.; Listosz, A. (2018) “The Efficiency and Reliability of Pollutant Removal in a Hybrid Constructed Wetland with Common Reed, Manna Grass, and Virginia Mallow”. *Water*. Vol. 10, 1445.

Marzo A., Ventura D., Cirelli G. L., Aiello R., Vanella D., Rapisarda R., Barbagallo S., Consoli, S. (2018) “Hydraulic reliability of a horizontal wetland for wastewater treatment in Sicily*”, Sc. of the Tot. Env*. Vol. 636 (September), 94–106.

Masi, F., Rizzo, A., Regelsberger, M. (2018). The role of constructed wetlands in a new circular economy, resource oriented, and ecosystem services paradigm, *Journal of Environmental Management*, (June) 216, 275-284.

Matos, M.P., Barreto, A.B., Vasconcellos, G.R., Matos, A.T. Simões, G.T, von Sperling M. (2017) “Difficulties and modifications in the use of available methods for hydraulic conductivity measurements in highly clogged horizontal subsurface flow constructed wetlands”. *Water Sci Technol* 76 (7): 1666–1675.

Matos, M.P., von Sperling, M., Matos, A.T. (2018) “Clogging in horizontal subsurface flow constructed wetlands: influencing factors, research methods and remediation techniques”. *Rev Environ Sci Biotechnol*, Vol. 17, 87–107

Matamoros, V., Rodríguez, Y., Bayona, J.M. (2017) “Mitigation of emerging contaminants by full-scale horizontal flow constructed wetlands fed with secondary treated wastewater”. *Ecol. Eng*. Vol. 99, 222–227.

Mestre, A., Pitt, R., 2005. The National Stormwater Quality Database, Version 1.1. The University of Alabama Tuscaloosa, AL. U.S. EPA Office of Water, Washington, D.C.

Milošković, A., Branković, S., Simić, V., Kovačević, S., Ćirković, M., Manojlović, D. (2013). “The accumulation and distribution of metals in water, sediment, aquatic macrophytes and fishes of the Gruža reservoir, Serbia”. *Bull. Environ. Contam. Toxicol.* 90 (5), 563–569.

Milani, M.; Consoli, S.; Marzo, A.; Pino, A.; Randazzo, C.; Barbagallo, S.; Cirelli, G.L. (2020) “Treatment of Winery Wastewater with a Multistage Constructed Wetland System for Irrigation Reuse”. *Water* Vol. 12, 1260.

Ministerial Decree 185 (2003) “Decreto Ministeriale 12 giugno 2003, n. 185”. 'Technical standards for wastewater reuse', GU n. 169, July 23th 2003.

Mitsch, W.J. and Wise, K.M. (1998). Water quality, fate of metals, and predictive model validation of a constructed wetland treating acid mine drainage. Water Res. 32, 1888–1900.

Nagajyoti, C.P., Lee, D.K., Sreekanth, M.V.T. (2010). Heavy metals, occurrence and toxicity for plants: a review. Environ. Chem. Lett. 8, 199–216.

Mares R., Barnard H.R., Mao D., Revil A., Singha K. (2016) “Examining diel patterns of soil and xylem moisture using electrical resistivity imaging. *J Hydrol* 536:327–338

Moreno. Z, Arnon-Zur A., Furman A. (2015) “Hydro-geophysical monitoring of orchard root zone dynamics in semi-arid region”. *Irrig Sci* 33(4):303–318

Morris R.H., Newton M.I., Knowles P.R., Bencsik M., Davies P.A., Griffin P., McHale G. (2011) “Analysis of clogging in constructed wetlands using magnetic resonance”. *Analyst* 136(11):2283-6

Morvannou A., Forquet N., S. Michel, S. Troesch, Pascal Molle. (2015) Treatment performances of French constructed wetlands: Results from a database collected over the last 30 years. *Water Science and Technology*, IWA Publishing, Vol. 71 (9), 333-1339.

Motisi A., Rossi F., Consoli S., Papa R., Minacapilli M., Rallo G., Cammalleri C., D’Urso G. (2012) “Eddy covariance and sap flow measurement of energy and mass exchanges of woody crops in a Mediterranean environment”. *Acta Hortic* 951:121–127.

NAVFAC (1986) Soil Mechanics. Design Manual 7.01. In Naval Facilities Engineering Command, Alexandria, Virginia, USA

Ni, J. Xu, M. Zhang (2016) “Constructed wetland planning-based bi-level optimization to balance the watershed ecosystem and economic development:

a case study at the Chaohu Lake watershed, China" *Ecol. Eng*., Vol. 97 (2016), 106-121.

Nivala J., Rousseau D.P.L. (2009) "Reversing clogging in subsurface-flow constructed wetlands by hydrogen peroxide treatment: two case studies". *Water Sci. Technol.* Vol. 1 2009; 59 (10): 2037–2046.

Nivala J., Knowles P., Dotro G., Garcia J., Wallace S. (2012). Clogging in subsurface-flow treatment wetlands: measurement, modelling and management. Water Res. 46, 1625–1640.

Nivala J., Headley T., Wallace S., Bernhard K., Brix H., Van Afferden M., Müller R. (2013) "Comparative analysis of constructed wetlands: The design and construction of the ecotechnology research facility" Langereichenbach, Germany. *Ecol. Eng*. Vol. 61(B): 527–543

Oral H.V., Carvalho P., Gajewska M., Ursino N., Masi F., Van Hullebusch E.D., Kazak J.K., Exposito A, Cipolletta G., Theis Raaschou Andersen T.R., Finger D.C, Simperler L., Regelsberger M., Rous V., Radinja M., Buttiglieri G., Krzeminski G.P., Rizzo A., Kaveh Dehghanian M.N., Zimmermann M. (2020) "A review of nature-based solutions for urban water management in European circular cities: a critical assessment based on case studies and literature". *Blue-Green Systems* Vol. 2 (1), 112–136

Paing J., A. Guilbert A., Gagnon V, Chazarenc F. (2015) "Effect of climate, wastewater composition, loading rates, system age and design on performances of French vertical flow constructed wetlands: a survey based on 169 full scale systems *Ecological Engineering*, 80, 46-52.

Pálfy T.G., Gerodolle M., Gourdon R., Meyer D., Troesch S., Molle P. (2017). Performance assessment of a vertical flow constructed wetland treating unsettled combined sewer overflow. *Water Sci. Technol*. 75, 2586-2597.

Passos R., Dias D., Matos M., Sperling M. (2018). Sodium chloride as a tracer for hydrodynamic characterization of a shallow maturation pond. Water Practice and Tech. 13 (1), 30–38.

Pedescoll A., Uggetti E, Llorens E, Granés F, Garcia D, García J (2009) Practical method based on saturated hydraulic conductivity used to assess clogging in subsurface flow constructed wetlands. Ecol. Eng. 35:1216–1224,

Pedescoll A., Sidrach-Cardona R.., Sanchez J.C., Carretero J., Garfi M., Becares E. (2013). Design configurations affecting flow pattern and solids accumulation in horizontal free water and subsurface flow constructed wetlands. Water Res. 47, 1448–1458,

Persson J., Somes N., Wong T. (1999). Hydraulics efficiency of constructed wetlands and ponds. Water Sci. Technol. 40, 291–300

Prost-Boucle S., Molle P. (2012) "Recirculation on a single stage of vertical flow constructed wetland: Treatment limits and operation modes", Ecol. Eng. Vol. 43, 2012, Pages 81-84.

Pucher B. and Langergraber G. (2019a) "Influence of design parameters on the treatment performance of VF wetlands – a simulation study". *Water Sci. Technol*. 80, 265-273.

Pucher B, Langergraber G. (2019b) "The State of the Art of Clogging in Vertical Flow Wetlands". *Water* 11(11):2400.

Puglisi I., Nicolosi E., Vanella D., Lo Piero A.R., Stagno F., Saitta D., Roccuzzo G., Consoli S., Baglieri A. (2019) "Physiological and biochemical responses of orange trees to different deficit irrigation regimes". *Plants* 8(10):42

R Core Team, 2014. R: A Language and Environment for Statistical Computing. R Foundation for Statistical Computing, Vienna, Austria http://www.R-project.org/.

Richir, J., Gobert, S. (2016) "Trace elements in marine environments: occurrence, threats and monitoring with special focus on the coastal Mediterranean". *J. Environ. Anal. Toxicol.* 6 (1), 349.

Rahman, M.E., Bin Halmi, M.I.E., Bin Abd Samad, M.Y., Uddin, M.K., Mahmud, K., Abd Shukor, M.Y., Sheikh Abdullah, S.R., Shamsuzzaman, SM. (2020) "Design, Operation and Optimization of Constructed Wetland for Removal of Pollutant". *Int. J. Environ. Res. Public Health*, Vol. 17, 8339.

Ranieri E., Gorgoglione A., Solimeno A. (2013). A comparison between model and experimental hydraulic performances in a pilot-scale horizontal subsurface flow constructed wetland. Ecol. Eng. 60, 45–49.

Rezania, S., Taib, S.M., Din, M.F.M., Dahalan, F.A., Kamyab, H. (2016) "Comprehensive review on phytotechnology: heavy metals removal by diverse aquatic plants species from wastewater". *J. Hazard. Mater.* 318, 587–599.

Robinson D.A., Campbell C.S., Hopmans J.W., Hornbuckle B.K., Jones S.B., Knight R., Ogden F., Selker J., Wendroth O. (2008) "Soil moisture measurements for ecological and hydrological watershed scale observatories: a review". *Vadose Zone J* 7:358–389

Robinson J.L., Slater L.D., Schäfer K.V.R. (2012)" Evidence for spatial variability in hydraulic redistribution within an oak-pine forest from resistivity imaging". *J Hydrol* 430–431:69–79.

Ronczka M., Rücker C, Günther T (2015) Numerical study of long-electrode electric resistivity tomography—accuracy, sensitivity, and resolution. Geophysics 80(6):E317–E328.

Rodgers, M.; Mulqueen, J. (2006) Field-saturated hydraulic conductivity of unsaturated soils from falling-head well tests. *Agric. Water Manag*. 79, 160–176.

Rodriguez-Dominguez M.A., Konnerup D., Brix H., Arias C.A. (2020) "Constructed Wetlands in Latin America and the Caribbean: A Review of Experiences during the Last Decade". *Water* 12 (6) 1744.

Rousseau D.P.L., Vanrolleghem P.A., De Pauw N. (2004) "Model-based design of horizontal subsurface flow constructed treatment wetlands: a review" *Water Research*, Vol. 38 (6) 1484-1493.

Rossi R., Amato M., Bitella G., Bochicchio R. (2013)" Electrical resistivity tomography to delineate greenhouse soil variability". *Int Agrophys* 27(2):211–218

Rousso B.Z, Pelissari C., Oliveira dos Santos M., Sezerino P.H. (2019) Hybrid constructed wetlands system with intermittent feeding applied for urban wastewater treatment in South Brazil. *Water, Sanitation and Hygiene for Development* 9 (3): 559–570.

Sacco A., Cirelli G.L., Ventura D., Barbagallo S., Licciardello F. (2021) Hydraulic performance of horizontal constructed wetlands for stormwater treatment: A pilot-scale study in the Mediterranean. *Ecol. Eng.* Volume 169, 106290.

Saitta D., Vanella D., Ramírez-Cuesta J.M., Longo-Minnolo G., Ferlito F., Consoli S. (2020) "Comparison of orange orchard evapotranspiration by eddy covariance, sap flow, and FAO-56 methods under different irrigation strategies". *J Irrig Drain* E ASCE 146(7):05020002

Samoüelian A., Cousin I., Tabbagh A., Bruand A., Richard G. (2005) "Electrical resistivity survey in soil science: a review". *Soil Til Res* 83:173–193.

Sanford W.E., Parlange J.Y, Steenhuis T.S., (1993). Hillslope Drainage with Sudden Drawdown: Closed Form Solution and Laboratory Experiments. Water Resour. Res. 1993, 29, 2313–2321.

Sanford W.E., Steenhuis T.S., Parlange J.Y., Surface J.M., Peverly J.H. (1995). Hydraulic conductivity of gravel sand as substrates in rock-reed filters. Ecol. Eng. 4, 321–336.

Schmitt N., Wanko A., Laurent J., Bois, P., Molle P., Mosé R. (2015). Constructed wetlands treating stormwater from separate sewer networks in a residential Strasbourg urban catchment area: Micropollutant removal and fate. Environ. Chem. Eng. 3, 2816–2824.

Scholz (2011) Wetland Systems Springer-Verlag London.

Scholz (2015) Wetland Systems to Control Urban Runoff Elsevier Science.

Schwartz B.F., Schreiber M.E., Yan T. (2008) "Quantifying field-scale soil moisture using electrical resistivity imaging". *J Hydrol* 362(3–4):234–246.

Seeger, E.M., Maier, U., Grathwohl, P., Kuschk, P., Kaestner, M. (2013) "Performance evaluation of different horizontal subsurface flow wetland types by characterization of flow behavior, mass removal and depth-

dependent contaminant load". *Water Res.* 47, 769–780.

Singha K., Day-Lewis F.D., Johnson T., Slater L.D. (2015) "Advances in interpretation of subsurface processes with time-lapse electrical imaging". *Hydrol Process* 29(6):1549–1576

Somarakis, G., Stagakis, S., & Chrysoulakis, N. (Eds.). (2019). "Think-Nature Nature-Based Solutions Handbook. Think-Nature project funded by the EU Horizon 2020 research and innovation programme under grant agreement" No. 730338.

Stefanakis A.I., Akratos C.S., Tsihrintzis V.A. (2014), "Vertical flow constructed wetlands: eco- engineering systems for wastewater and sludge treatment, 1st ed. Elsevier Science, Amsterdam

Stefanakis A.I. and Akratos C.S. (2016), "Removal of Pathogenic Bacteria in Constructed Wetlands: Mechanisms and Efficiency". In: Ansari A., Gill S., Gill R., Lanza G., Newman L. (eds) Phytoremediation. Springer, Cham.

Stefanakis A.I. Bardiau M., Trajano D., Couceiro F., Williams J.B., Taylor H. (2019) "Presence of bacteria and bacteriophages in full-scale trickling filters and an aerated constructed wetland", *Sci. Total Environ*., 659, 1135-1145.

Stefanakis A.I., (2020) "Constructed Wetlands for Sustainable Wastewater Treatment in Hot and Arid Climates: Opportunities, Challenges and Case Studies in the Middle East" *Water* Vol 12 (6), 1665.

Suliman, F.; French, H.K.; Haugen, L.E.; Søvik, A.K (2006) "Change in flow and transport patterns in horizontal subsurface flow constructed wetlands as a result of biological growth". *Ecol. Eng.* 27, 124–133,

Tang P., Yu B., Zhou Y., Zhang Y., Li J. (2017) "Clogging development and hydraulic performance of the horizontal subsurface flow stormwater constructed wetlands: a laboratory study". *Environ. Sci. Pollut*. 24, 9210–9219.

Tang, Y.; Yao, X.; Chen, Y.; Zhou, Y.; Zhu, D.Z.; Zhang, Y.; Zhang, T.; Peng, Y (2020) "Experiment research on physical clogging mechanism in the porous media and its impact on permeability". *Gr. Matter* 22, 37.

Thalla, A.K., Devatha, C.P., Anagh, K., Sony E. (2019) "Performance

evaluation of horizontal and vertical flow constructed wetlands as tertiary treatment option for secondary effluents. *Appl. Water Sci* Vol. 9, 147.

Torrens A., Molle P., Boutin C., Salgot M. (2009) "Impact of design and operation variables on the performance of vertical-flow constructed wetlands and intermittent sand filters treating pond effluent" *Water Research*, Vol. 43 (7), 1851-1858.

Tchounwou, P.B., Yedjou, C.G., Patlolla, A.K., Sutton, D.J., 2012. Heavy metal toxicity and the environment. In: Luch, A. (Ed.), Molecular, *Clinical and Environmental Toxicology*. Springer, Basel, pp. 133–164. Tsonev, T., Cebola Lidon, F.J., Zinc in plants — an overview. Emir. J. Food Agric. 24 (4), 322–333.

United Nations, 2015. Transforming our World: The 2030 Agenda for Sustainable Development. General Assembly, 17th Session, Items 15 and 116. Volume 16301 pp. 1–35.

United Nations, 2017. The Sustainable Development Goals Report. NewYork.https://unstats.un.org/sdgs/files/report/2017/thesustainabledevelopmentgoalsreport2017.pdf Accessed on 9/01/2020.

United States Environmental Protection Agency (US EPA 2000). "Manual Constructed Wetlands Treatment of Municipal Wastewaters". EPA/625/R-99/010, Washington DC – USA.

Urban Water Reuse Handbook. 1st ed. CRC Press. Available at: https://www.perlego.com/book/1599053/urban-water-reuse-handbook-pdf

Walaszek, M., Lenormand, E., Bois, P., Laurent, J., Wanko, A. (2017) "Urban stormwater constructed wetland: micropollutants removal linked to rain events characteristics andaccumulation. Chem. Eng. J. 359, 1065–1074.

Weis, J. and Weis, P. (2004). "Metal uptake, transport and release by wetland plants, implications for phytoremediation and restoration. *Environ. Int.* 30 (5), 685–700.

Van Leeuwen J., Awan J., Myers B., Pezzaniti D. (2019). Introduction to Urban Stormwater: A Global Perspective. In Urban Stormwater and Flood

management: Enhancing live-ability of Cities: A Global Perspective, 1st ed.; Springer International Publishing, Switzerland AG. Volume 1:1–199,

Vanella D and Consoli S (2018) “Eddy Covariance fluxes versus satellite-based modelisation in a deficit irrigated orchard”. Ital *J Agrometeorol* 23(2):41–52.

Vanella D., Cassiani G., Busato L., Boaga J., Barbagallo S., Binley A., Consoli S. (2018) “Use of small-scale electrical resistivity tomography to identify soil-root interactions during deficit irrigation”. *J Hydrol* 556:310–324

Vanella D., Ramírez-Cuesta J.M., Intrigliolo D.S., Consoli S. (2019) “Combining electrical resistivity tomography and satellite images for improving evapotranspiration estimates of citrus orchards”. *Remote Sens* 11(4):373

Varma M., Gupta A.K., Ghosal P.S., Majumder A., (2021) “A review on performance of constructed wetlands in tropical and cold climate: Insights of mechanism, role of influencing factors, and system modification in low temperature”, Sc. of The Tot. Env., Vol. 755 (2), 142540.

Ventura D., Consoli S., Barbagallo, S., Marzo A., Vanella D., Licciardello F., Cirelli G. L. (2019a) “How to overcome barriers for wastewater agricultural reuse in Sicily (Italy)?” *Water*, Vol. 11 (2), 335.

Ventura D., Barbagallo S., Consoli S., Ferrante M., Milani M., Licciardello F. Cirelli G.L. (2019b). On the performance of a pilot hybrid constructed wetland for stormwater recovery in Mediterranean climate, Water Science and Technology, 79(6), 1051–1059.

Ventura, D., Barbagallo S., Consoli, S., Milani M., Sacco A., Rapisarda R., Cirelli, G.L. (2020). On the Performance of a novel hybrid constructed wetland for stormwater treatment and irrigation reuse in Mediterranean climate. Lecture Notes in Civil Engineering, 2020, 67, pp. 151–159.

Ventura D., Ferrante M., Copat C., Grasso A., Milani M., Sacco A.,

Licciardello F., Cirelli G.L. (2021) Metal removal processes in a pilot hybrid constructed wetland for the treatment of semi-synthetic stormwater, Sci. of the Tot. Env,754, 142221.

Vereecken H., Huisman J.A., Bogena H., Vanderborght J., Vrugt J.A., Hopmans J.W. (2008) "On the value of soil moisture measurements in vadose zone hydrology: a review". *Water Resour Res* 44:1–21

Verlicchi P. and Zambello E. (2014) "How efficient are constructed wetlands in removing pharmaceuticals from untreated and treated urban wastewaters? A review", *Sc. of The Tot. Envir*., Vol. 470–471, 1281-1306,

Vodyanitskii, Y.N. and Shoba S.A. (2015). Biogeochemistry of carbon, iron, and heavy metals in wetlands (analytical review). Moscow Univ. Soil Sci. Bull. 70 (3), 89–97.

Vymazal J. (1996) "The use of subsurface-flow constructed wetlands for wastewater treatment in the Czech Republic" *Ecological Eng.*, Volume 7 (1), 1-14.

Vymazal J., Brix h., Cooper P., Green M., Haberl R. (1998) "Removal mechanisms and types of constructed wetlands, in: Constructed Wetlands for Wastewater Treatment in Europe" Backhuys Publishers, Leiden, The Netherlands, 17-66

Vymazal J. (2004) "Removal of Phosphorus in Constructed Wetlands with Horizontal Sub-Surface Flow in the Czech Republic". *Water, Air, & Soil Pollution*: Focus 4, 657–670.

Vymazal J. (2013). "The use of hybrid constructed wetlands for wastewater treatment with special attention to nitrogen removal: A review of a recent development" *Water Res.*, Vol. 47 (14), 4795-4811.

Vymazal J., Březinová T. (2016) "Accumulation of heavy metals in aboveground biomass of Phragmites australis in horizontal flow constructed wetlands for wastewater treatment: A review", *Chemical Engineering Journal*, Vol. 290, 232-242.

Vymazal J., Dvořáková Březinová T., Koželuh M., Kule L. (2017) "Occurrence and removal of pharmaceuticals in four full-scale constructed wetlands in the Czech Republic – the first year of monitoring", *Ecological Engineering*, Vol. 98, 354-364.

Vymazal J., (2018). Does clogging affect long-term removal of organics and suspended solids in gravel-based horizontal subsurface flow constructed wetland? *Chemical Engineering Journal*, Vol. 331, 663-674.

Vymazal J. (2019) "Is removal of organics and suspended solids in horizontal sub-surface flow constructed wetlands sustainable for twenty and more years?", *Ch. Eng. Journal*, Vol. 378, 122117.

Wada, Y., M. Flörke, N. Hanasaki, S. Eisner, G. Fischer, S. Tramberend, Y. Satoh, M.T.H. van Vliet, P. Yillia, C. Ringler, and D. Wiberg (2016) "Modeling global water use for the 21st century: Water Futures and Solutions (WFaS) initiative and its approaches. *Geosci. Model Dev.*, **9**, 175-222,

Wahl M.D., Brown L.C., Soboyejo A.O., Martin J., Dong B. (2010). Quantifying the hydraulic performance of treatment wetlands using the moment index. Ecol. Eng. 36, 1691–1699,

Wallace, S.D. System for Removing Pollutants from Water. U.S. Patent 6,200,469 B1, 13 March 2001.

Wang H., Sheng L., Xu J. (2021) Clogging mechanisms of constructed wetlands: A critical review, *Journal of Cleaner Production*, Vol. 295, 2021, 126455

Wang H. and Jawitz J.W. (2006). Hydraulic analysis of cell-network treatment wetlands. Hydrol. 330, 721–734,

Wang Z, Liu CX, Li PY, Dong J, Liu L, Zhu GF. (2012) "Study on phosphorus removal capability of constructed wetlands filled with broken bricks". *Huan Jing Ke Xue*, Vol. 33 (12), 4373-9. Chinese. PMID: 23379167.

Wetzel R.G. (2001) "Fundamental processes within natural and constructed wetland ecosystems: short-term versus long-term objectives". *Water Science and Technology*, Vol. 44 (11-12), 1–8.

Whitmer S., Baker L., Wass R. (2000). Loss of bromide in a wetland tracer experiment. Environ. Qual. 29, 2043–2045,

Williams M.R., Buda A.R., Singha K., Folmar G.J., Elliott H.A., Schmidt J.P. (2017) "Imaging hydrological processes in headwater riparian seeps with time-lapse electrical resistivity". *Groundwater* 55(1):136–148

Wojciechowska, E. (2013). Removal of persistent organic pollutants from landfill leachates treated in three constructed wetland systems, *Water Science and Technology*, Vol. 68 (5), 1164– 172.

Wu G.L., Liu Y., Yang Z., Cui Z., Deng L., Chang X.F., Shi Z.H. (2017) "Root channels to indicate the increase in soil matrix water infiltration capacity of arid reclaimed mine soils". *J Hydrol* 546:133–139

Wu H., Zhang J., Huu H.N., Guo W., Zhen H., Liang S, Fan J., Hai Liu H. (2015) "A review on the sustainability of constructed wetlands for wastewater treatment: Design and operation", *Bioresource Technology*, 175, 2015, 594-601.

Wu S., Carvalho P.N., Müller J. A., Manoj V. R., Dong R., (2016) "Sanitation in constructed wetlands: A review on the removal of human pathogens and faecal indicators", *Sc. of The Tot. Envir.*, Vol. 541, 8-22.

Wu Y., Han R., Yang X., Zhang Y., Zhang R. (2017). Long-term performance of an integrated constructed wetland for advanced treatment of mixed wastewater. Ecol. Eng. 99, 91-98,

Yadav A., Chazarenc F., Mutnuri S. (2018) "Development of the "French system" vertical flow constructed wetland to treat raw domestic wastewater in India, *Ecological Engineering*, Vol. 113, 88-93.

Zapater-Pereyra M., Ilyas H., Lavrnić S., van Bruggen J.J.A., Lens P.N.L. "Evaluation of the performance and space requirement by three different hybrid constructed wetlands in a stack arrangement", Eco. Eng., Vol. 82, 290-300

Zeb B.S, Qaisar M., Saima J., Arshid P., Muhammad I., Muhammad B., Zulfiqar Ahmad B. (2013) "Combined Industrial Wastewater Treatment in Anaerobic Bioreactor Post-treated in Constructed Wetland" BioMed Res. Inter. Vol. 2013, Article ID 957853

Zhang S.Y., Hopkins I., Guo L., Lin H. (2019) "Dynamics of infiltration rate and field-saturated soil hydraulic conductivity in a wastewater-irrigated cropland". *Water* 11(8):1632

Zhang Y., Niu J., Zhang M., Xiao Z., Zhu W. (2017) "Interaction between plant roots and soil water flow in response to preferential flow paths in northern China". *Land Degrad Dev* 28(2):648–663

Zhi W., Ji G. (2012) “Constructed wetlands, 1991–2011: A review of research development, current trends, and future directions”, *Science of The Total Environment*, Vol. 441, 19-27.

Zhao Y., Ji B., Liu R., Ren B., Wei T. (2020) “Constructed treatment wetland: Glance of development and future perspectives” *Water Cycle*, Vol. 1, 104-112.

Zhou X., Chen Z., Li Z., Wu H. (2020) “Impacts of aeration and biochar addition on extracellular polymeric substances and microbial communities in constructed wetlands for low C/N wastewater treatment: implications for clogging” *Chem. Eng. J.*, Vol. 396 125349.

List of publication

Peer-reviewed journals

Article

Sacco, A., Cirelli, G.L., Ventura, D., Barbagallo, S., Licciardello, F. (2021) - Hydraulic performance of horizontal constructed wetlands for stormwater treatment: A pilot-scale study in the Mediterranean - Ecological Engineering, 2021, 169, 106290
https://doi.org/10.1016/j.ecoleng.2021.106290

Ventura D., Ferrante M., Copat C., Grasso A., Milani M., **Sacco A**., Licciardello F., Cirelli G.L. (2021) - Metal removal processes in a pilot hybrid constructed wetland for the treatment of semi-synthetic stormwater in Sc. of total environment Volume 754, 1 Feb 21 https://doi.org/10.1016/j.scitotenv.2020.142221

Article – open access

Licciardello F., **Sacco A.**, Barbagallo S., Ventura D., Cirelli G.L. (2020) - “Evaluation of Different Methods to Assess the Hydraulic Behavior in Horizontal Treatment Wetlands” Water 12, no. 8: 2286. https://doi.org/10.3390/w12082286

Vanella D., Ramírez-Cuesta J.M., **Sacco** A., Longo-Minnolo G.; Cirelli G. L., Consoli S. (2020) - Electrical resistivity imaging for monitoring soil water motion patterns under different drip irrigation scenarios in Springer - Irrigation Science Volume 39, 12 Sep 20 https://doi.org/10.1007/s00271-020-00699-8

Book chapter

Ventura, D., Consoli, S., Milani, M., **Sacco, A**., Rapisarda, R., Cirelli, G.L. (2019c) - On the performance of a novel hybrid constructed wetland for stormwater treatment and irrigation reuse in Mediterranean climate". In: Innovative biosystems engineering for sustainable agriculture, forestry and food production, by Springer International Publishing - AG, AIIA International Mid-Term Conference 2019.

Congress and conferences contributions

Ventura, D., Consoli, S., Milani, M., **Sacco, A.**, Rapisarda, R., Cirelli, G.L. (2019) - On the performance of a novel hybrid constructed wetland for stormwater treatment and irrigation reuse in Mediterranean climate. AIIA International Mid-Term Conference 2019.

Ventura, D., Ferrante, M., Copat, C., Grasso, A., Milani, M., **Sacco, A.**, Rapisarda, R., Cirelli., G.L (2019) - A synthetic stormwater recipe for assessing a pilot hybrid constructed wetland reliability in Mediterranean climate. 8th WETPOL - International Symposium on Wetland Pollutant Dynamics and Control, Aarhus University, Denmark, June 17-21, 2019.

Sacco A., Barbera A.C., Leonardi G., Licciardello F., Milani M., Cirelli G.L. (2021) - Effects of clogging on vegetation development and CO_2 emission in a Mediterranean horizontal flow constructed wetland. 9th WETPOL - International Symposium on Wetland Pollutant Dynamics and Control, Boku University, Austria, September 13-17, 2021.